

Response to reviewers' comments on the paper "Interferences on Aerosol Acidity Quantification due to Gas-phase Ammonia Uptake onto Acidic Sulfate Filter Samples"

We would like to thank both reviewers for their time and for their useful comments that have helped improve and clarify our paper. For ease, comments from reviewers are in black, responses in blue, and new text added to paper in **bold blue**.

Reviewer #1

1.0. Nault et al. identify and characterize apparent artifacts associated with NH₃ uptake onto acidic aerosol collected on filters during aircraft campaigns. This is important work and certainly relevant and useful for readers of AMt. It should be pointed out, however, that their results are not terribly surprising. It has long been recognized that filter samples of acidic aerosol need to be protected from human breath and other sources of ammonia during handling and storage. The fact that some practitioners of aerosol sampling by filters in aircraft campaigns (where acidic aerosol are even more likely to be encountered than at the typically more ammonia-rich surface) have ignored these lessons outlined in the literature is unfortunate.

We agree that the importance of NH₃ uptake onto filters has been discussed in prior studies, which we already included in lines 84 through 87 of the AMTD version (Klockow et al., 1979; Hayes et al., 1980; Koutrakis et al., 1988). However, because the SAGA has been on many major airborne campaigns since the 1980s, the measurements from SAGA filters have been used to constrain chemical transport models (e.g., Wang et al., 2008a, 2008b; Ge et al., 2018), and the recent ATom campaigns that measured very remote air over Pacific, Atlantic, Southern, and Arctic Ocean. Thus, we felt it was important to analyze this uptake in regards to the SAGA system to ensure documentation as well as proper interpretation of past measurements in any future study, as we expect, e.g., the data collected from ATom to be used in numerous future studies. Finally, the very high speed of neutralization that we document is a novel and important aspect that has not been fully discussed in the prior studies we listed above.

I have several comments for the authors to consider in preparing a revised manuscript.

1.1. Abstract lines 45-47 and manuscript lines 376-379: the authors need to more fully specify the LOD they provide for filter sampling. This depends on a variety of factors, including sampled air volume and (depending on the stage where contamination occurs) filter extraction volume. At a minimum they should state their LOD estimate is appropriate for typical SAGA filter collection and extraction protocols.

Here and throughout the rest of the manuscript, we have specified specifically for the SAGA system as flown on the DC-8 and have also noted that similar type analysis should be conducted for other filter systems but will lead to different results.

For line 47, we have changed it to say:

“Finally, a more meaningful limit-of-detection for SAGA filters collected during airborne campaigns is $\sim 0.2 \mu\text{g sm}^{-3}$ ammonium, which is substantially higher than the limit-of-detection of the ion chromatography. A similar analysis should be conducted for filters that collect inorganic aerosol and do not have ammonia scrubbers and/or are handled in the presence of human ammonia emissions.”

For line 404, we have changed it to say:

“Thus, this analysis suggests that for SAGA filters, a more meaningful ammonium limit-of-detection would be equivalent to $1 \mu\text{g sm}^{-3}$ sulfate, which would be $\sim 0.2 \mu\text{g sm}^{-3}$ ammonium. This also provides the framework to define limit-of-detection for other filter-based measurements not associated with ion chromatography.”

For line 650, we have changed it to say:

“For example, for filters that collect aerosols similar to those described here (no ammonia scrubber and/or exposed to human emissions of ammonia), values of ammonium $< 0.2 \mu\text{g sm}^{-3}$ should be used with caution or instead use *on-line* measurements of ammonium (specifically for SAGA measurements but a similar analysis should be conducted for other filter-based measurements).”

Finally, for line 678, we have changed it to say:

“Thus, due to the interaction of ammonia in the cabin of research aircraft, we suggest a more realistic limit-of-detection of ammonium for the SAGA filters is 200 ng sm^{-3} , versus the 10 ng sm^{-3} typically cited based on the ion chromatography measurement.”

1.2. Line 92: Please change “cations” to “anions.” Sulfate and nitrate are anions.

Changed.

1.3. Lines 178-181: Can the authors exclude loss of NH_4^+ volatiles from the warming/drying of the AMS stream as a cause of some of the difference vs. filter NH_4^+ levels?

Yes. This has been analyzed in depth in prior studies (Guo et al., 2016, 2017; Shingler et al., 2016). For example, Guo et al. (2016) showed that for the residence time of the PILS inlet sample (~2 s) and the heating between ambient and cabin air (~17 K), the observed ammonium nitrate was inconsistent with a calculation that considered evaporation of ammonium nitrate. Instead, the observations were consistent with the calculation that assumed the ambient (277 K) vs the cabin (294 K) temperature. As the residence time for the AMS is faster than PILS (< 1 s) (Nault et al., 2018; Schroder et al., 2018; Guo et al., 2020), we do not expect any losses of these semivolatile compounds.

We have added the following lines, starting at line 195:

“To minimize any potential losses of volatile aerosol components, the residence time between the inlet and AMS was less than 1 s (Nault et al., 2018; Schroder et al., 2018; Guo et al., 2020). Prior studies (Guo et al., 2016; Shingler et al., 2016) have shown minimal loss of semivolatile components for this residence time.”

1.4. Lines 223-224: Plastics are common sources of NH₄⁺ contamination vs. offgassing of NH₃ adsorbed onto the plastic surface. Many researchers who are worried about artifact neutralization of acidity on aerosol filter samples use acid-coated substrates as NH₃ sinks inside bags or other containers used for sample storage. Did the authors evaluate the polyethylene bags as a potential source of contamination? Were acid scrubbers inserted into the bags to prevent such an artifact from offgassed NH₃?

The following text has been added to SI (Sect. S4):

“Research from co-authors on a prior paper showed that films of water are the most likely reason for the retention and slow release of sticky volatile gases from surfaces coated by Teflon and other surfaces. An upper limit water thickness is ~10 μm (Liu et al., 2019). The Henry’s Law Coefficient for ammonia is 62 M atm⁻¹ (Seinfeld. and Pandis, 2006). With the bags being ~1.6×10⁴ mm² (~1.6×10⁻² m²), that would put an upper limit of water volume of ~1.6×10⁻⁷ m³ (~1.6×10⁻⁴ L). The average ammonia in the cabin of the DC-8 was ~45 ppbv (~4.5×10⁻⁹ atm), leading to ~2.8×10⁻⁷ M ammonia partitioned to the water in the bag. Thus, that would lead to ~4.5×10⁻¹¹ mol ammonia on the walls, or ~2.7×10¹³ molecules ammonia. The average number of sulfate molecules on the filters was ~3.8×10¹⁵. Thus, at the upper limit for the water thickness of the bags, there is ~0.7% ammonia:sulfate molecules. As the bags are blown with dry air prior to placing the filters into the bags, the water thickness is expected to be lower (~0.1 μm), leading to a three order magnitude decrease for ammonia

molecules in the bag. Thus, the bags are not expected to be a large source of ammonia contamination. However, this effect has not been directly investigated experimentally.”

And the following text has been added to main text (Line 508) to reference SI:

“Some studies have suggested that the bags used to store the filters may be a source of ammonia (e.g., Hayes et al., 1980); however, calculations indicate the bags would be a small source of ammonia (see Sect. S4).”

Finally, the following text has been added to the paper to address the second point at Line 250:

“No acid scrubbers were inserted into the bags to prevent any artifact from offgassing of ammonia.”

1.5. Lines 225-226: I was shocked to see that collected filter samples were extracted with 20 mL of water. This represented a huge dilution when extracting a sample that has collected only 2-3 m³ of air. By diluting aqueous concentrations to low levels, any background NH₄⁺ in the extract solution has an outsize effect on raising calculated aerosol ammonium concentrations and the uncertainty associated with measuring low extract ion concentration is also magnified. Can the authors justify this large extraction volume and assess possible contributions to the concluded artifacts in the filter samples? A modern conventional IC analysis needs only 20-100 μL of injected volume (some capillary systems use far less) and even an autosampler can easily work with a total extract volume of several hundred μL.

The following has been added to SI (Sect. S2):

“The 20 mL is thought to be a balance between a couple of competing factors. (1) The SAGA team wants to be confident that they are completely extracting the soluble material from the filters (recall, the filters are 90 mm in diameter). They had conducted testing when they first started operating on the NASA DC-8 (late 1980’s-early 1990’s) and established that this amount of water was necessary to fully extract the material. (2) To counter the dilution, the SAGA team uses a pre-concentrator column and large volume injections into the IC (~5 mL). These two aspects compensate for the greater dilution. (3) Finally, 5 mL is injected for both anions and cations (total 10 mL), and enough sample is left to conduct a follow-up injection if there was any concern about the data.”

1.6. Section 2.2.3. I am puzzled why the authors rely on PALMS data to get an independent (of AMS) estimate of online particle ammonium balance. The PALMS sulfate acidity indicator, as pointed out by the authors, is calibrated by comparison to PILS ion concentration ratios. The

WINTER campaign flew with a PILS onboard. The authors should use that PILS ion balance directly rather than the PILS-calibrated PALMS data, which the authors point out can be influenced by changes in laser power. By its design and reliance on direct IC measurement of ion concentrations in aerosol extracts, the PILS should provide the most definitive measure of ratios of NH_4^+ to SO_4^{2-} .

For ATom, PALMS is the only other instrument that offers information on submicron aerosol acidity. Even if somewhat indirect, it is still useful, since the remote atmosphere is where the largest differences appear. PILS is not available except for WINTER and ARCTAS. Unfortunately, the PILS data from WINTER could not be used for this analysis. As discussed in Guo et al. (2016), the cation IC exhibited higher baseline noise during the WINTER campaign compared to the anion IC, leading to insufficient sensitivity for reliable ammonium measurements. Further, Schroder et al. (2018) found that the PILS sulfate mass concentration was lower than the AMS sulfate concentration (slope of AMS vs. PILS = 1.5, $R^2 = 0.75$), even though there was good agreement with the AMS and SAGA filter sulfate mass concentration (slope of AMS vs. SAGA = 1.0, $R^2 = 0.92$). Similarly, as shown below, the PILS sulfate was lower than the SAGA sulfate during WINTER. Thus, these factors make comparing against PILS during WINTER unreliable. Finally, a similar disagreement between PILS and SAGA was observed during ARCTAS campaigns, the only other campaign that PILS, SAGA, and AMS were co-located on the same plane, whereas SAGA and AMS showed similar agreement as WINTER (Aknan, 2015).

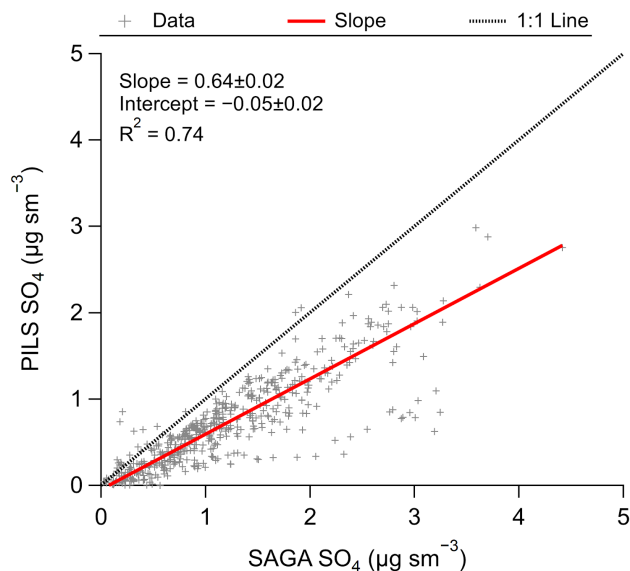


Figure 1. Scatter plot of PILS and SAGA sulfate during WINTER campaign.

We have added the following at line 384:

“The only useful comparison, other than SAGA versus AMS, is with PALMS during ATom.”

1.7. Section 2.3.1. The FIREX campaign targeted smoke plumes. Biomass burning smoke can be very rich in NH₃. How much might penetration of smoky air into aircraft cabin influenced the NH₃ concentrations measured here? The authors’ air exchange measurements and calculated concentrations with assumed human emission rates suggest that smoke NH₃ might not have been a major factor in determining cabin NH₃ concentrations. That surprised me!

We have conducted further investigation and added the following figure to the SI:

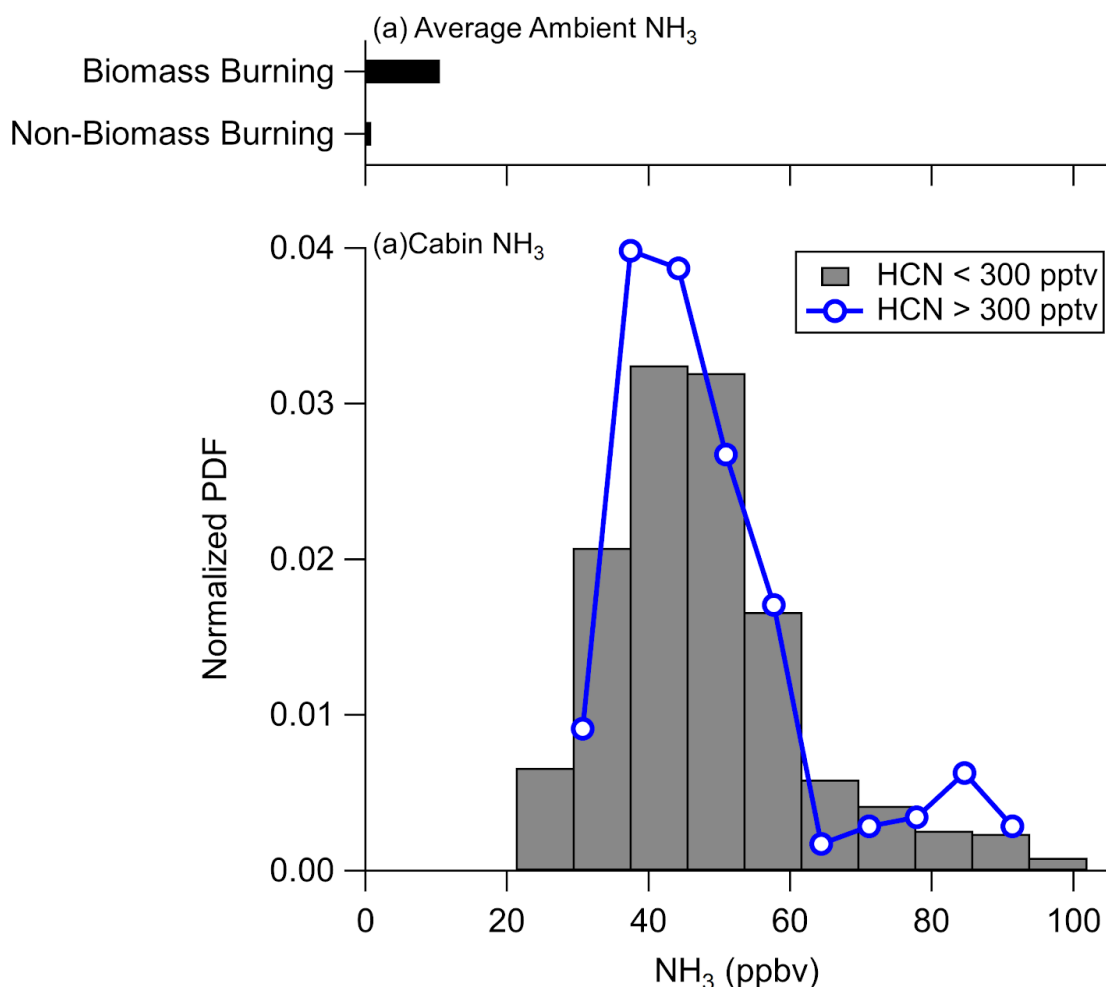


Figure S7. (top) Average ambient ammonia, measured by PTR-MS (Müller et al., 2014), sampled in air influenced (HCN > 300 pptv) and not influenced (HCN < 300 pptv) by biomass burning during the time period cabin was being sampled by Picarro. Note, this sampling was weighted towards the time period that the DC-8 was sampling agricultural fires, where the plumes were significantly smaller (seconds) versus the western fires at the

beginning of the campaign (minutes - hours). (b) Normalized probability density function (PDF) of gas-phase ammonia (NH_3) measured in the cabin of the DC-8 during FIREX-AQ for when the DC-8 was sampling air influenced by biomass burning ($\text{HCN} > 300$ pptv) and not influenced by biomass burning ($\text{HCN} < 300$ pptv).

And the following lines, starting at line 472:

“During FIREX-AQ, the DC-8 frequently sampled air impacted by biomass burning, which is an important source of ammonia (Sutton et al., 2013) and could potentially increase the background ammonia being brought into and mixing with the cabin air being sampled by the Picarro. Splitting the cabin ammonia ratios between sampling air impacted by biomass burning versus nominally background air, the normalized PDF did not shift to higher ammonia mixing ratios (Fig. S7). Further, the averages of the observed cabin ammonia was statistically similar, at the 95% confidence interval, between the DC-8 sampling biomass burning and nominally background air (48.1 ± 13.4 versus 44.1 ± 14.4 ppbv for biomass burning and background air, respectively). Finally, the majority of the time the cabin air was sampled by the Picarro for cabin ammonia, the DC-8 was sampling agricultural fires in Southeast US, which are shorter in duration (seconds) versus the large wildfires in Western US (minutes to hours). This is reflected in the low average ambient value for ammonia, as measured by a proton transfer reaction mass spectrometer (Müller et al., 2014), when the DC-8 was sampling biomass burning-influenced air observed during this time (~ 10 ppbv) and very low average value for non-biomass burning-influenced air (~ 0.8 ppbv) (Fig. S7). Thus, ammonia from biomass burning would at most be a small impact on the ammonia measured in the cabin of the DC-8, further indicating the ammonia in the cabin was mainly from human emissions.”

1.8. Line 393: The filter storage bag here is specified to be Teflon vs. the polyethylene bag referred to earlier in the manuscript.

Corrected. The correct bag material is polyethylene bag.

1.9. I like that the authors consider the timescale for diffusion to the collected aerosol particles in the filter. I do want to be sure they are calculating the timescale correctly. Can the authors please verify that the timescale expression they used (Eqn. 1) applies to a porous membrane? I am surprised that there is no dependence on pore size included. Also, what is the relevant timescale for NH_3 to diffuse into acidic particle itself? It needs to do more than just reach the surface.

The following has been added at line 518:

“Even though the filters have a porous membrane, for molecular diffusion, the membrane only increases the pathway that the ammonia molecules have to travel slightly; thus, not changing the estimated time. Second, as the particles are liquid (Wilson, 1921), the diffusion will be similar as through water. A typical value for diffusivity in water is $\sim 1 \times 10^{-5} \text{ cm}^2 \text{ s}^{-1}$ (Seinfeld and Pandis, 2006). For the size ranges observed (Fig. 7, $\sim 40 - 700 \text{ nm}$), this corresponds to a timescale of 1.6×10^{-7} to $5.0 \times 10^{-5} \text{ s}$. Thus, the diffusion through the filter and through the PM is nearly instantaneous for ammonia.”

1.10. Pp. 26-27. The discussion of CSN and CASTNet NH_4^+ differences is interesting, although other factors beyond those discussed are likely at play. Both filter sampling systems can lose volatile NH_4^+ (e.g., NH_4NO_3). The degree of loss will increase in the denuded system as the equilibrium with the gas phase is strongly perturbed. Difference in sample handling, shipping, and storage may also be important.

The following has been added at line 638:

“Other aspects that could impact this comparison, and are beyond the scope of this study (but that have been discussed in other studies (Hering and Cass, 1999; Schauer et al., 2003; Chow et al., 2005, 2010; Dzepina et al., 2007; Watson et al., 2009; Nie et al., 2010; Liu et al., 2014, 2015; Cheng and He, 2015; Heim et al., 2020) include the loss of volatile ammonium from the evaporation of ammonium nitrate or differences in the handling, shipping, and/or storage of the filters or extracted samples.”

1.11. Lines 589-592: The authors’ computed $0.2 \mu\text{g}/\text{m}^3$ threshold is relevant for the SAGA system as used here but should not be more generally claimed for other filter-based sampling approaches with different sample volumes. Post-collection NH_3 uptake will yield different impacts on aerosol LODs in other systems.

Please see response to 1.1 above.

Reviewer #2

This manuscript provides a detailed analysis and discussion on artefacts related to filter handling and analysis during atmospheric measurements. For this discussion, the authors grouped together six different airborne measurement campaigns where both offline filters and online aerosol mass spectrometry were used to measure aerosol chemical composition. The authors highlight discrepancies in measurements that are thought to be largely related to handling artefacts and exposures of filters samples to ambient ammonia from the laboratory environment and from human interference. This work illustrates how artefacts related to sampling and handling of

offline measurements can result in observations that can lead to the misinterpretation of atmospheric measurements, which will then inherently lead to discrepancies when comparing with global transport models. The authors recommend that the limit of detection of ammonia on filters is increased and that when possible a denuder is used for filter sampling.

This manuscript is well written with well-illustrated figures and detailed supplementary information, and I recommend this manuscript for publication. I have a small number of remarks below related to additional information that could be included in the discussion.

Minor comments:

2.1 Line 176: The AMS samples behind the NCAR inlet (HIMIL); the upper size cut of this inlet is not mentioned. (Line 216: The SAGA inlet is stated to have an aerodynamic diameter cut of 4.1 microns). Can the author include the upper size cut of the HIMIL inlet and that it was isokinetic sampling?

We have added the following lines, at line 183:

“The best estimated upper size cut-off for the HIMIL inlet is ~1 μm diameter (geometric, David Rogers, pers. comm. 2011). This diameter is larger than the size cut-off than that of the AMS inlet (~0.5-0.7 μm diameter, geometric, depending on the composition), with no losses in the tubing between the HIMIL and AMS inlet expected (see Guo et al. (2020) for more details). Multiple comparisons with instruments sampling from an isokinetic inlet PM_4 inlet (Brock et al., 2019; Guo et al., 2020) indicate that no significant sampling biases were incurred over the size range of the AMS.”

2.2 What was the flow rate of the SAGA inlet?

We have added the following lines, at line 245:

“The aerosol inlet flow is close to 400 slpm in the marine boundary layer and approximately 150 slpm at maximum altitude.”

2.3 What is the lower size cut of these two inlets? Given that the discrepancies between the two methods were highest as lowest mass concentrations, could they be a result of different sampling efficiencies for particles with diameters < 80 nm?

The following has been added to line 238:

“The lower size cut-offs for SAGA and AMS are similar (Guo et al., 2020). As discussed by Guo et al. (2020; their Fig. 8) the difference in mass sampled at the smaller sizes between SAGA and AMS is generally negligible at all altitudes.”

2.4 In section 2.2.2 Aerosol filters. There was no mention of filter blanks. Can the authors state how blank filter measurements were made (each flight or every couple of flights)?

The following has been added to line 247:

“Further, 2 blank filters are collected each flight.”

2.5 There were several instruments operating together on the plane. Was mass closure check performed on the AMS measurements to illustrate that this instrument was measuring all the NR-PM1? How did this mass closure change with altitude?

We have added the following lines, at line 215:

“Mass and/or volume closure has been investigated between the AMS and other measurements for all campaigns discussed here (Cubison et al., 2011; Aknan, 2015; Liu et al., 2017; Nault et al., 2018; Schroder et al., 2018; Guo et al., 2020). The closure was complete for the size range of the AMS and did not show any dependence with altitude (Guo et al., 2020).”

2.6 If measured, how did the OC/OM concentrations measured on the filters compare to the organic mass measured by the AMS instrument? Was the PILS instrument available on any of the flights? How did the PILS data compare with offline filters?

The only organic molecule reported from SAGA filters is oxalate (Talbot et al., 1992; Dibb et al., 1997). Thus, a comparison of OC/OM between filters and AMS cannot be conducted.

Please see comment 1.6 above concerning PILS.

References

- Aknan, A.: NASA Airborne Science Data for Atmospheric Composition, TABMEP2 POLARCAT Preliminary Assessment Reports [online] Available from: <http://www-air.larc.nasa.gov/> (Accessed 3 June 2020), 2015.
- Brock, C. A., Williamson, C., Kupc, A., Froyd, K. D., Erdesz, F., Wagner, N., Richardson, M., Schwarz, J. P., Gao, R.-S., Katich, J. M., Campuzano-Jost, P., Nault, B. A., Schroder, J. C., Jimenez, J. L., Weinzierl, B., Dollner, M., Bui, T. and Murphy, D. M.: Aerosol size distributions during the Atmospheric Tomography Mission (ATom): methods, uncertainties, and data products, *Atmos. Meas. Tech.*, 12(6), 3081–3099, 2019.
- Cheng, Y. and He, K.-B.: Measurement of carbonaceous aerosol with different sampling configurations and frequencies, *Atmos. Meas. Tech.*, 8(7), 2639–2648, 2015.
- Chow, J. C., Watson, J. G., Lowenthal, D. H. and Magliano, K. L.: Loss of PM_{2.5} Nitrate from Filter Samples in Central California, *J. Air Waste Manage. Assoc.*, 55(8), 1158–1168, 2005.
- Chow, J. C., Watson, J. G., Chen, L.-W. A., Rice, J. and Frank, N. H.: Quantification of PM_{2.5} organic carbon sampling artifacts in US networks, *Atmos. Chem. Phys.*, 10(12), 5223–5239, 2010.
- Cubison, M. J., Ortega, A. M., Hayes, P. L., Farmer, D. K., Day, D. A., Lechner, M. J., Brune, W. H., Apel, E., Diskin, G. S., Fisher, J. A., Fuelberg, H. E., Hecobian, A., Knapp, D. J., Mikoviny, T., Riemer, D., Sachse, G. W., Sessions, W., Weber, R. J., Weinheimer, A. J., Wisthaler, A. and Jimenez, J. L.: Effects of aging on organic aerosol from open biomass burning smoke in aircraft and laboratory studies, *Atmos. Chem. Phys.*, 11(23), 12049–12064, 2011.
- Dibb, J. E., Talbot, R. W., Lefer, B. L., Scheuer, E., Gregory, G. L., Browell, E. V., Bradshaw, J. D., Sandholm, S. T. and Singh, H. B.: Distributions of beryllium 7 and lead 2109, and soluble aerosol-associated ionic species over the western Pacific: PEM West B, February–March 1994, *J. Geophys. Res.*, 102(D23), 28287–28302, 1997.
- Dzepina, K., Arey, J., Marr, L. C., Worsnop, D. R., Salcedo, D., Zhang, Q., Onasch, T. B., Molina, L. T., Molina, M. J. and Jimenez, J. L.: Detection of particle-phase polycyclic aromatic hydrocarbons in Mexico City using an aerosol mass spectrometer, *Int. J. Mass Spectrom.*, 263(2), 152–170, 2007.
- Ge, C., Zhu, C., Francisco, J. S., Zeng, X. C. and Wang, J.: A molecular perspective for global modeling of upper atmospheric NH₃ from freezing clouds, *Proc. Natl. Acad. Sci. U. S. A.*, 115(24), 6147–6152, 2018.
- Guo, H., Sullivan, A. P., Campuzano-Jost, P., Schroder, J. C., Lopez-Hilfiker, F. D., Dibb, J. E., Jimenez, J. L., Thornton, J. A., Brown, S. S., Nenes, A. and Weber, R. J.: Fine particle pH and the partitioning of nitric acid during winter in the northeastern United States, *J. Geophys. Res. D: Atmos.*, 121(17), 10,355–10,376, 2016.

Guo, H., Liu, J., Froyd, K. D., Roberts, J. M., Veres, P. R., Hayes, P. L., Jimenez, J. L., Nenes, A. and Weber, R. J.: Fine particle pH and gas–particle phase partitioning of inorganic species in Pasadena, California, during the 2010 CalNex campaign, *Atmos. Chem. Phys.*, 17(9), 5703–5719, 2017.

Guo, H., Campuzano-Jost, P., Nault, B. A., Day, D. A., Schroder, J. C., Dibb, J. E., Dollner, M., Weinzierl, B. and Jimenez, J. L.: The Importance of Size Ranges in Intercomparison of Aerosol Volume Concentration Measurements: A Case Study for Aerosol Mass Spectrometer in the ATom Mission, *Atmos. Meas. Tech. Discuss.*, In Review, doi:10.5194/amt-2020-224, 2020.

Hayes, D., Snetsinger, K., Ferry, G., Oberbeck, V. and Farlow, N.: Reactivity of stratospheric aerosols to small amounts of ammonia in the laboratory environment, *Geophys. Res. Lett.*, 7(11), 974–976, 1980.

Heim, E. W., Dibb, J., Scheuer, E., Jost, P. C., Nault, B. A., Jimenez, J. L., Peterson, D., Knote, C., Fenn, M., Hair, J., Beyersdorf, A. J., Corr, C. and Anderson, B. E.: Asian dust observed during KORUS-AQ facilitates the uptake and incorporation of soluble pollutants during transport to South Korea, *Atmos. Environ.*, 224, 117305, 2020.

Hering, S. and Cass, G.: The Magnitude of Bias in the Measurement of PM_{2.5} Arising from Volatilization of Particulate Nitrate from Teflon Filters, *J. Air Waste Manag. Assoc.*, 49(6), 725–733, 1999.

Klockow, D., Jablonski, B. and Nießner, R.: Possible artifacts in filter sampling of atmospheric sulphuric acid and acidic sulphates, *Atmos. Environ.*, 13(12), 1665–1676, 1979.

Koutrakis, P., Wolfson, J. M. and Spengler, J. D.: An improved method for measuring aerosol strong acidity: Results from a nine-month study in St Louis, Missouri and Kingston, Tennessee, *Atmos. Environ.*, 22(1), 157–162, 1988.

Liu, C.-N., Lin, S.-F., Awasthi, A., Tsai, C.-J., Wu, Y.-C. and Chen, C.-F.: Sampling and conditioning artifacts of PM_{2.5} in filter-based samplers, *Atmos. Environ.*, 85, 48–53, 2014.

Liu, C.-N., Lin, S.-F., Tsai, C.-J., Wu, Y.-C. and Chen, C.-F.: Theoretical model for the evaporation loss of PM_{2.5} during filter sampling, *Atmos. Environ.*, 109, 79–86, 2015.

Liu, X., Huey, L. G., Yokelson, R. J., Selimovic, V., Simpson, I. J., Müller, M., Jimenez, J. L., Campuzano-Jost, P., Beyersdorf, A. J., Blake, D. R., Butterfield, Z., Choi, Y., Crouse, J. D., Day, D. A., Diskin, G. S., Dubey, M. K., Fortner, E., Hanisco, T. F., Hu, W., King, L. E., Kleinman, L., Meinardi, S., Mikoviny, T., Onasch, T. B., Palm, B. B., Peischl, J., Pollack, I. B., Ryerson, T. B., Sachse, G. W., Sedlacek, A. J., Shilling, J. E., Springston, S., St. Clair, J. M., Tanner, D. J., Teng, A. P., Wennberg, P. O., Wisthaler, A. and Wolfe, G. M.: Airborne measurements of western U.S. wildfire emissions: Comparison with prescribed burning and air quality implications, *J. Geophys. Res. D: Atmos.*, 122(11), 6108–6129, 2017.

Liu, X., Deming, B., Pagonis, D., Day, D. A., Palm, B. B., Talukdar, R., Roberts, J. M., Veres, P. R., Krechmer, J. E., Thornton, J. A., de Gouw, J. A., Ziemann, P. J. and Jimenez, J. L.: Effects of

gas–wall interactions on measurements of semivolatile compounds and small polar molecules, , doi:10.5194/amt-12-3137-2019, 2019.

Müller, M., Mikoviny, T., Feil, S., Haidacher, S., Hanel, G., Hartungen, E., Jordan, A., Märk, L., Mutschlechner, P., Schottkowsky, R., Sulzer, P., Crawford, J. H. and Wisthaler, A.: A compact PTR-ToF-MS instrument for airborne measurements of volatile organic compounds at high spatiotemporal resolution, , doi:10.5194/amt-7-3763-2014, 2014.

Nault, B. A., Campuzano-Jost, P., Day, D. A., Schroder, J. C., Anderson, B., Beyersdorf, A. J., Blake, D. R., Brune, W. H., Choi, Y., Corr, C. A., de Gouw, J. A., Dibb, J., DiGangi, J. P., Diskin, G. S., Fried, A., Huey, L. G., Kim, M. J., Knote, C. J., Lamb, K. D., Lee, T., Park, T., Pusede, S. E., Scheuer, E., Thornhill, K. L., Woo, J.-H. and Jimenez, J. L.: Secondary Organic Aerosol Production from Local Emissions Dominates the Organic Aerosol Budget over Seoul, South Korea, during KORUS-AQ, *Atmos. Chem. Phys.*, 18, 17769–17800, 2018.

Nie, W., Wang, T., Gao, X., Pathak, R. K., Wang, X., Gao, R., Zhang, Q., Yang, L. and Wang, W.: Comparison among filter-based, impactor-based and continuous techniques for measuring atmospheric fine sulfate and nitrate, *Atmos. Environ.*, 44(35), 4396–4403, 2010.

Schauer, C., Niessner, R. and Pöschl, U.: Polycyclic aromatic hydrocarbons in urban air particulate matter: decadal and seasonal trends, chemical degradation, and sampling artifacts, *Environ. Sci. Technol.*, 37(13), 2861–2868, 2003.

Schroder, J. C., Campuzano-Jost, P., Day, D. A., Shah, V., Larson, K., Sommers, J. M., Sullivan, A. P., Campos, T., Reeves, J. M., Hills, A., Hornbrook, R. S., Blake, N. J., Scheuer, E., Guo, H., Fibiger, D. L., McDuffie, E. E., Hayes, P. L., Weber, R. J., Dibb, J. E., Apel, E. C., Jaeglé, L., Brown, S. S., Thornton, J. A. and Jimenez, J. L.: Sources and Secondary Production of Organic Aerosols in the Northeastern US during WINTER, *J. Geophys. Res. D: Atmos.*, doi:10.1029/2018JD028475, 2018.

Seinfeld., J. H. and Pandis, S. N.: *Atmospheric Chemistry and Physics: From Air Pollution to Climate Change*, Second., John Wiley & Sons, Inc., Hoboken, NJ USA., 2006.

Shingler, T., Crosbie, E., Ortega, A., Shiraiwa, M., Zuend, A., Beyersdorf, A., Ziemba, L., Anderson, B., Thornhill, L., Perring, A. E., Schwarz, J. P., Campuzano-Jost, P., Day, D. A., Jimenez, J. L., Hair, J. W., Mikoviny, T., Wisthaler, A. and Sorooshian, A.: Airborne characterization of subsaturated aerosol hygroscopicity and dry refractive index from the surface to 6.5 km during the SEAC⁴ RS campaign, *J. Geophys. Res. D: Atmos.*, 121(8), 4188–4210, 2016.

Sutton, M. A., Reis, S., Riddick, S. N., Dragosits, U., Nemitz, E., Theobald, M. R., Tang, Y. S., Braban, C. F., Vieno, M., Dore, A. J., Mitchell, R. F., Wanless, S., Daunt, F., Fowler, D., Blackall, T. D., Milford, C., Flechard, C. R., Loubet, B., Massad, R., Cellier, P., Personne, E., Coheur, P. F., Clarisse, L., Van Damme, M., Ngadi, Y., Clerbaux, C., Skjøth, C. A., Geels, C., Hertel, O., Wichink Kruit, R. J., Pinder, R. W., Bash, J. O., Walker, J. T., Simpson, D., Horváth, L., Misselbrook, T. H., Bleeker, A., Dentener, F. and de Vries, W.: Towards a climate-dependent

paradigm of ammonia emission and deposition, *Philos. Trans. R. Soc. Lond. B Biol. Sci.*, 368(1621), 20130166, 2013.

Talbot, R. W., Vijgen, A. S. and Harriss, R. C.: Soluble species in the Arctic summer troposphere: Acidic gases, aerosols, and precipitation, *J. Geophys. Res.*, 97(D15), 16531, 1992.

Wang, J., Hoffmann, A. A., Park, R. J., Jacob, D. J. and Martin, S. T.: Global distribution of solid and aqueous sulfate aerosols: Effect of the hysteresis of particle phase transitions, *J. Geophys. Res.*, 113(D11), 1770, 2008a.

Wang, J., Jacob, D. J. and Martin, S. T.: Sensitivity of sulfate direct climate forcing to the hysteresis of particle phase transitions, *J. Geophys. Res.*, 113(D11), 13791, 2008b.

Watson, J. G., Chow, J. C., Chen, L. W. A. and Frank, N. H.: Methods to assess carbonaceous aerosol sampling artifacts for IMPROVE and other long-term networks, *J. Air Waste Manag. Assoc.*, 59(8), 898–911, 2009.

Wilson, R. E.: Humidity Control by Means of Sulfuric Acid Solutions, with Critical Compilation of Vapor Pressure Data, *J. Ind. Eng. Chem.*, 13(4), 326–331, 1921.

1 **Interferences on Aerosol Acidity Quantification due to Gas-phase Ammonia Uptake onto**
2 **Acidic Sulfate Filter Samples**

3 Benjamin A. Nault^{1,2,*}, Pedro Campuzano-Jost^{1,2}, Douglas A. Day^{1,2}, Hongyu Guo^{1,2}, Duseong S.
4 Jo^{1,2,**}, Anne V. Handschy^{1,2}, Demetrios Pagonis^{1,2}, Jason C. Schroder^{1,2,***}, Melinda K.
5 Schueneman^{1,2}, Michael J. Cubison³, Jack E. Dibb⁴, Alma Hodzic⁵, Weiwei Hu⁶, Brett B. Palm⁷,
6 Jose L. Jimenez^{1,2}

7

8 1. Department of Chemistry, University of Colorado, Boulder, CO, USA

9 2. Cooperative Institute for Research in Environmental Sciences, University of Colorado,
10 Boulder, CO, USA

11 3. TOFWERK AG, Boulder, CO USA

12 4. Earth Systems Research Center, Institute for the Study of Earth, Oceans, and Space,
13 University of New Hampshire, Durham, NH, USA

14 5. Atmospheric Chemistry Observations and Modeling Laboratory, National Center for
15 Atmospheric Research, Boulder, CO, USA

16 6. State Key Laboratory at Organic Geochemistry, Guangzhou, Institute of Geochemistry,
17 Chinese Academy of Sciences, Guangzhou, China

18 7. Department of Atmospheric Sciences, University of Washington, Seattle, WA, USA

19 * Now at: Center for Aerosols and Cloud Chemistry, Aerodyne Research, Inc., Billerica, MA,
20 USA

21 ** Now at: Advanced Study Program, National Center for Atmospheric Research, Boulder, CO
22 USA

23 *** Now at: Colorado Department of Public Health and Environment, Denver, CO, USA

24

25 Correspondence: Jose L. Jimenez (jose.jimenez@colorado.edu)

26

27 *For submission to Atmospheric Measurement Techniques*

28 Abstract

29 Measurements of the mass concentration and chemical speciation of aerosols are important to
30 investigate their chemical and physical processing from near emission sources to the most
31 remote regions of the atmosphere. A common method to analyze aerosols is to collect them onto
32 filters and to analyze filters off-line; however, biases in some chemical components are possible
33 due to changes in the accumulated particles during the handling of the samples. Any biases
34 would impact the measured chemical composition, which in turn affects our understanding of
35 numerous physico-chemical processes and aerosol radiative properties. We show, using filters
36 collected onboard the NASA DC-8 and NSF C-130 during six different aircraft campaigns, a
37 consistent, substantial difference in ammonium mass concentration and ammonium-to-anion
38 ratios, when comparing the aerosols collected on filters versus the Aerodyne Aerosol Mass
39 Spectrometer (AMS). Another *on-line* measurement is consistent with the AMS in showing that
40 the aerosol has lower ammonium-to-anion ratios than obtained by the filters. Using a gas uptake
41 model with literature values for accommodation coefficients, we show that for ambient ammonia
42 mixing ratios greater than 10 ppbv, the time scale for ammonia reacting with acidic aerosol on
43 filter substrates is less than 30 s (typical filter handling time in the aircraft) for typical aerosol
44 volume distributions. Measurements of gas-phase ammonia inside the cabin of the DC-8 show
45 ammonia mixing ratios of 45 ± 20 ppbv, consistent with mixing ratios observed in other indoor
46 environments. This analysis enables guidelines for filter handling to reduce ammonia uptake.
47 Finally, a more meaningful limit-of-detection for SAGA filters collected during airborne
48 ~~campaigns that either do not have an ammonia scrubber and/or are handled in the presence of~~
49 ~~human emissions~~ is $\sim 0.2 \mu\text{g sm}^{-3}$ ammonium, which is substantially higher than the
50 limit-of-detection of the ion chromatography. A similar analysis should be conducted for filters
51 that collect inorganic aerosol and do not have ammonia scrubbers and/or are handled in the
52 presence of human ammonia emissions.

53 Introduction

54 Particulate matter (PM), or aerosol, impacts human health, ecosystem health, visibility,
55 climate, cloud formation and lifetime, and atmospheric chemistry (Meskhidze et al., 2003;
56 Abbatt et al., 2006; Seinfeld and Pandis, 2006; Jimenez et al., 2009; Myhre et al., 2013; Cohen et
57 al., 2017; Hodzic and Duvel, 2018; Heald and Kroll, 2020; Pye et al., 2020). Quantitative
58 measurements of the chemical composition and aerosol mass concentration are necessary to
59 understand these impacts and to constrain and improve chemical transport models (CTMs). The
60 inorganic portion of aerosol, which includes both volatile (e.g., nitrate, ammonium) and
61 non-volatile (e.g., calcium, sodium) species, controls many of these impacts through the
62 regulation of charge balance, aerosol pH, and aerosol liquid water concentration (Guo et al.,
63 2015, 2018; Hennigan et al., 2015; Nguyen et al., 2016; Pye et al., 2020). Further, the inorganic
64 portion of aerosol is an important fraction of the aerosol budget, both in polluted cities (e.g.,
65 (Jimenez et al., 2009; Song et al., 2018)), and remote regions (e.g., (Hodzic et al., 2020)), and the
66 chemistry controlling the inorganic portion of the aerosol is still not well known (e.g., (Liu et al.,
67 2020)).

68 There are numerous methods to quantify the inorganic aerosol composition and mass
69 concentration, including by mass spectrometry (DeCarlo et al., 2006; Canagaratna et al., 2007;
70 Pratt and Prather, 2010; Froyd et al., 2019), *on-line* ion chromatography (Talbot et al., 1997;
71 Weber et al., 2001; Nie et al., 2010), and collection onto filters to be extracted and measured
72 off-line by ion chromatography (Malm et al., 1994; Dibb et al., 2002, 2003; Coury and Dillner,
73 2009; Watson et al., 2009). Each method has different advantages and disadvantages (e.g., time
74 resolution, sample preparation, range of species identified, cost, and personnel needs). These

75 results, in turn, have been used to inform and improve the results of CTMs, influencing our
76 understanding in processes such as the direct radiative effect (Wang et al., 2008b), transport of
77 ammonia in deep convection (Ge et al., 2018), aerosol pH (Pye et al., 2020; Zakoura et al., 2020)
78 and subsequent chemistry, and precursor emissions (Henze et al., 2009; Heald et al., 2012;
79 Walker et al., 2012; Mezuman et al., 2016).

80 Filter measurements have been shown to be most prone to artifacts during sample
81 collection, handling, storage of the filter, or extraction of the aerosol from the filter prior to
82 analysis. These artifacts include evaporation of volatile compounds such as organics (Watson et
83 al., 2009; Chow et al., 2010; Cheng and He, 2015) and ammonium nitrate (Hering and Cass,
84 1999; Chow et al., 2005; Nie et al., 2010; Liu et al., 2014, 2015; Heim et al., 2020), as well as
85 chemical reactions of gas-phase species with the accumulated particles (e.g., (Schauer et al.,
86 2003; Dzepina et al., 2007)). Further, early research indicated potential artifacts from gas-phase
87 ammonia uptake onto acidic aerosol collected onto filters, leading to a positive bias for
88 particulate ammonium (Klockow et al., 1979; Hayes et al., 1980; Koutrakis et al., 1988). This led
89 to debates about whether aerosol in the lower stratosphere was sulfuric acid or ammonium
90 sulfate (Hayes et al., 1980); however, after improved filter handling practices and *on-line*
91 measurements (i.e., mass spectrometry), it has been generally well accepted that the sulfate in the
92 stratosphere is mainly sulfuric acid (Murphy et al., 2014).

93 This artifact may impact aerosol collected in remote locations (e.g., the lower
94 stratosphere, but also the free troposphere over the Pacific Ocean basin). Comparisons for a
95 major cation, ammonium, in a similar location (middle of the Pacific Ocean) have shown very
96 different results (Dibb et al., 2003; Paulot et al., 2015). This, in turn, affects the observed charge

97 balance of ~~anions~~ (sulfate and nitrate) with ammonium, which can indicate different
98 aerosol phase state (Colberg et al., 2003; Wang et al., 2008a) and aerosol pH (Pye et al., 2020),
99 leading to potentially important chemical and physical differences between the real state of the
100 particles and that concluded from the measurements. An example of the differences in observed
101 charge balance of ammonium to sulfate for different studies of the same remote Pacific Ocean
102 region is highlighted in Fig. 1. This difference leads to the inorganic portion of the aerosol
103 potentially being solid (filters) and hence good ice-nucleating particles (Abbatt et al., 2006),
104 versus it being liquid (*on-line* measurements), leading to important differences in the calculated
105 radiative balance. It should be noted that other measurements (both filter and *on-line*) in a similar
106 location from another study (bar at surface (Paulot et al., 2015)) are more in-line with the *on-line*
107 observations. A large decrease in the ambient ammonia mixing ratio is required to change from
108 ammonium sulfate-like aerosols to sulfuric acid-like aerosols between the years, contradictory to
109 the increasing trends of ammonia globally (Warner et al., 2016, 2017; Weber et al., 2016; Liu et
110 al., 2019; Tao and Murphy, 2019). Further, oceanic emissions of ammonia are not high enough to
111 lead to full charge neutralization of sulfate, since these emissions are approximately an order of
112 magnitude less than those of sulfate precursors (Faloona, 2009; Paulot et al., 2015). A debate
113 about the acidity and potential impact of ammonia-uptake artifacts on acidic filters for remote
114 locations has not occurred as it did for stratospheric observations.

115 Previous laboratory studies have suggested that exposure of acidic aerosol, both
116 suspended in air in a flow tube or on a filter, to gas-phase ammonia will lead to formation of
117 ammonium salts in short time (≤ 10 s) (Klockow et al., 1979; Huntzicker et al., 1980); however,
118 it has not been investigated if this time frame applies for acidic aerosol collected on filters

119 handled in a typical indoor environment. Though human emissions of ammonia are variable and
120 depend on various factors (e.g., temperature, clothing, etc.) (Li et al., 2020), the emissions of
121 ammonia, specifically from perspiration but also from breath, can lead to high, accumulated
122 mixing ratios of ammonia indoor (e.g., (Ampollini et al., 2019; Finewax et al., 2020)) and
123 references therein), depending on the ventilation rate. The mixing ratios of ammonia can be
124 factor of 2 to 2000 higher indoor versus outdoor. This higher mixing ratio of ammonia leads to
125 similarly high mixing ratios used in prior studies to lead to partially to fully neutralize sulfuric
126 acid (Klockow et al., 1979; Huntzicker et al., 1980; Daumer et al., 1992; Liggio et al., 2011).

127 Here, we investigate whether previously observed laboratory observations of ammonium
128 uptake to acidic particulate lead to the large differences in ammonium, both in mass
129 concentration and in ammonium-to-sulfate ratios or ammonium-to-anion ratios, between *in-situ*
130 measurements and *off-line* filter measurement during five NASA and one NSF airborne
131 campaigns that sampled air over remote continental and oceanic regions. An uptake model for
132 gas-phase ammonia interacting with acidic PM on a filter along with constraints from
133 observations of gas-phase ammonia in the cabin of the airplane are used to further probe the
134 reason behind the differences between the *in-situ* and *off-line* measurements of ammonium. The
135 results provide insight into how to interpret prior aircraft measurements and other filter based
136 measurements where the filters were handled in environments (i.e., indoors), where rapid uptake
137 of ammonia to acidic PM will occur.

138

139 **2. Methods**

140 **2.1 Aircraft Campaigns**

141 Five different NASA aircraft campaigns on-board the DC-8 research aircraft and one
142 NSF aircraft campaign on-board the C-130 research aircraft are used in this study. As described
143 below, though the campaigns were sampling ambient (outside) air in various locations around the
144 world, the filters were handled and exposed to both aircraft cabin air and indoor temporary
145 laboratory air, where between 20 and 40 people were operating instruments. The campaigns
146 include the Arctic Research of the Composition of the Troposphere from Aircraft and Satellites
147 (ARCTAS) -A (April 2008) and -B (June – July 2008) campaigns (Jacob et al., 2010), the
148 Studies of Emissions and Atmospheric Composition, Clouds, and Climate Coupling by Regional
149 Surveys (SEAC⁴RS, August – September 2013) campaign (Toon et al., 2016), the Wintertime
150 INvestigation of Transport, Emissions, and Reactivity (WINTER, February – March 2015)
151 (Schroder et al., 2018), and the Atmospheric Tomography (ATom) -1 (July – August 2016) and
152 -2 (January – February 2017) campaigns (Hodzic et al., 2020). ARCTAS-A was based in
153 Fairbanks, Alaska, Thule, Greenland, and Iqaluit, Nunavut, and sampled the Arctic Ocean and
154 Arctic regions of Alaska, Canada, and Greenland; while, ARCTAS-B was based in Cold Lake,
155 Alberta, Canada, and sampled the boreal Canadian forest, including wildfire smoke. SEAC⁴RS
156 was based in Houston, Texas, and sampled biomass burning from western forest fires and
157 agricultural burns along the Mississippi River and the Southern United States, isoprene
158 chemistry over Southern United States and midwestern deciduous forests, and deep convection
159 associated with isolated thunderstorms, the North American Monsoon, and tropical depressions.
160 Finally, ATom-1 and -2 sampled the remote atmosphere over the Arctic, Pacific, Southern, and
161 Atlantic Oceans during the Northern (Southern) Hemispheric summer (winter) and winter
162 (summer).

163 For ARCTAS-A, -B, and SEAC⁴RS, the general sampling scheme was regional, sampling
164 large regions at level flight tracks. ATom-1 and -2, being global in nature, only sampled at level
165 legs for short durations (5 – 15 min) at low (~300 m) and high (10 – 12 km) altitude, and did not
166 measure at level altitudes between the low and high altitude. Due to the sampling time of the
167 filters (see Sect. 2.2.2), the entirety of the ascent and descent time was needed for one filter
168 sample. Therefore, all data during the ascents and descents have not been considered in this
169 study to minimize any issues due to the mixing of aerosols of different compositions and
170 acidities.

171

172 **2.2 Aerosol Measurements**

173 **2.2.1 Aerosol Mass Spectrometer**

174 An Aerodyne High-Resolution Time-of-Flight Aerosol Mass Spectrometer, flown by the
175 University of Colorado-Boulder (CU for short), was flown during the five campaigns used here.
176 The general features of the AMS have been described in prior studies (DeCarlo et al., 2006;
177 Canagaratna et al., 2007), and the specifics of the CU AMS for each campaign has been
178 described elsewhere (Cubison et al., 2011; Liu et al., 2017; Nault et al., 2018; Schroder et al.,
179 2018; Guo et al., 2020; Hodzic et al., 2020). In brief, the AMS measured the mass concentration
180 of non-refractory species in PM₁ (PM with an aerodynamic diameter less than 1 μm, see Guo et
181 al. (2020) for details). Ambient air was sampled by drawing air through an NCAR
182 High-Performance Instrumental Platform for Environmental Modular Inlet (HIMIL; Stith et al.
183 (2009)) at a constant standard flow rate of 9 L min⁻¹ (T = 273.15 K and P = 1013 hPa). **The best**
184 **estimated upper size cut-off for the HIMIL inlet is ~1 μm diameter (geometric, David Rogers,**

185 pers. comm. 2011). This diameter is larger than the size cut-off than that of the AMS inlet
186 (~0.5-0.7 μm diameter, geometric, depending on the composition), with no losses in the tubing
187 between the HIMIL and AMS inlet expected (see Guo et al. (2020) for more details). Multiple
188 comparisons with instruments sampling from an isokinetic inlet PM_{10} inlet (Brock et al. 2019;
189 Guo et al. 2020) indicate that no significant sampling biases were incurred over the size range of
190 the AMS. No active drying of the sampling flow was used to minimize artifacts for semi-volatile
191 species, but the temperature differential between ambient and cabin typically ensured the relative
192 humidity (RH) inside the sampling line less than 40% (e.g., (Nault et al., 2018)). An exception to
193 this was during ATom-1 and -2, where the cabin temperature, along with the high RH in tropics,
194 led to higher RH in the sample lines in a few instances in the boundary layer, which was
195 accounted for in the final mass concentrations (Guo et al., 2020). To minimize any potential
196 losses of volatile aerosol components, the residence time between the inlet and AMS was less
197 than 1 s (Nault et al., 2018; Schroder et al., 2018; Guo et al., 2020). Prior studies (Guo et al.,
198 2016; Shingler et al., 2016) have shown minimal loss of semivolatile components for this
199 residence time.

200 The air sample was introduced into the AMS via an aerodynamic focusing lens (Zhang et
201 al., 2002, 2004), which was operated at 2.00 hPa (1.50 Torr), via a pressure-controlled inlet,
202 which was operated at various pressures (94-325 Torr) (Bahreini et al., 2008), depending on the
203 ceiling of the campaign and lens transmission calibrations (Hu et al., 2017b; Nault et al., 2018).
204 The aerosol, once focused, was introduced into a detection chamber after three differential
205 pumping stages. The aerosol impacted on an inverted cone porous tungsten “standard” vaporizer
206 under high vacuum, which was held at $\sim 600^\circ\text{C}$. Upon impaction, the non-refractory portion of

207 the aerosol (organic, ammonium, nitrate, sulfate, and chloride) were flash-vaporized, and the
208 vapors were ionized by 70 eV electron ionization. The ions were then extracted and analyzed
209 with a H-TOF time-of-flight mass spectrometer (Tofwerk AG). The AMS was operated in the
210 “V-mode” ion path (DeCarlo et al., 2006), with spectral resolution ($m/\Delta m$) of 2500 at m/z 44 and
211 2800 at m/z 184. The collection efficiency (CE) for AMS was estimated with the
212 parameterization of Middlebrook et al. (2012), which has been shown to perform well for
213 ambient aerosols (Hu et al., 2017a, 2020). The AMS nominally samples aerosol with vacuum
214 aerodynamic diameter between 40 nm and 1400 nm, which was calibrated for in SEAC⁴RS,
215 ATom-1, and -2 (Liu et al., 2017; Guo et al., 2020). Mass and/or volumen closure has been
216 investigated between the AMS and other measurements for all campaigns discussed here
217 (Cubison et al., 2011; Aknan, 2015; Liu et al., 2017; Nault et al., 2018; Schroder et al., 2018;
218 Guo et al., 2020). The closure was complete for the size range of the AMS and did not show any
219 dependence with altitude (Guo et al., 2020). Software packages Squirrel and PIKA under Igor
220 Pro 7 (WaveMetrics, Lake Oswego, OR) (DeCarlo et al., 2006; Sueper, 2018) were used to
221 analyze all AMS data.

222 A cryogenic pump, to reduce background of ammonium and organics (Nault et al., 2018;
223 Schroder et al., 2018), was flown on the AMS for SEAC⁴RS, ATom-1, and -2; but not for
224 ARCTAS-A and -B. The cryogenic pump lowers the temperature of a copper cylinder
225 surrounding the vaporizer to ~90 K. This freezes out the background gases and ensures low
226 detection limits from the beginning of the flight, which is critical since aircraft instruments can
227 typically not be pumped continuously and hence suffer from high backgrounds at switch-on. The

228 2σ accuracy for the AMS for inorganic aerosol is estimated to be 35% (Bahreini et al., 2009; Guo
229 et al., 2020).

230

231 **2.2.2 Aerosol Filters**

232 Fast collection of aerosol particles onto filters during airborne sampling, via the
233 University of New Hampshire Soluble Acidic Gases and Aerosol (SAGA) technique, has been
234 described elsewhere (Dibb et al., 2002, 2003), and was flown during the five campaigns
235 investigated here. Briefly, air is sampled into the airplane via a curved leading edge nozzle (Dibb
236 et al., 2002). The inlet is operated isokinetically during flight, and typically has a 50% collection
237 efficiency for aerosol with an aerodynamic diameter of $4.1\ \mu\text{m}$ (Dibb et al., 2002; McNaughton
238 et al., 2007), with some altitude dependence (Guo et al., 2020). The lower size cut-offs for
239 SAGA and AMS are similar (Guo et al., 2020). As discussed by Guo et al. (2020; their Fig. 8)
240 the difference in mass sampled at the smaller sizes between SAGA and AMS is generally
241 negligible at all altitudes.

242 - Aerosol was collected onto Millipore Fluoropore Teflon filters (90 mm diameter with 1
243 μm pore size). Collection time was dependent on altitude and estimated mass concentration, but
244 generally 2 to 3 sm^3 (where sm^3 is standard m^{-3} at temperature = 273 K and pressure = 1013 hPa)
245 volume of air is collected to ensure detectable masses of species (Dibb et al., 2002). The aerosol
246 inlet flow is close to 400 slpm in the marine boundary layer and approximately 150 slpm at
247 maximum altitude. Further, 2 blank filters are collected each flight. The filters were contained in
248 a Delrin holder during collection. After collection, the filters were transferred to a particle free
249 polyethylene “clean room” bag, which was filled with zero air, sealed, and stored over dry ice.

250 No acid scrubbers were inserted into the bags to prevent any artifact from offgassing of
251 ammonia. The samples from the filters were then extracted during non-flight days with 20 mL
252 ultrapure water and preserved with 100 μ L chloroform (see Sect. S2). The preserved samples
253 were sent to the University of New Hampshire, to be analyzed by ion chromatography. The
254 estimated limit of detection for both sulfate and ammonium is $0.01 \mu\text{g sm}^{-3}$ for all missions
255 evaluated here (Dibb et al., 1999).

256

257 2.2.3 Other Aerosol Measurements

258 The NOAA Particle Analysis by Laser Mass Spectrometer (herein PALMS) was flown
259 during ATom-1 and -2. Details of the PALMS instrument configured for ATom-1 and -2 are
260 described in Froyd et al. (2019). Briefly, PALMS measures the chemical composition of single
261 aerosol particles via laser-ablation/ionization (Murphy and Thomson, 1995; Thomson et al.,
262 2000), where the ions are extracted and detected by a time of flight mass spectrometer. The
263 instrument measures particles between 100 nm and $4.8 \mu\text{m}$ (geometric diameter) (Froyd et al.,
264 2019). The measurement of PALMS used in this study is the “sulfate acidity indicator” (Froyd et
265 al., 2009). These authors reported that in the negative ion mode, there is a prominent peak at m/z
266 97, corresponding to HSO_4^- , and another peak at m/z 195, corresponding to the cluster
267 $\text{HSO}_4^-(\text{H}_2\text{SO}_4)$. The first peak was independent of acidity; whereas, the second peak was
268 dependent on acidity. Froyd et al. (2009) calibrated the PALMS ratio of
269 $\text{HSO}_4^-(\text{H}_2\text{SO}_4)/(\text{HSO}_4^-+\text{HSO}_4^-(\text{H}_2\text{SO}_4))$ to Particle-into-Liquid Sampler (PILS) measurements to
270 achieve an estimate of ammonium balance.

271 Besides the chemical composition, the particle number and volume distributions are used
272 here. For SEAC⁴RS, the measurements have been described elsewhere (e.g., (Liu et al., 2016)).
273 The laser aerosol spectrometer (from TSI), which measured aerosol from geometric diameter 100
274 nm to 6.3 μm , is used here for volume distribution. For the ATom missions, the measurements
275 have been described elsewhere (Kupc et al., 2018; Williamson et al., 2018; Brock et al., 2019).
276 Briefly, the dry particle size distribution, from geometric diameter of 2.7 nm to 4.8 μm , were
277 measured by a series of optical particle spectrometers, including the Nucleation Model Aerosol
278 Size Spectrometer (3 nm to 60 nm, custom built (Williamson et al., 2018)), an Ultra-High
279 Sensitivity Aerosol Spectrometer (60 nm to 1 μm) from Droplet Measurement Technologies
280 (Kupc et al., 2018)), and Laser Aerosol Spectrometer (120 nm to 4.8 μm) from TSI). These
281 measurements have been split in nucleation mode (3 to 12 nm), Aitken mode (12 to 60 nm),
282 accumulation mode (60 to 500 nm) and coarse mode (500 nm to 4.8 μm).

283

284 **2.3 Gas-Phase and Other Measurements**

285 **2.3.1 Ammonia Measurements**

286 Gas-phase ammonia was measured inside the cabin of the NASA DC-8 during the
287 FIREX-AQ campaign (Warneke et al., 2018), a subsequent DC-8 campaign which shared many
288 instrument installations and a similar level of aircraft personnel with the campaigns analyzed
289 here. The location of the instrument and where it sampled cabin ammonia (in relation to where
290 the SAGA filters are located) is shown in Fig. S1. Ammonia was measured by a Picarro G2103
291 Gas Concentration Analyzer (von Bobruzki et al., 2010; Sun et al., 2015; Kamp et al., 2019).
292 The instrument is a continuous, cavity ring-down spectrometer. Cabin air is brought into a cavity

293 at low pressure (18.7 kPa, 140 Torr), where laser light is pulsed into the cavity. The light is
294 reflected by mirrors in the cavity, providing an effective path length of kilometers. A portion of
295 the light penetrates the mirrors, reaching the detectors, where the intensity of the light is
296 measured to determine the mixing ratio of ammonia from the time decay of the light intensity via
297 Beer-Lambert Law. The instrument measures the absorption of infrared light from 6548.5 to
298 6549.2 cm^{-1} (Martin et al., 2016). Absorption of gas-phase water is also measured and corrected
299 for. This water vapor measurement is also used to calculate RH inside the cabin of the DC-8
300 (Filges et al., 2018). Data was logged at 1 Hz.

301

302 **2.3.2 Carbon Dioxide and Temperature Measurements**

303 Carbon dioxide inside the cabin of the NASA DC-8 during FIREX-AQ was measured by
304 a HOBO MX1102 Carbon Dioxide Data Logger (HOBO by Onset). It is a self-calibrating carbon
305 dioxide sensor with a range of 0 to 5,000 ppm carbon dioxide and an accuracy of ± 50 ppm. A
306 non-dispersive infrared sensor is used to measure carbon dioxide. Data was acquired once every
307 10 s to once every 2 min. Besides carbon dioxide, RH and temperature are also recorded by the
308 instrument. Prior to each flight, the instrument was turned on and measured ambient carbon
309 dioxide, outside the cabin of the DC-8, to ensure the accuracy of the instrument compared to
310 ambient carbon dioxide measurements.

311 Ambient carbon dioxide during FIREX-AQ was measured by an updated version of the
312 instrument known as Atmospheric Vertical Observations of CO_2 in the Earth's Troposphere
313 (AVOCET) (Vay et al., 2003, 2011). The updated instrument used a modified LI-COR model
314 7000 non-dispersive infrared spectrometer and measured carbon dioxide at 5 Hz.

315 Temperature in the cabin was measured by a thermocouple (SEAC⁴RS) or thermistor
316 (ATom-1 and 2) located in the AMS rack or a Vaisala probe located at the front of the airplane
317 (ARCTAS-A, -B, and SEAC⁴RS).

318

319 **2.4 Theoretical Ammonia Flux Model**

320 To investigate the possibility that the ammonia mixing ratio in the cabin of the DC-8 is
321 high enough to be taken up by acidic PM on a filter during the short time the filter is exposed to
322 cabin air prior to final storage, a theoretical uptake model was constructed to estimate the time
323 scale for ammonia to interact with all the acidic particles (Seinfeld and Pandis, 2006). The
324 equations used for the model can be found in the Supplemental Information (Sect. S32). The
325 model was initialized with a range of ammonia mixing ratios (1 to 200 ppb) and a range of PM
326 diameters (10 to 1000 nm). The calculations were conducted at 298 K, which is within ± 10 K of
327 typical temperatures inside the cabin of the NASA DC-8 during the five campaigns (Fig. S2). An
328 accommodation coefficient of 1 for ammonia onto acidic PM was assumed (Hanson and
329 Kosciuch, 2003), with a density of 1.8 g cm^{-3} for sulfuric acid (Rumble, 2019). For the mass
330 transfer calculations, the transition regime (between the free molecular and continuum regimes)
331 equations were used, using the Fuchs and Sutugin parameterization (Fuchs and Sutugin, 1971).
332 The model was used to estimate the ammonia molecular flux to acidic PM on the filter (Eq. S3).
333 Finally, the molecular flux was used to estimate the time it would take all the particles to be
334 partially neutralized by ammonia in the cabin (Eq. S4), though this may be a lower limit
335 (Robbins and Cadle, 1958; Daumer et al., 1992).

336

337 3. Results and Discussion

338 3.1 Comparison of On-Line and Off-Line Ion Balances across the Tropospheric Column

339 SAGA and AMS co-sampled aerosols during multiple aircraft campaigns. Nitrate quickly
340 evaporates from aerosols as the aerosols are transported away from source regions and is
341 typically small in the global troposphere (DeCarlo et al., 2008; Hennigan et al., 2008; Hodzic et
342 al., 2020). Thus, in Fig. 2 the mass concentrations for the two most important submicron
343 contributors to ammonium balance, ammonium and sulfate, are compared from the aircraft
344 campaigns. The campaigns generally sampled remote air, either continental or oceanic, except
345 for biomass burning sampled during ARCTAS-B and SEAC⁴RS and downwind of urban areas
346 during WINTER. The measurements, for mass concentrations greater than $0.1 \mu\text{g sm}^{-3}$, are
347 generally within the combined uncertainties of the two instruments. Sulfate generally remains on
348 the one-to-one line, even at low mass concentrations. However, ammonium shows a large
349 divergence between the two measurements for mass concentrations less than $0.1 \mu\text{g sm}^{-3}$ during
350 all six aircraft campaigns. As shown in Fig. 2, the divergence in ammonium occurs well above
351 the limit-of-detection for both instruments, namely $\sim 4 \text{ ng sm}^{-3}$ for AMS for a 5-minute average
352 (DeCarlo et al., 2006; Guo et al., 2020) and 10 ng sm^{-3} for SAGA (Dibb et al., 1999), for both
353 ammonium and sulfate.

354 This divergence in ammonium mass concentration is thus reflected in the ammonium
355 balance, defined as the ratio of ammonium to sulfate plus nitrate, in moles (Fig. 3). For all
356 campaigns, the two measurements show differences in ammonium balance, especially at higher
357 altitudes, where the aerosols is distant from ammonia emissions (Dentener and Crutzen, 1994;
358 Paulot et al., 2015), but sulfate production can continue due to vertical transport of precursors

359 such as SO₂. On average, the SAGA measurements indicate ammonium balance rarely below 0.5
360 throughout the troposphere; whereas, the AMS measurements indicate that ammonium balance
361 generally drops to below 0.2 for pressures less than 400 hPa. Fig. 2 and Fig. 3 indicate either
362 differences in the ammonium balance due to differences in aerosols population sampled, as
363 SAGA measures larger aerosols diameters than AMS (Guo et al., 2020), or potential artifacts
364 with one of the measurements.

365 Both the AMS and the filters sample most of the submicron aerosols (see Guo et al.
366 (2020) for details), but the filters also sample supermicron particles that the AMS does not.
367 Therefore it is possible in principle that the difference could be due to ammonium present in
368 supermicron particles. As discussed in Guo et al. (2020), nearly 100% of the measured volume
369 occurs for aerosols < 1 μm above the marine boundary layer, where the largest difference in
370 ammonium balance between the filters and AMS occurs (Fig. 3). Further, ammonium has been
371 observed to be a small fraction of the supermicron mass (Kline et al., 2004; Cozic et al., 2008;
372 Pratt and Prather, 2010), except for instances of continental fog (Yao and Zhang, 2012) and
373 Asian dust events (Heim et al., 2020). An upper estimate of supermicron ammonium can be
374 calculated using results from prior studies (Kline et al., 2004; Cozic et al., 2008). In these prior
375 studies, ~90% of the ammonium was submicron. With the average ammonium observed during
376 ATom-1 and -2 (~10 to 50 ng sm⁻³) (Hodzic et al., 2020), that would suggest an upper limit of ~1
377 to 5 ng sm⁻³ ammonium in the supermicron aerosols. This upper estimate does not explain the
378 differences between AMS and filters during ATom-1 and -2 (Fig. S3), as the percent difference
379 increases with decreasing estimated supermicron ammonium volume. As the largest differences
380 between the AMS and filters occur well above the boundary layer (Fig. 3), away from

381 continental ammonia sources (Dentener and Crutzen, 1994) and Asian dust events, we conclude
382 that the sampling of supermicron aerosols by filters is not leading to the observed differences in
383 ammonium.

384 The only useful comparison, other than SAGA versus AMS, is with PALMS during
385 ATom. Prior studies by PALMS have shown aerosols observed for pressure < 400 hPa to be
386 acidic, depending on potential recent influence of boundary layer air via convection (Froyd et al.,
387 2009; Liao et al., 2015), similar to observations by other single particle mass spectrometers (Pratt
388 and Prather, 2010). Though not reaching similarly low $\text{NH}_4/(2\times\text{SO}_4)$ values as the AMS, the
389 PALMS acidity marker shows much lower values than were determined by the aerosols collected
390 on the filters (Fig. S4). Different reasons for PALMS not achieving as low values as AMS may
391 include differences in aerosols sizes sampled by PALMS versus AMS (Guo et al., 2020), and the
392 sensitivity of the acidity marker to laser power (Liao et al., 2015). Thus, two different *on-line*
393 measurements indicate that the ammonium balance is lower than the aerosols collected on filters,
394 suggesting potentially more acidic aerosols.

395 Differences in ammonium balance between AMS and SAGA are detectable for sulfate
396 mass concentrations $\leq 1 \mu\text{g sm}^{-3}$ (Fig. 4) for all six aircraft campaigns. As the sulfate mass
397 concentration decreases, the relative differences in ammonium, and thus ammonium balance,
398 increase. The large majority of the troposphere contains sulfate mass concentrations in which the
399 differences in ammonium are observed, highlighting the importance of this problem (Fig. 4a).
400 Thus, except for more polluted conditions ($> 1 \mu\text{g sm}^{-3}$ sulfate), which mainly occurs in
401 continental (Jimenez et al., 2009; Kim et al., 2015; Malm et al., 2017) and urban regions
402 (Jimenez et al., 2009; Hu et al., 2016; Kim et al., 2018; Nault et al., 2018), this bias between

403 filters and *on-line* measurements is critically important, especially since airborne measurements
404 are often the only meaningful observational constraints for remote regions. Thus, this analysis
405 ~~suggests~~suggest that for SAGA filters ~~handled in indoor environments with large ammonia~~
406 ~~mixing ratios (see below)~~, a more meaningful ammonium limit-of-detection would be equivalent
407 to $1 \mu\text{g sm}^{-3}$ sulfate, which would be $\sim 0.2 \mu\text{g sm}^{-3}$ ammonium. This also provides the framework
408 to define limit-of-detection for other filter-based measurements not associated with ion
409 chromatography.

410

411 3.2 Ammonia Levels on the NASA DC-8 Cabins

412 Prior studies have suggested that various sources of ammonia could impact acidic filter
413 measurements (Klockow et al., 1979; Hayes et al., 1980; Koutrakis et al., 1988). Some of these
414 studies found that the materials of the containers where the filters are stored, unless thoroughly
415 cleaned and not stored around humans, are a source of ammonia gas that reacts with the sulfuric
416 acid on the filters to become ammonium, leading to ammonium bisulfate or ammonium sulfate
417 (Hayes et al., 1980). Further, handling of acidic filters in rooms with people or acidic aerosol in
418 the presence of human breath can also lead to near to complete neutralization of acidic aerosol
419 (Larson et al., 1977; Hayes et al., 1980; Clark et al., 1995). Finally, various studies have
420 suggested that the SAGA filters specifically may be impacted by various ammonia sources prior
421 to sampling with the ion chromatography (Dibb et al., 1999, 2000; Fisher et al., 2011).

422 During SAGA sampling, the filters with collected aerosol are moved from the sample
423 collector to a ~~Teflon~~polyethylene bag that is filled with clean air. During this step, the filter is
424 exposed to the cabin air of the DC-8 for ~ 10 s. As humans are a source of ammonia (Larson et

425 al., 1977; Clark et al., 1995; Sutton et al., 2000; Finewax et al., 2020; Li et al., 2020), this source
426 sustains significant ammonia concentrations in indoor environments, which could potentially
427 bias the filter measurements. *On-line* measurements would not be subject to this effect since the
428 sampled air is not exposed to cabin air before measurement. While inlet lines for *on-line*
429 instruments could in theory lead to some memory effects, there is no evidence of such effects in
430 the data (e.g., the response going from a large, neutralized plume into the acidic FT is nearly
431 instantaneous (Schroder et al., 2018)).

432 During a recent 2019 NASA DC-8 aircraft campaign, FIREX-AQ, ammonia was
433 measured on-board the DC-8 during several research flights. An example time series of cabin
434 ammonia, temperature, and RH is shown in Fig. 5. Prior to take-off, as scientists were slowly
435 boarding the airplane, the ammonia mixing ratio was low (< 20 ppbv) and similar to ambient
436 levels of ammonia outside the aircraft. As scientists started boarding before take-off, the
437 ammonia mixing ratio increased. Upon doors closing, the mixing ratio leveled off at ~ 40 ppbv.
438 After take-off, the mixing ratio remained ~ 40 ppbv, though there were changes related to
439 changes in cabin temperature and humidity, which would affect emission rates and also
440 adsorption of ammonia onto cabin surfaces (Sutton et al., 2000; Finewax et al., 2020; Li et al.,
441 2020) and movement of scientists throughout the cabin, which would affect emission rates and
442 their location.

443 The average ($\pm 1\sigma$ spread of the observations) and median ammonia in the cabin of the
444 DC-8 during FIREX-AQ was 45.4 ± 19.9 and 41.9 ppbv (Fig. 6). There was a large positive tail in
445 ammonia mixing ratio, related to high temperatures (Fig. S5), which causes the scientists to
446 perspire more and release more ammonia (Sutton et al., 2000; Finewax et al., 2020; Li et al.,

447 2020). Compared to outdoor ammonia mixing ratios, ranging from urban to remote locations, the
448 ammonia in the cabin of the DC-8 is higher by a factor of 2 to 2000 (Fig. 6). On the other hand,
449 the ammonia measured in the cabin of the DC-8 is similar but towards the lower end of the
450 mixing ratios measured during various indoor studies (Table S1 for compilation of references).

451 The ammonia mixing ratios observed in the cabin were verified by investigating the cabin
452 air exchange rates (see SI Sect. S3). Using carbon dioxide measurements, the exchange rate in
453 the cabin was calculated to be 9.9 hr^{-1} (Fig. S6), which is similar to literature values for the cabin
454 exchange rate of other passenger airliners (Hunt and Space, 1994; Hocking, 1998; Brundrett,
455 2001; National Research Council, 2002). This value is a factor of 2 to 5 higher than typical
456 exchange rates for commercial buildings (Hunt and Space, 1994; Pagonis et al., 2019), which
457 would suggest lower mixing ratios than observed in other indoor environments. Using this
458 exchange rate, and the literature total ammonia emission rates from humans ($1940 \mu\text{g hr}^{-1}$
459 person^{-1} (Sutton et al., 2000)) and the average of ambient ammonia mixing ratios as an outdoor
460 background onto which the human emissions in the cabin are added ($\sim 4.4 \text{ ppbv}$, Fig. 6), the
461 ammonia mixing ratio in the cabin of the DC-8 was estimated to be 43.4 ppbv , which is within
462 the uncertainty of the average ammonia ($45.4 \pm 19.9 \text{ ppbv}$) inside the cabin of the DC-8. Thus, the
463 observed ammonia mixing ratios in the cabin of the DC-8 are consistent with the cabin air
464 exchange rates and literature human ammonia emissions. These mixing ratios are approximately
465 a factor of nine higher than in a typical laboratory environment (Fig. S7), as there are fewer
466 people (1 to 4 versus 20 to 40), making the cabin of the DC-8 an extreme laboratory environment
467 for handling acidic filters. As shown in Fig. 6, ammonia mixing ratios in indoor environments
468 are high enough to change the thermodynamics of inorganic aerosol, leading to higher

469 ammonium balances (Weber et al., 2016). Thus, similar to the conclusions of other studies, the
470 cabin of the DC-8 is an important source of ammonia that could lead to biases with acidic
471 aerosols collected on filters.

472 During FIREX-AQ, the DC-8 frequently sampled air impacted by biomass burning,
473 which is an important source of ammonia (Sutton et al., 2013) and could potentially increase the
474 background ammonia being brought into and mixing with the cabin air being sampled by the
475 Picarro. Splitting the cabin ammonia ratios between sampling air impacted by biomass burning
476 versus nominally background air, the normalized PDF did not shift to higher ammonia mixing
477 ratios (Fig. S7). Further, the averages of the observed cabin ammonia was statistically similar, at
478 the 95% confidence interval, between the DC-8 sampling biomass burning and nominally
479 background air (48.1 ± 13.4 versus 44.1 ± 14.4 ppbv for biomass burning and background air,
480 respectively). Finally, the majority of the time the cabin air was sampled by the Picarro for cabin
481 ammonia, the DC-8 was sampling agricultural fires in Southeast US, which are shorter in
482 duration (seconds) versus the large wildfires in Western US (minutes to hours). This is reflected
483 in the low average ambient value for ammonia, as measured by a proton transfer reaction mass
484 spectrometer (Müller et al., 2014), when the DC-8 was sampling biomass burning-influenced air
485 observed during this time (~ 10 ppbv) and very low average value for non-biomass
486 burning-influenced air (~ 0.8 ppbv) (Fig. S7). Thus, ammonia from biomass burning would at
487 most be a small impact on the ammonia measured in the cabin of the DC-8, further indicating the
488 ammonia in the cabin was mainly from human emissions.

489

490 3.3 Can Uptake of Cabin Ammonia Explain the Higher Ammonium Concentrations on 491 Filters?

492 As shown in Fig. 6, the cabin of the DC-8 is an important source of ammonia from the
493 breathing and perspiring of scientists. Prior studies (Klockow et al., 1979; Huntzicker et al.,
494 1980; Daumer et al., 1992; Liggio et al., 2011) have shown in laboratory settings that 10 s is fast
495 enough to partially to fully neutralize sulfuric acid. Thus, here we investigate whether the time of
496 the filter handling of 10 s will lead to partial to full neutralization of sulfuric acid from cabin
497 ammonia, or whether this time is fast enough to limit exposure of the acidic filter to cabin
498 ammonia. Huntzicker et al. (1980) showed that for typical aerosol modal distributions (Fig. 7)
499 and cabin RH (Fig. S9), an initial pure sulfuric acid aerosol, suspended in a flow reactor, reaches
500 equal molar amounts of ammonium and sulfate (i.e., ammonium bisulfate) when exposed to 70
501 ppb ammonia in 10 s. This indicates the plausibility that acidic aerosol filters, which typically
502 have lower sulfate mass concentrations than Huntzicker et al. (1980) ($\sim 2 \mu\text{g}$ versus $\sim 55 \mu\text{g}$
503 sulfate equivalent on filters), would interact with cabin ammonia to form at least ammonium
504 bisulfate. Further, other studies found that in less than 10 s, sulfuric acid aerosol, suspended in a
505 flow reactor, at $\text{RH} \leq 45\%$, will completely react with gas-phase ammonia to form ammonium
506 sulfate (Robbins and Cadle, 1958; Daumer et al., 1992). The latter study used ammonia mixing
507 ratios similar to the amount observed in the cabin of the DC-8 ($\sim 30 \text{ ppbv}$); whereas, the former
508 study used excess ammonia ($\sim 9 \text{ ppmv}$). Some studies have suggested that the bags used to store
509 the filters may be a source of ammonia (e.g., [\(Hayes et al. 1980\)](#)); however, calculations indicate
510 the bags would be a small source of ammonia (see Sect. S4).

511 First, the time of diffusion of ammonia gas from the surface to the interior of the filter
512 was investigated, as there is a potential for the PM to be embedded deep into the filter. Eq. 1
513 (Seinfeld and Pandis, 2006):

$$514 \quad \tau_{diffusion} = \frac{d_t^2}{8D_g} \quad \text{Eq. 1}$$

515 where d_t^2 is the depth of the Teflon (~ 0.015 cm) and D_g is the diffusion coefficient of ammonia in
516 air (0.228 cm² s⁻¹) (Spiller, 1989). Therefore, the estimated timescale for ammonia to diffuse
517 through the depth of the Teflon filter is $\sim 1 \times 10^{-4}$ s, meaning that the surface of PM will always be
518 in contact with cabin-level mixing ratios of ammonia. Even though the filters have a porous
519 membrane, for molecular diffusion, the membrane only increases the pathway that the ammonia
520 molecules have to travel slightly; thus, not changing the estimated time. Second, as the particles
521 are liquid (Wilson 1921), the diffusion will be similar as through water. A typical value for
522 diffusivity in water is $\sim 1 \times 10^{-5}$ cm² s⁻¹ (Seinfeld. and Pandis 2006). For the size ranges observed
523 (Fig. 7, ~ 40 - 700 nm), this corresponds to a timescale of 1.6×10^{-7} to 5.0×10^{-5} s. Thus, the
524 diffusion through the filter and through the PM is nearly instantaneous for ammonia.

525 A theoretical uptake model for ammonia to acidic PM on filters was run for a range of
526 ammonia mixing ratios and PM diameters (Fig. 7). As shown in Fig. 7, only at the lowest
527 ammonia mixing ratios (< 10 ppbv), the flux of ammonia to acidic PM is slower (> 20 s) than the
528 typical filter handling time (~ 10 s) for typical aerosol diameters in the remote atmosphere. For
529 the conditions of the DC-8, similar to other indoor environments (> 20 ppbv ammonia, Fig. 6),
530 and ambient aerosol diameters in the accumulation mode that contains most ambient sulfate
531 (Fig. 7), the amount of time needed for cabin ammonia to interact with acidic PM on filters to
532 form ammonium bisulfate is ≤ 10 s, similar to the results of Huntzicker et al. (1980). Also,

533 studies show that the kinetic limitation to form ammonium sulfate ((NH₄)₂SO₄) versus
534 ammonium bisulfate (NH₄HSO₄) is relatively low and can occur within the 10 s time frame
535 (Robbins and Cadle, 1958; Daumer et al., 1992). A laboratory setting with ~5 ppbv NH₃ would
536 result in the filters needing to be exposed to laboratory air for at least 40 s to form ammonium
537 bisulfate (Fig. S8) versus the 3 to 10 s for conditions in the cabin of the DC-8 (Fig. 7), further
538 exemplifying the challenging conditions of the DC-8 cabin for filter sampling.

539 The prior analysis made the assumption that the PM maintained a spherical shape upon
540 impacting the Teflon filter. More viscous (i.e., solid) PM is more likely to maintain a spherical
541 shape on filters whereas less viscous (i.e., liquid) PM will spread and become more similar to
542 cylindrical shape (e.g., (Slade et al., 2019)). As more acidic aerosol is more likely to be liquid
543 (e.g., (Murray and Bertram, 2008)), an exploration of cylindrical shape was conducted.
544 Depending on the assumed height of the cylindrical shape, the timescale for a molecule of
545 ammonia to interact with a molecule of sulfuric acid decreases from ~5 s (for maximum
546 ammonia and aerosol volume) to ~4 s (assuming height of cylinder equals radius of sphere) to
547 less than 1 s as height decreases from 25 nm or less. The aerosol deforming and spreading upon
548 impacting the filters increases the particle surface area, and decreases the amount of time for
549 cabin ammonia to interact with the acidic PM. Thus, less viscous aerosol has more rapid
550 uptake and interaction with ammonia due to the higher surface area.

551 A potential limitation to the model is the accommodation coefficient of ammonia to
552 acidic PM, as there are conflicting reports on its value (Hanson and Kosciuch, 2004; Worsnop et
553 al., 2004). However, as shown in Worsnop et al. (2004), once the sulfuric acid weight percentage
554 is 50% or greater, the different studies converge to an accommodation coefficient of ~1. Various

555 studies indicate that the RH in the cabin of jet airplanes is low due to how air is brought into the
556 airplane, typically < 20% (Hunt and Space, 1994; Brundrett, 2001; National Research Council,
557 2002). Even though the ambient RH may be higher than the RH in the cabin of the DC-8, the
558 water equilibration is rapid (< 1 s) for the temperature of the cabin of the DC-8, even for very
559 viscous aerosol (Shiraiwa et al., 2011; Price et al., 2015; Ma et al., 2019), meaning the PM on the
560 filter would rapidly reach equilibrium with the cabin RH upon exposure. This would result in a \geq
561 60% sulfuric acid weight percentage (Wilson, 1921) for the typical RH ranges in the cabin of
562 typical airlines. However, various measurements in the DC-8 cabin indicate the RH is \leq 40%
563 (Fig. S9), leading to sulfuric acid weight percentage of 50% or greater (Wilson, 1921).
564 Therefore, the accommodation coefficient of ~ 1 is well-constrained by the literature. Thus, the
565 handling of the filters between the sampling inlet to the polyethylene Teflon bag exposes the
566 acidic PM to enough gas-phase ammonia towards forming ammonium bisulfate or ammonium
567 sulfate, biasing high ammonium from the filters. This explains the differences seen in Fig. 1 –
568 Fig. 4.

569 Another potential limitation is that the PM on the filters could form a layer, as multiple
570 particles pile up on top of each other, slowing the diffusion of ammonia to be taken up by acidic
571 PM. The filters have a one-sided surface area of $6.4 \times 10^{-3} \text{ m}^2$, while an individual particle at the
572 mode of the volume distribution (Fig. 7) has a projected surface area of $\sim 7.1 \times 10^{-14} \text{ m}^2$. Thus,
573 $\sim 9.0 \times 10^{10}$ particles would need to be collected to form a single layer of PM on the filter. The
574 number of molecules in a single particle of the mode size is $\sim 1.4 \times 10^8$ molecules (Eq. S2).
575 Therefore, $\sim 1.3 \times 10^{19}$ molecules need to be collected onto the filters in order to form a monolayer
576 of PM, which is equivalent to $\sim 2.2 \times 10^3 \text{ } \mu\text{g}$ total aerosol collected or $\sim 700 \text{ } \mu\text{g sm}^{-3}$ aerosol

577 concentration. As the mass concentration in ATom was typically $\sim 1 \mu\text{g sm}^{-3}$ (Hodzic et al.,
578 2020), and total aerosol concentrations that high is rarely seen except for extreme events (such as
579 the thickest fresh wildfire plumes), it is very unlikely that more particle layering would delay the
580 diffusion of ammonia to acidic PM.

581 Various sensitivity analyses of the uptake of ammonia to sulfuric acid were conducted.
582 First, there is minimal impact of cabin temperature on the results. Though there was a 25 K range
583 in cabin temperature (Fig. S2), the impact on the molecular speed of ammonia in the model
584 (Eq. S1) leads to a $\pm 2\%$ change in molecular speed, resulting in small changes in the time.
585 Further, only large changes in the accommodation coefficient with temperature occurs for
586 sulfuric acid weight percentages $< 40\%$ (Swartz et al., 1999), which is smaller than the weight
587 percentage expected for the filters in the cabin of the DC-8. For the temperature range of the
588 cabin of the DC-8 (Fig. S2), the coefficient changes by less than 10%, which leads to a total
589 maximum change in Fig. 7 of $\pm 12\%$. The largest impact on the results in Fig. 7 is changing the
590 accommodation coefficient. Reducing the accommodation coefficient by a factor of 10, though
591 not representative of the DC-8 cabin conditions, would mean the acidic PM would need to be
592 exposed to ammonia for ≥ 1 minute (Fig. S10). It is expected that the lower accommodation
593 coefficient will occur for conditions with higher RH ($> 80\%$), suggesting typical laboratory
594 conditions (along with the lower ammonia mixing ratios) or ambient conditions may experience
595 lower ammonia uptake to acidic PM. Finally, organic coatings may impact the accommodation
596 coefficient of ammonia to sulfuric acid; however, the amount of reduction on the accommodation
597 coefficient has varied among studies (e.g., (Daumer et al., 1992; Liggio et al., 2011)). Daumer et
598 al. (1992) showed no impact; whereas, Liggio et al. (2011) found a similar impact to reducing the

599 accommodation coefficient by a factor of 10 (Fig. S10). Thus, the results in Fig. 7 are in line
600 with Daumer et al. (1992) while the results in Fig. S10 are in line with Liggio et al. (2011).

601

602 **3.4 Impacts of Ammonia Uptake on Acidic Filters**

603 As discussed throughout this study, uptake of cabin ammonia during the handling of
604 acidic filters can lead to biases in ammonium mass concentrations. However, other potential
605 sources of biases include the material used for sampling and storing the filter (Hayes et al.,
606 1980), and the preparation of the filter in the field to be sampled by ion chromatography. As the
607 preparation of the filters occurs indoors, as well, the filters will be exposed to similar ammonia
608 mixing ratios to those shown in Fig. 6.

609 Further, filter collection of aerosols is a widely used technique outside of aircraft
610 campaigns, including for regulatory purposes and long-term monitoring at various locations
611 around the world. For many of these sites, ammonia denuders are used to minimize biases of
612 ammonium on filters (e.g. (Baltensperger et al., 2003)). Data from remote, high altitude locations
613 have indicated that the ammonium balance is less than one (Cozic et al., 2008; Sun et al., 2009;
614 Freney et al., 2016; Zhou et al., 2019), similar to the observations from the AMS shown in
615 Fig. 3. However, this is dependent on air mass origin and type (Cozic et al., 2008; Sun et al.,
616 2009; Fröhlich et al., 2015). Thus, sampling of remote aerosols with filters does provide
617 evidence of ammonium balances less than one due to a combination of procedures to minimize
618 interaction of gas-phase ammonia with the acidic filters and the lower human presence (and
619 potentially cooler temperatures at high, remote, mountaintop locations such as Jungfrauoch).

620 However, there are some long-term monitoring stations that do not use denuders or other
621 practices to minimize the interaction of ammonia with acidic aerosols. For example, the Clean
622 Air Status and Trends Network (CASTNET), which is located throughout the continental United
623 States, measures ammonium, sulfate, and nitrate (Solomon et al., 2014). The CASTNET system
624 uses an open-face system to collect aerosols on Teflon filters for approximately one week for
625 each filter (Lavery et al., 2009). In comparison, the Chemical Speciation Monitoring Network
626 (CSN), which also samples the continental United States and collects the aerosols on Nylon or
627 Teflon filters, a denuder is used to scrub gas-phase ammonia to minimize interaction of ammonia
628 with acidic aerosols on filters (Solomon et al., 2000, 2014). The comparison between these two
629 long-term monitoring sites show very different trends of ammonium balance versus total
630 inorganic mass concentration (Fig. S11). For CSN, the ammonium balance decreases with mass
631 concentration whereas CASTNET remains nearly constant. This is similar to the comparison
632 between SAGA and AMS in Fig. 4. This difference between the two sampling techniques may
633 be due to the lack of denuder in CASTNET to remove gas-phase ammonia. The use of the
634 denuders has led to CSN and other monitoring networks that use denuders to be more in-line
635 with in-situ observations (Kim et al., 2015; Weber et al., 2016). Further, as shown in Fig. S8,
636 exposure of an unprotected acidic filter for time greater than 1 day will lead to ammonia reacting
637 with the acid to form ammonium bisulfate or ammonium sulfate, even at low ammonia mixing
638 ratios. Other aspects that could impact this comparison, and are beyond the scope of this study
639 (but has been discussed in other studies (Hering and Cass, 1999; Schauer et al., 2003; Chow et
640 al., 2005, 2010; Dzepina et al., 2007; Watson et al., 2009; Nie et al., 2010; Liu et al., 2014, 2015;
641 Cheng and He, 2015; Heim et al., 2020)), include the loss of volatile ammonium from the

642 evaporation of ammonium nitrate or differences in the handling, shipping, and/or storage of the
643 filters or extracted samples. Thus, without denuders, or handling of filters with more than one
644 person present, will lead to similar differences between in-situ sampling versus filter collection
645 of inorganic aerosols observed during various aircraft campaigns.

646 Further, the uptake of ammonia onto acidic aerosols will impact comparisons with
647 chemical transport models (CTMs) and the understanding of various physical processes. For
648 example, various CTMs predict different results for the mass concentration of ammonium in the
649 upper troposphere (Wang et al., 2008a; Fisher et al., 2011; Ge et al., 2018), and selection of one
650 measurement versus the other will lead to different degrees of agreement. For example, for filters
651 that collect aerosols similar to those described here (no ammonia scrubber and/or exposed to
652 human emissions of ammonia), values of ammonium $< 0.2 \mu\text{g sm}^{-3}$ should ~~not~~ be used with
653 caution ~~and either disregarded~~ or instead use *on-line* measurements of ammonium (specifically
654 for SAGA measurements but a similar analysis should be conducted for other filter-based
655 measurements). This different agreement impacts our understanding of important processes, such
656 as the direct radiative impact of inorganic aerosol (Wang et al., 2008b) or deposition of inorganic
657 gases and aerosols (Nenes et al., 2020a), as the gas-phase species have a faster deposition rate
658 than the aerosol-phase. Finally, the measurement biases can impact the suggested regulations to
659 improve air quality (Nenes et al., 2020b) and the calculated aerosol pH, as the pH is sensitive to
660 the partitioning of ammonia between the aerosol- and gas-phase (e.g., (Hennigan et al., 2015)).

661

662 **Conclusions**

663 Collection of aerosols onto filters to measure aerosol mass concentration and composition
664 is valuable for improving our understanding of the emissions and chemistry of inorganic aerosol,
665 and longstanding, multi-decadal filter-based records of atmospheric composition are invaluable
666 to analyze atmospheric change. However, as had been discussed in earlier studies, acidic aerosols
667 collected on filters are susceptible to uptake of gas-phase ammonia, which interacts with the
668 acidic aerosol to form an ammonium salt (e.g., ammonium bisulfate or ammonium sulfate). This
669 artifact in filter measurements can bias our understanding on the chemical composition of the
670 aerosol, which impacts numerous atmospheric processes.

671 We show that across six different aircraft campaigns, the aerosol collected on filters
672 showed a substantially higher ammonium mass concentration and ammonium balance compared
673 to AMS measurements. Further, another *on-line* measurement (PALMS) also shows lower
674 ammonium-to-sulfate ratios than for the filters. These differences are not due to differences in
675 the aerosol size ranges sampled by the PALMS and the filters. Instead, we show that the mixing
676 ratio of gas-phase ammonia in the cabin of the DC-8 is high enough (mean ~ 45 ppbv), and
677 similar to other indoor environments, to interact with acidic aerosol collected on filters in ≤ 10 s,
678 to form ammonium salts. These results are consistent with prior studies investigating this
679 interference. Thus, due to the interaction of ammonia in the cabin of research aircraft, we suggest
680 that a more realistic limit-of-detection of ammonium **for the SAGA filters** is 200 ng sm^{-3} , versus
681 the 10 ng sm^{-3} typically cited based on the ion chromatography measurement. Finally, even
682 though methods to reduce this bias have been implemented in several ground-based long-term
683 filter measurements of inorganic aerosols, there are still some networks that collect inorganic
684 aerosol without denuders to remove gas-phase ammonia, leading to similar discrepancies

685 between ground networks as observed between filters and AMS on the various aircraft
686 campaigns. Careful practice in both the aerosol collection and filtering handling is necessary to
687 better understand the emissions, chemistry, and chemical and physical properties of inorganic
688 aerosol.

689

690 **Acknowledgements**

691

692 This study was supported by NASA grants NNX15AH33A, NNX15AJ23G, 80NSSC18K0630,
693 and 80NSSC19K0124. We thank Glenn Diskin and the DACOM team for the use of the CO₂
694 measurements from FIREX-AQ, [Armin Wisthaler for the use of the NH₃ measurements from](#)
695 [FIREX-AQ](#), [Paul Wennberg for the use of HCN measurements from FIREX-AQ](#), Bruce
696 Anderson, Luke Ziemba, and the LARGE team for the use of the LAS volume distribution from
697 SEAC⁴RS, Karl Froyd, Gregory Schill, and Daniel Murphy for the use of the PALMS
698 observations from ATom-1 and -2, and Charles Brock, Agnieszka Kupc, and Christina
699 Williamson for the volume distribution measurements during ATom-1 and -2. Also, we thank J.
700 Andrew Neuman for the use of the Picarro G2103 during FIREX-AQ. We thank the crew of the
701 DC-8 and C-130 aircraft for extensive support in the field deployments. We specifically thank
702 Adam Webster and the crew of the NASA DC-8 in their assistance and persistence in allowing us
703 to install the Picarro G2103 during FIREX-AQ in order to measure ammonia in the cabin.

704

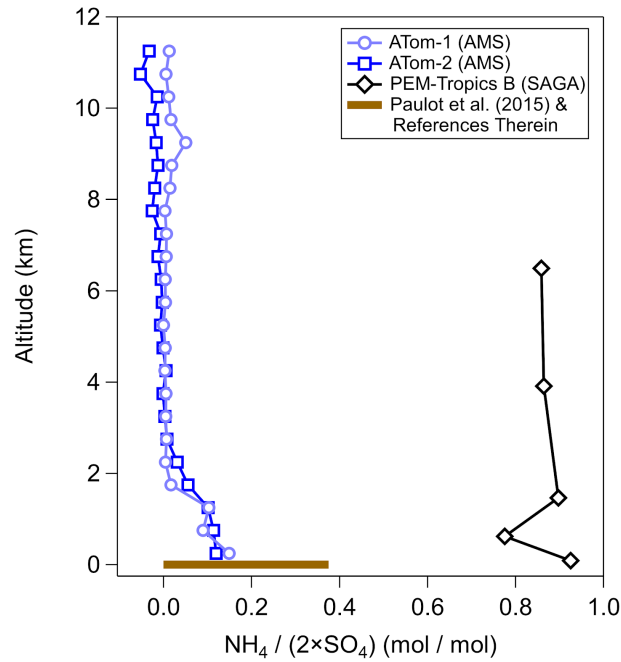
705 **Data Availability**

706

707 ARCTAS-A and -B measurements are available at
708 <http://doi.org/10.5067/SUBORBITAL/ARCTAS2008/DATA001>, last access 27 April 2020.
709 SEAC⁴RS measurements are available at
710 <http://doi.org/10.5067/Aircraft/SEAC4RS/Aerosol-TraceGas-Cloud>, last access 27 April 2020.
711 WINTER measurements are available at https://data.eol.ucar.edu/master_lists/generated/winter/,
712 last access 27 April 2020. ATom-1 and -2 measurements are available at
713 <https://doi.org/10.3334/ORNLDAAAC/1581>, last access 27 April 2020. Ammonia and carbon
714 dioxide measurements from the cabin of the DC-8 are available as an attachment . CSN and
715 CASTNET measurements are available at
716 <http://views.cira.colostate.edu/fed/QueryWizard/Default.aspx>, last access 27 April 2020.

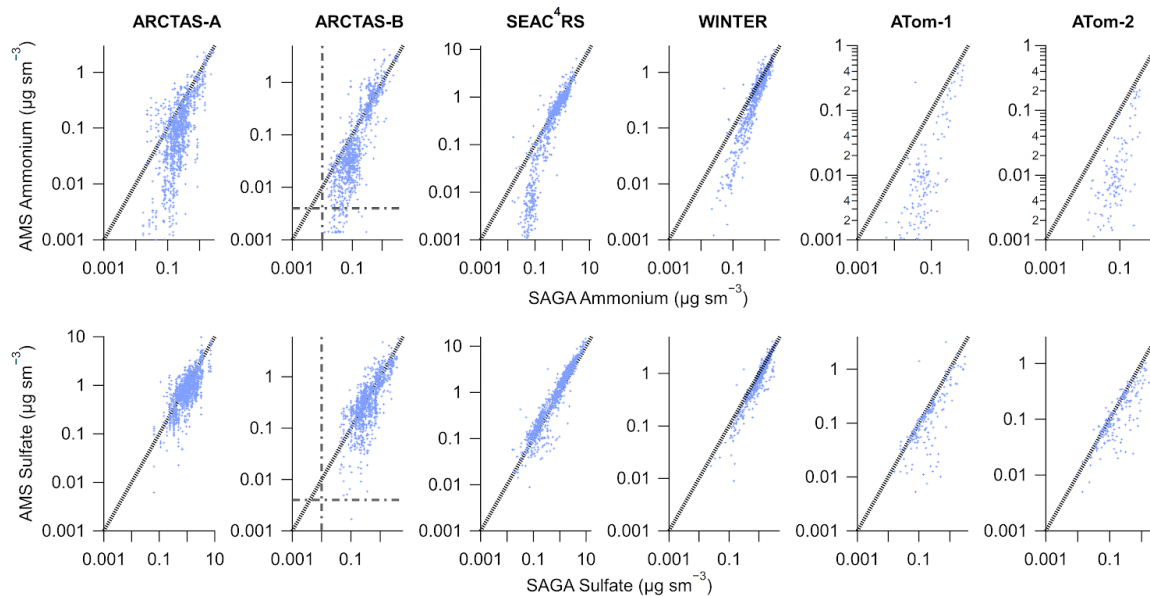
717 **Figures**

718



719 Figure 1. Vertical profile of sulfate-only ion molar balance ($moles(NH_4)/moles(SO_4)$) measured
 720 during PEM-Tropics by collecting the aerosol on filters and analyzing it off-line with ion
 721 chromatography (Dibb et al., 2002) and during ATom-1 and -2 by AMS (Hodzic et al., 2020).
 722 The ammonium balance profile is for observations collected during ATom-1 and -2 between
 723 $-20^\circ S$ and $20^\circ N$ in the Pacific basin, so that the observations were in a similar location as the
 724 PEM-Tropics samples. Also shown is the ammonium balance from observations summarized in
 725 Paulot et al. (2015), and reference therein, for the area around the same location as
 726 PEM-Tropics.

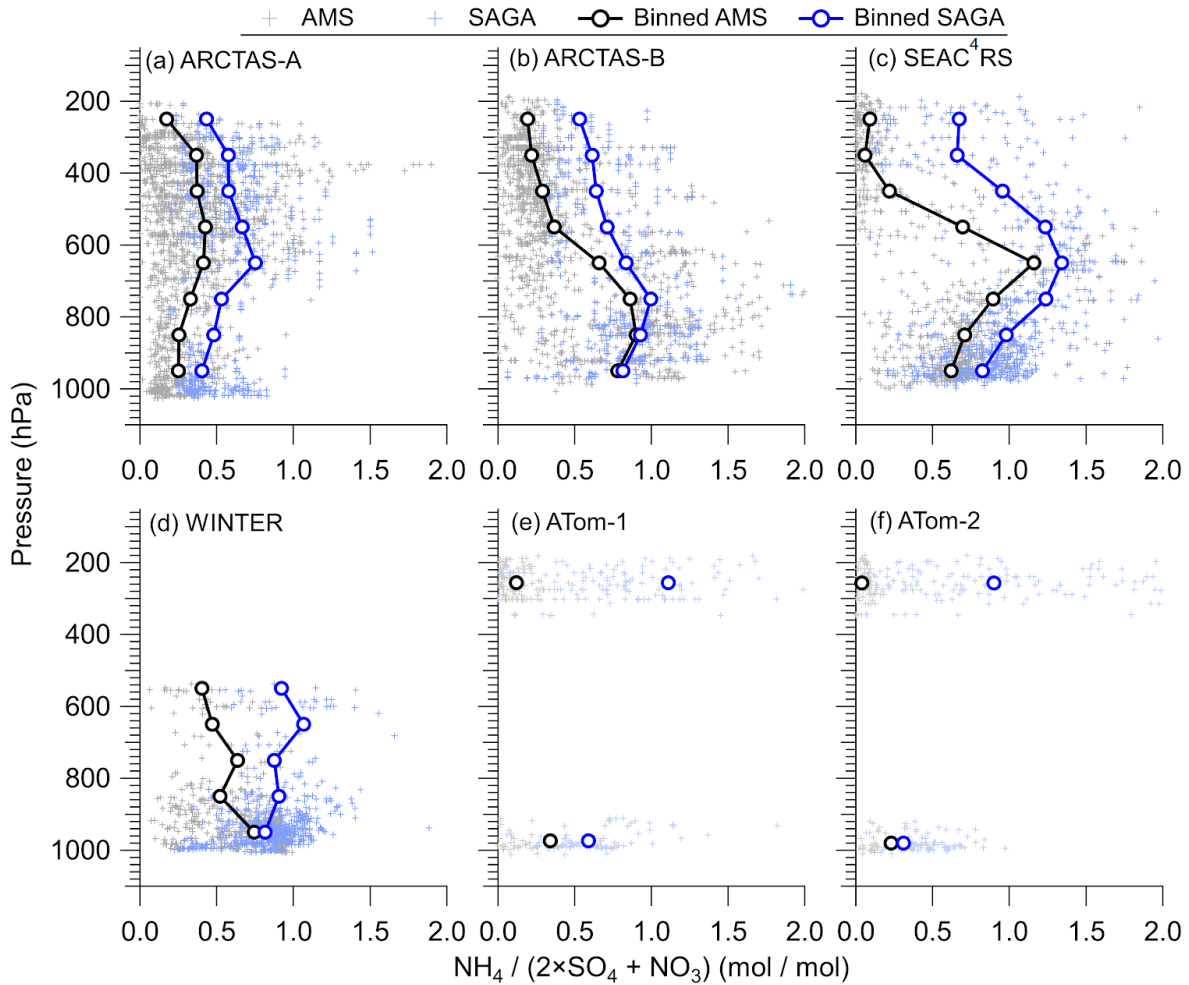
727



728

729 Figure 2. Scatter plot of AMS (y-axis) versus SAGA filter (x-axis) ammonium (top) and sulfate
 730 (bottom) mass concentration from 6 different aircraft campaigns. AMS data have been averaged
 731 over the SAGA filter collection times. Black line is the one-to-one line and the grey dash-dot
 732 lines are the estimated detection limits for AMS (DeCarlo et al., 2006; Guo et al., 2020) at the
 733 SAGA filter collection interval (~5 minutes) and the estimated detection limits for SAGA (Dibb et
 734 al., 1999). Data has been averaged to the sampling time of SAGA and has not been filtered for
 735 supermicron particles. For ATom-1 and -2, data during ascent and descent has been removed
 736 (only level sampling at low altitude and high altitude).

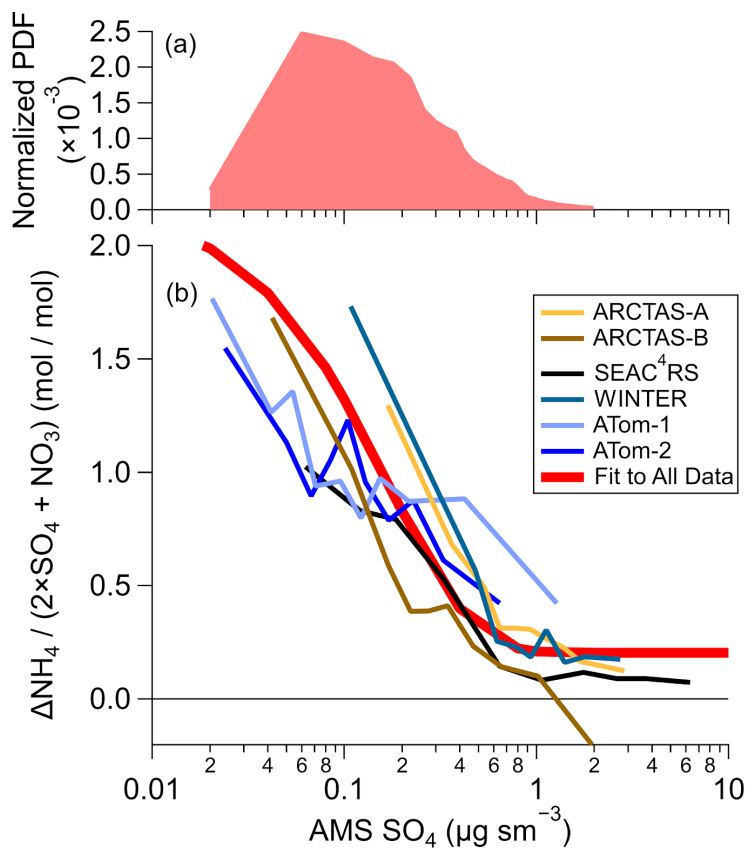
737



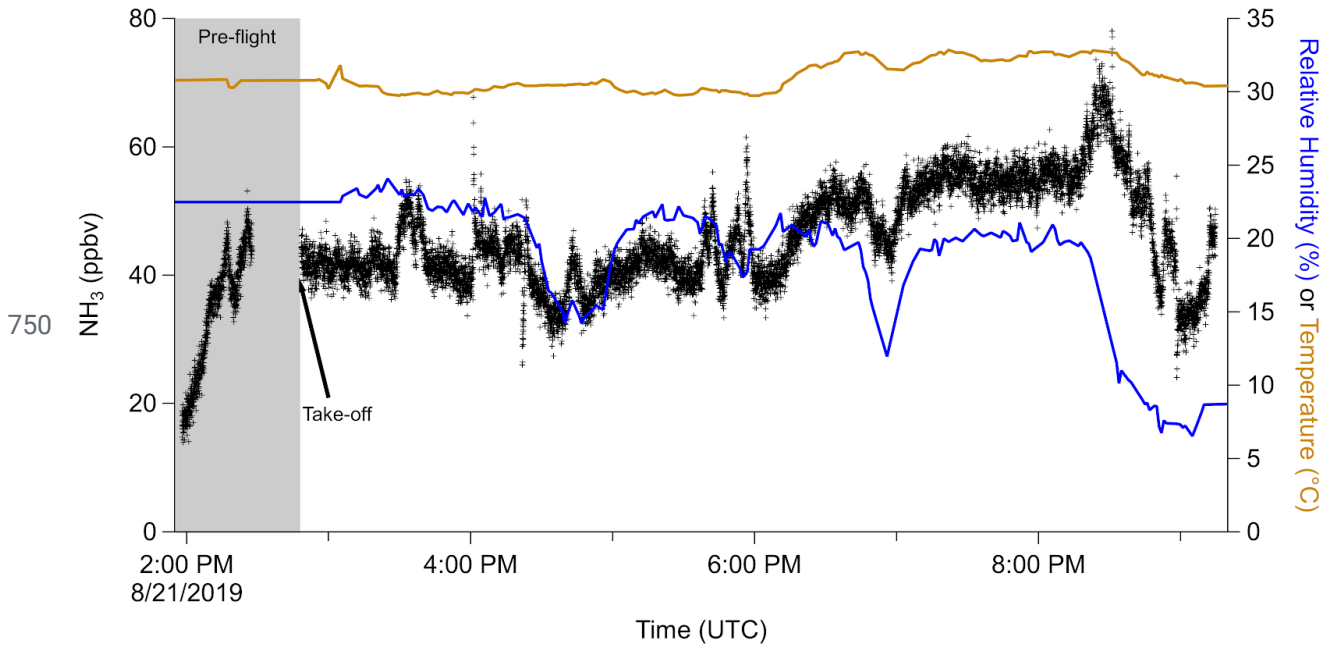
738 Figure 3. Vertical profiles of ammonium balance $((\text{NH}_4/18)/(2\times\text{SO}_4/96+\text{NO}_3/62))$ for (a)
 739 ARCTAS-A, (b) ARCTAS-B, (c) SEAC⁴RS, (d) WINTER, (e) ATom-1, and (f) ATom-2, for AMS
 740 and SAGA. The binned data is the mean for each 100 hPa pressure level. The data has been
 741 averaged to the sampling time of SAGA filters.

742

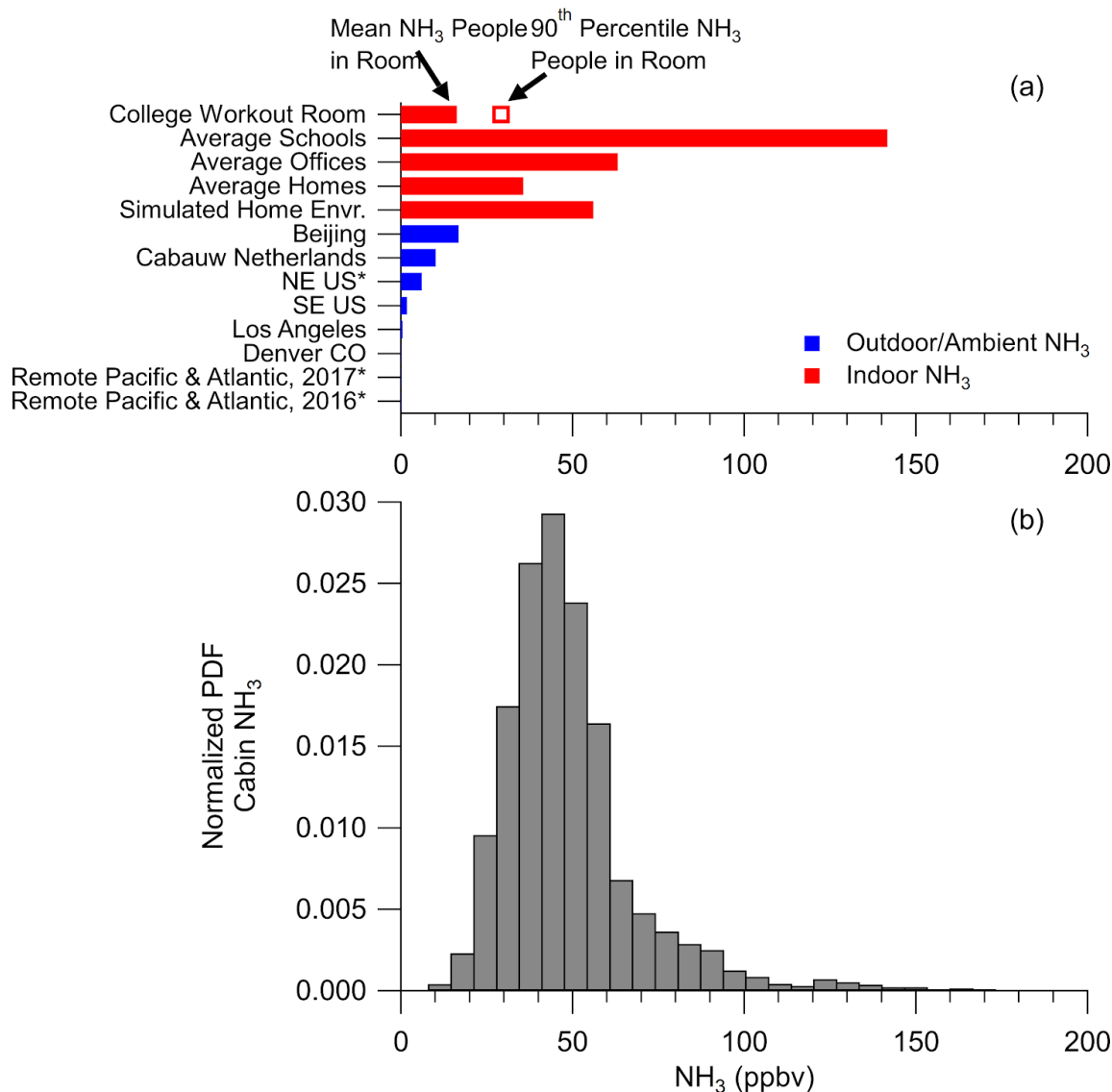
743



744 Figure 4. (a) Predicted normalized probability distribution function (PDF) for tropospheric
 745 (pressure > 250 hPa) sulfate from GEOS-Chem for one model year (see SI). (b) Difference
 746 between SAGA and AMS ammonium, in mol sm^{-3} , divided by AMS sulfate and nitrate, in mol
 747 sm^{-3} , versus AMS sulfate ($\mu\text{g sm}^{-3}$), for the six different airborne campaigns. The values shown
 748 are binned deciles for the five different airborne campaigns. The fit shown in (b) is for all data
 749 from all campaigns.



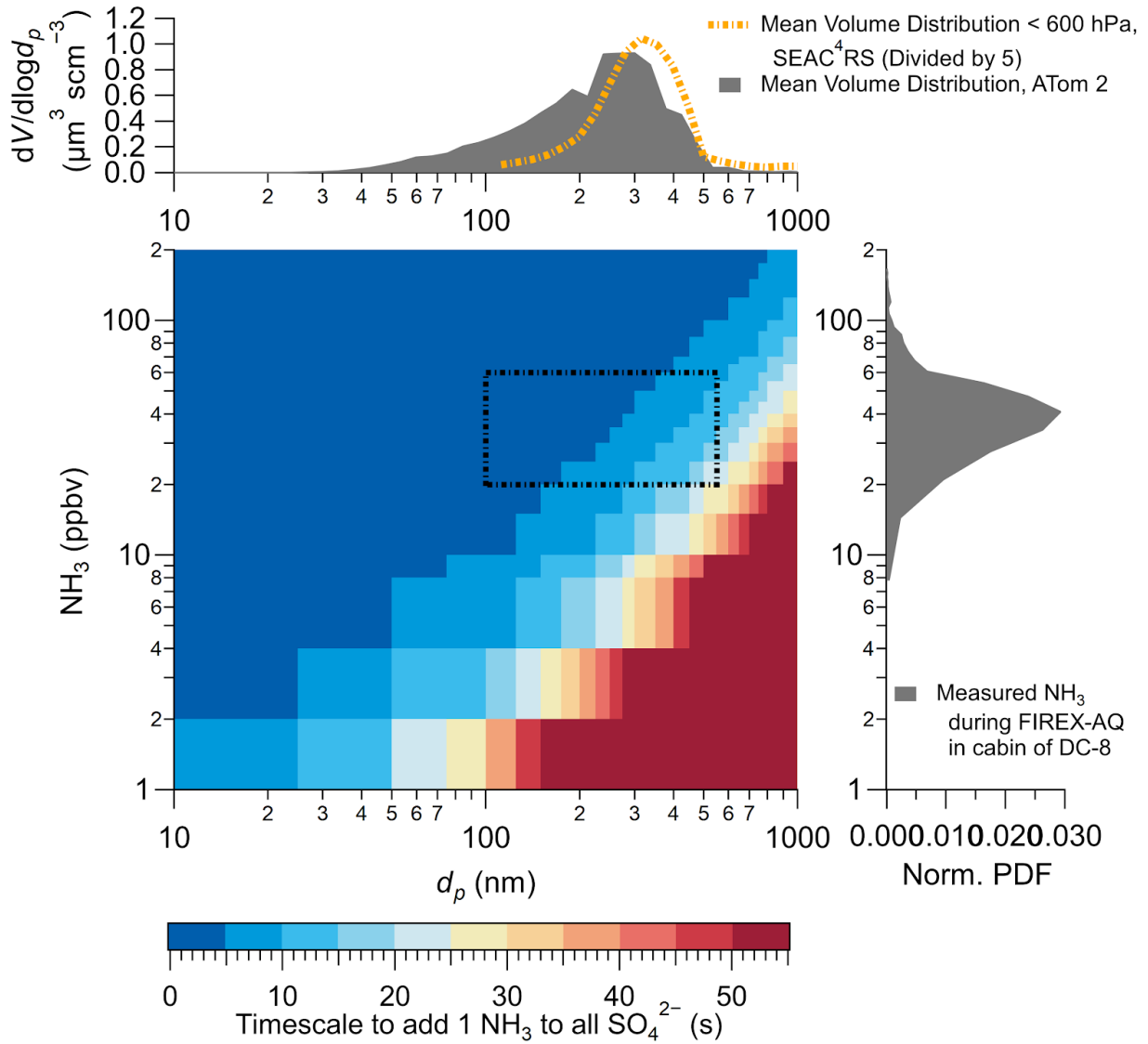
751 Figure 5. Time series of ammonia (left) and relative humidity and temperature (right) measured
 752 inside the cabin of the NASA DC-8 during a flight during the FIREX-AQ campaign. Time spent
 753 prior to take-off is marked with a grey background.



754

755 Figure 6. (a) Ammonia (NH_3) (ppbv) reported for studies. See Table S1 for references. Asterisk
 756 after study name indicates NH_3 predicted by thermodynamic model instead of being measured.
 757 (b) Normalized probability distribution function (PDF) for NH_3 , measured in the cabin of the
 758 NASA DC-8 during FIREX-AQ.

759



760 Figure 7. Theoretical calculation for the amount of time it would take for all the sulfuric acid on
 761 the filter to react with one ammonia molecule to become ammonium bisulfate. Volume
 762 distribution is the average from SEAC⁴RS and ATom-2 (adapted from Guo et al. (2020)) and the
 763 normalized probability distribution function (Norm. PDF) is from Fig. 6. The representative
 764 diameter and ammonia mixing ratio are shown as dashed lines in the calculated timescale.

765 **References**

- 766 Abbatt, J. P. D., Benz, S., Cziczo, D. J., Kanji, Z., Lohmann, U. and Möhler, O.: Solid
767 ammonium sulfate aerosols as ice nuclei: a pathway for cirrus cloud formation, *Science*,
768 313(5794), 1770–1773, 2006.
- 769 Aknan, A.: NASA Airborne Science Data for Atmospheric Composition, TABMEP2
770 POLARCAT Preliminary Assessment Reports [online] Available from:
771 <http://www-air.larc.nasa.gov/> (Accessed 3 June 2020), 2015.
- 772 Ampollini, L., Katz, E. F., Bourne, S., Tian, Y., Novoselac, A., Goldstein, A. H., Lucic, G.,
773 Waring, M. S. and DeCarlo, P. F.: Observations and Contributions of Real-Time Indoor
774 Ammonia Concentrations during HOMEChem, *Environ. Sci. Technol.*, 53(15), 8591–8598,
775 2019.
- 776 Bahreini, R., Dunlea, E. J., Matthew, B. M., Simons, C., Docherty, K. S., DeCarlo, P. F., Jimenez,
777 J. L., Brock, C. A. and Middlebrook, A. M.: Design and Operation of a Pressure-Controlled Inlet
778 for Airborne Sampling with an Aerodynamic Aerosol Lens, *Aerosol Sci. Technol.*, 42(6),
779 465–471, 2008.
- 780 Bahreini, R., Ervens, B., Middlebrook, A. M., Warneke, C., De Gouw, J. A., DeCarlo, P. F.,
781 Jimenez, J. L., Brock, C. A., Neuman, J. A., Ryerson, T. B., Stark, H., Atlas, E., Brioude, J.,
782 Fried, A., Holloway, J. S., Peischl, J., Richter, D., Walega, J., Weibring, P., Wollny, A. G. and
783 Fehsenfeld, F. C.: Organic aerosol formation in urban and industrial plumes near Houston and
784 Dallas, Texas, *J. Geophys. Res. D: Atmos.*, 114(16), 1–17, 2009.
- 785 Baltensperger, U., Barrie, L., Frohlich, C., Gras, J., Jäger, H., Jennings, S. G., Li, S.-M., Ogren,
786 J., Widensohler, A., Wehrli, C. and Wilson, J.: WMO/GAW Aerosol Measurement Procedures
787 Guidelines and Recommendations, WMO GAW. [online] Available from:
788 https://library.wmo.int/doc_num.php?explnum_id=9244, 2003.
- 789 von Bobruzki, K., Braban, C. F., Famulari, D., Jones, S. K., Blackall, T., Smith, T. E. L., Blom,
790 M., Coe, H., Gallagher, M., Ghalaieny, M., McGillen, M. R., Percival, C. J., Whitehead, J. D.,
791 Ellis, R., Murphy, J., Mohacsi, A., Pogany, A., Junninen, H., Rantanen, S., Sutton, M. A. and
792 Nemitz, E.: Field inter-comparison of eleven atmospheric ammonia measurement techniques,
793 *Atmos. Meas. Tech.*, 3(1), 91–112, 2010.
- 794 Brock, C. A., Williamson, C., Kupc, A., Froyd, K. D., Erdesz, F., Wagner, N., Richardson, M.,
795 Schwarz, J. P., Gao, R.-S., Katich, J. M., Campuzano-Jost, P., Nault, B. A., Schroder, J. C.,
796 Jimenez, J. L., Weinzierl, B., Dollner, M., Bui, T. and Murphy, D. M.: Aerosol size distributions
797 during the Atmospheric Tomography Mission (ATom): methods, uncertainties, and data products,
798 *Atmos. Meas. Tech.*, 12(6), 3081–3099, 2019.
- 799 Brundrett, G.: Comfort and health in commercial aircraft: a literature review, *J. R. Soc. Promot.*
800 *Health*, 121(1), 29–37, 2001.
- 801 Canagaratna, M. R., Jayne, J. T., Jimenez, J. L., Allan, J. D., Alfarra, M. R., Zhang, Q., Onasch,

802 T. B., Drewnick, F., Coe, H., Middlebrook, A., Delia, A., Williams, L. R., Trimborn, A. M.,
803 Northway, M. J., DeCarlo, P. F., Kolb, C. E., Davidovits, P. and Worsnop, D. R.: Chemical and
804 microphysical characterization of ambient aerosols with the aerodyne aerosol mass spectrometer,
805 *Mass Spectrom. Rev.*, 26(2), 185–222, 2007.

806 Cheng, Y. and He, K.-B.: Measurement of carbonaceous aerosol with different sampling
807 configurations and frequencies, *Atmos. Meas. Tech.*, 8(7), 2639–2648, 2015.

808 Chow, J. C., Watson, J. G., Lowenthal, D. H. and Magliano, K. L.: Loss of PM_{2.5} Nitrate from
809 Filter Samples in Central California, *J. Air Waste Manage. Assoc.*, 55(8), 1158–1168, 2005.

810 Chow, J. C., Watson, J. G., Chen, L.-W. A., Rice, J. and Frank, N. H.: Quantification of PM_{2.5}
811 organic carbon sampling artifacts in US networks, *Atmos. Chem. Phys.*, 10(12), 5223–5239,
812 2010.

813 Clark, K. W., Anderson, K. R., Linn, W. S. and Gong, H., Jr: Influence of breathing-zone
814 ammonia on human exposures to acid aerosol pollution, *J. Air Waste Manag. Assoc.*, 45(11),
815 923–925, 1995.

816 Cohen, A. J., Brauer, M., Burnett, R., Anderson, H. R., Frostad, J., Estep, K., Balakrishnan, K.,
817 Brunekreef, B., Dandona, L., Dandona, R., Feigin, V., Freedman, G., Hubbell, B., Jobling, A.,
818 Kan, H., Knibbs, L., Liu, Y., Martin, R., Morawska, L., Pope, C. A., Shin, H., Straif, K.,
819 Shaddick, G., Thomas, M., van Dingenen, R., van Donkelaar, A., Vos, T., Murray, C. J. L. and
820 Forouzanfar, M. H.: Estimates and 25-year trends of the global burden of disease attributable to
821 ambient air pollution: an analysis of data from the Global Burden of Diseases Study 2015,
822 *Lancet*, 389(10082), 1907–1918, 2017.

823 Colberg, C. A., Luo, B. P., Wernli, H., Koop, T. and Peter, T.: A novel model to predict the
824 physical state of atmospheric H₂SO₄/NH₃/H₂O aerosol particles, *Atmos. Chem. Phys.*, 3(4),
825 909–924, 2003.

826 Coury, C. and Dillner, A. M.: ATR-FTIR characterization of organic functional groups and
827 inorganic ions in ambient aerosols at a rural site, *Atmos. Environ.*, 43(4), 940–948, 2009.

828 Cozic, J., Verheggen, B., Weingartner, E., Crosier, J., Bower, K. N., Flynn, M., Coe, H.,
829 Henning, S., Steinbacher, M., Henne, S., Collaud Coen, M., Petzold, A. and Baltensperger, U.:
830 Chemical composition of free tropospheric aerosol for PM₁ and coarse mode at the high alpine
831 site Jungfraujoch, *Atmos. Chem. Phys.*, 8(2), 407–423, 2008.

832 Cubison, M. J., Ortega, A. M., Hayes, P. L., Farmer, D. K., Day, D. A., Lechner, M. J., Brune, W.
833 H., Apel, E., Diskin, G. S., Fisher, J. A., Fuelberg, H. E., Hecobian, A., Knapp, D. J., Mikoviny,
834 T., Riemer, D., Sachse, G. W., Sessions, W., Weber, R. J., Weinheimer, A. J., Wisthaler, A. and
835 Jimenez, J. L.: Effects of aging on organic aerosol from open biomass burning smoke in aircraft
836 and laboratory studies, *Atmos. Chem. Phys.*, 11(23), 12049–12064, 2011.

837 Daumer, B., Niessner, R. and Klockow, D.: Laboratory studies of the influence of thin organic
838 films on the neutralization reaction of H₂SO₄ aerosol with ammonia, *J. Aerosol Sci.*, 23(4),

839 315–325, 1992.

840 DeCarlo, P. F., Kimmel, J. R., Trimborn, A., Northway, M. J., Jayne, J. T., Aiken, A. C., Gonin,
841 M., Fuhrer, K., Horvath, T., Docherty, K. S., Worsnop, D. R. and Jimenez, J. L.:
842 Field-deployable, high-resolution, time-of-flight aerosol mass spectrometer, *Anal. Chem.*,
843 78(24), 8281–8289, 2006.

844 DeCarlo, P. F., Dunlea, E. J., Kimmel, J. R., Aiken, A. C., Sueper, D., Crouse, J., Wennberg, P.
845 O., Emmons, L., Shinozuka, Y., Clarke, A., Zhou, J., Tomlinson, J., Collins, D. R., Knapp, D.,
846 Weinheimer, A. J., Montzka, D. D., Campos, T. and Jimenez, J. L.: Fast airborne aerosol size and
847 chemistry measurements above Mexico City and Central Mexico during the MILAGRO
848 campaign, *Atmos. Chem. Phys.*, 8(14), 4027–4048, 2008.

849 Dentener, F. J. and Crutzen, P. J.: A three-dimensional model of the global ammonia cycle, *J.*
850 *Atmos. Chem.*, 19(4), 331–369, 1994.

851 Dibb, J. E., Talbot, R. W., Scheuer, E. M., Blake, D. R., Blake, N. J., Gregory, G. L., Sachse, G.
852 W. and Thornton, D. C.: Aerosol chemical composition and distribution during the Pacific
853 Exploratory Mission (PEM) Tropics, *J. Geophys. Res.*, 104(D5), 5785–5800, 1999.

854 Dibb, J. E., Talbot, R. W. and Scheuer, E. M.: Composition and distribution of aerosols over the
855 North Atlantic during the Subsonic Assessment Ozone and Nitrogen Oxide Experiment
856 (SONEX), *J. Geophys. Res. D: Atmos.*, 105(D3), 3709–3717, 2000.

857 Dibb, J. E., Talbot, R. W., Seid, G., Jordan, C., Scheuer, E., Atlas, E., Blake, N. J. and Blake, D.
858 R.: Airborne sampling of aerosol particles: Comparison between surface sampling at Christmas
859 Island and P-3 sampling during PEM-Tropics B, *J. Geophys. Res.*, 108(D2), 11335, 2002.

860 Dibb, J. E., Talbot, R. W., Scheuer, E. M., Seid, G., Avery, M. A. and Singh, H. B.: Aerosol
861 chemical composition in Asian continental outflow during the TRACE-P campaign: Comparison
862 with PEM-West B, *J. Geophys. Res.: Atmos.*, 108(D21), 8815, 2003.

863 Dzepina, K., Arey, J., Marr, L. C., Worsnop, D. R., Salcedo, D., Zhang, Q., Onasch, T. B.,
864 Molina, L. T., Molina, M. J. and Jimenez, J. L.: Detection of particle-phase polycyclic aromatic
865 hydrocarbons in Mexico City using an aerosol mass spectrometer, *Int. J. Mass Spectrom.*, 263(2),
866 152–170, 2007.

867 Faloon, I.: Sulfur processing in the marine atmospheric boundary layer: A review and critical
868 assessment of modeling uncertainties, *Atmos. Environ.*, 43(18), 2841–2854, 2009.

869 Filges, A., Gerbig, C., Rella, C. W., Hoffnagle, J., Smit, H., Krämer, M., Spelten, N., Rolf, C.,
870 Bozóki, Z., Buchholz, B. and Ebert, V.: Evaluation of the IAGOS-Core GHG package H₂O
871 measurements during the DENCHAR airborne inter-comparison campaign in 2011, *Atmos.*
872 *Meas. Tech.*, 11(9), 5279–5297, 2018.

873 Finewax, Z., Pagonis, D., Claflin, M. S., Handschy, A. V., Brown, W. L., Ba, J. O. N., Lerner, B.
874 M., Jimenez, J. L., Ziemann, P. J. and de Gouw, J. A.: Quantification and source characterization

875 of volatile organic compounds from exercising and application of chlorine-based cleaning
876 products in a university athletic center, *Indoor Air*, Submitted, 2020.

877 Fisher, J. A., Jacob, D. J., Wang, Q., Bahreini, R., Carouge, C. C., Cubison, M. J., Dibb, J. E.,
878 Diehl, T., Jimenez, J. L., Leibensperger, E. M., Lu, Z., Meinders, M. B. J., Pye, H. O. T., Quinn,
879 P. K., Sharma, S., Streets, D. G., van Donkelaar, A. and Yantosca, R. M.: Sources, distribution,
880 and acidity of sulfate–ammonium aerosol in the Arctic in winter–spring, *Atmos. Environ.*,
881 45(39), 7301–7318, 2011.

882 Freney, E., Sellegri Karine, S. K., Eija, A., Clemence, R., Aurelien, C., Jean-Luc, B., Aurelie, C.,
883 Hervo Maxime, H. M., Nadege, M., Laetia, B. and David, P.: Experimental Evidence of the
884 Feeding of the Free Troposphere with Aerosol Particles from the Mixing Layer, *Aerosol Air*
885 *Qual. Res.*, 16(3), 702–716, 2016.

886 Fröhlich, R., Cubison, M. J., Slowik, J. G., Bukowiecki, N., Canonaco, F., Croteau, P. L., Gysel,
887 M., Henne, S., Herrmann, E., Jayne, J. T., Steinbacher, M., Worsnop, D. R., Baltensperger, U.
888 and Prévôt, A. S. H.: Fourteen months of on-line measurements of the non-refractory submicron
889 aerosol at the Jungfraujoch (3580 m a.s.l.) – chemical composition, origins and organic aerosol
890 sources, *Atmos. Chem. Phys.*, 15(19), 11373–11398, 2015.

891 Froyd, K. D., Murphy, D. M., Sanford, T. J., Thomson, D. S., Wilson, J. C., Pfister, L. and Lait,
892 L.: Aerosol composition of the tropical upper troposphere, *Atmos. Chem. Phys.*, 9(13),
893 4363–4385, 2009.

894 Froyd, K. D., Murphy, D. M., Brock, C. A., Campuzano-Jost, P., Dibb, J. E., Jimenez, J.-L.,
895 Kupc, A., Middlebrook, A. M., Schill, G. P., Thornhill, K. L., Williamson, C. J., Wilson, J. C.
896 and Ziemba, L. D.: A new method to quantify mineral dust and other aerosol species from
897 aircraft platforms using single-particle mass spectrometry, *Atmos. Meas. Tech.*, 12(11),
898 6209–6239, 2019.

899 Fuchs, N. A. and Sutugin, A. G.: High-Dispersed Aerosols, in *Topics in Current Aerosol*
900 *Research*, edited by G. M. Hidy and J. R. Brock, Pergamon., 1971.

901 Ge, C., Zhu, C., Francisco, J. S., Zeng, X. C. and Wang, J.: A molecular perspective for global
902 modeling of upper atmospheric NH₃ from freezing clouds, *Proc. Natl. Acad. Sci. U. S. A.*,
903 115(24), 6147–6152, 2018.

904 Guo, H., Xu, L., Bougiatioti, A., Cerully, K. M., Capps, S. L., Hite, J. R., Carlton, A. G., Lee,
905 S.-H., Bergin, M. H., Ng, N. L., Nenes, A. and Weber, R. J.: Fine-particle water and pH in the
906 southeastern United States, *Atmos. Chem. Phys.*, 15(9), 5211–5228, 2015.

907 Guo, H., Sullivan, A. P., Campuzano-Jost, P., Schroder, J. C., Lopez-Hilfiker, F. D., Dibb, J. E.,
908 Jimenez, J. L., Thornton, J. A., Brown, S. S., Nenes, A. and Weber, R. J.: Fine particle pH and
909 the partitioning of nitric acid during winter in the northeastern United States, *J. Geophys. Res. D:*
910 *Atmos.*, 121(17), 10,355–10,376, 2016.

911 Guo, H., Nenes, A. and Weber, R. J.: The underappreciated role of nonvolatile cations in aerosol

912 ammonium-sulfate molar ratios, *Atmos. Chem. Phys.*, 18(23), 17307–17323, 2018.

913 Guo, H., Campuzano-Jost, P., Nault, B. A., Day, D. A., Schroder, J. C., Dibb, J. E., Dollner, M.,
914 Weinzierl, B. and Jimenez, J. L.: The Importance of Size Ranges in Intercomparison of Aerosol
915 Volume Concentration Measurements: A Case Study for Aerosol Mass Spectrometer in the
916 ATom Mission, *Atmos. Meas. Tech. Discuss.*, In Review, doi:10.5194/amt-2020-224, 2020.

917 Hanson, D. and Kosciuch, E.: The NH₃ Mass Accommodation Coefficient for Uptake onto
918 Sulfuric Acid Solutions, *J. Phys. Chem. A*, 107(13), 2199–2208, 2003.

919 Hanson, D. R. and Kosciuch, E.: Reply to “Comment on ‘The NH₃ Mass Accommodation
920 Coefficient for Uptake onto Sulfuric Acid Solutions,’” *J. Phys. Chem. A*, 108(40), 8549–8551,
921 2004.

922 Hayes, D., Snetsinger, K., Ferry, G., Oberbeck, V. and Farlow, N.: Reactivity of stratospheric
923 aerosols to small amounts of ammonia in the laboratory environment, *Geophys. Res. Lett.*, 7(11),
924 974–976, 1980.

925 Heald, C. L. and Kroll, J. H.: The fuel of atmospheric chemistry: Toward a complete description
926 of reactive organic carbon, *Sci Adv*, 6(6), eaay8967, 2020.

927 Heald, C. L., Collett, J. L., Jr., Lee, T., Benedict, K. B., Schwandner, F. M., Li, Y., Clarisse, L.,
928 Hurtmans, D. R., Van Damme, M., Clerbaux, C., Coheur, P.-F., Philip, S., Martin, R. V. and Pye,
929 H. O. T.: Atmospheric ammonia and particulate inorganic nitrogen over the United States,
930 *Atmos. Chem. Phys.*, 12(21), 10295–10312, 2012.

931 Heim, E. W., Dibb, J., Scheuer, E., Jost, P. C., Nault, B. A., Jimenez, J. L., Peterson, D., Knote,
932 C., Fenn, M., Hair, J., Beyersdorf, A. J., Corr, C. and Anderson, B. E.: Asian dust observed
933 during KORUS-AQ facilitates the uptake and incorporation of soluble pollutants during transport
934 to South Korea, *Atmos. Environ.*, 224, 117305, 2020.

935 Hennigan, C. J., Sullivan, A. P., Fountoukis, C. I., Nenes, A., Hecobian, A., Vargas, O., Peltier,
936 R. E., Hanks, A. T. C., Huey, L. G., Lefer, B. L., Russell, A. G. and Weber, R. J.: On the
937 volatility and production mechanisms of newly formed nitrate and water soluble organic aerosol
938 in Mexico City, *Atmos. Chem. Phys.*, 8(14), 3761–3768, 2008.

939 Hennigan, C. J., Izumi, J., Sullivan, A. P., Weber, R. J. and Nenes, A.: A critical evaluation of
940 proxy methods used to estimate the acidity of atmospheric particles, *Atmos. Chem. Phys.*, 15(5),
941 2775–2790, 2015.

942 Henze, D. K., Seinfeld, J. H. and Shindell, D. T.: Inverse modeling and mapping US air quality
943 influences of inorganic PM_{2.5} precursor emissions using the adjoint of GEOS-Chem, *Atmos.*
944 *Chem. Phys.*, 9(16), 5877–5903, 2009.

945 Hering, S. and Cass, G.: The Magnitude of Bias in the Measurement of PM_{2.5} Arising from
946 Volatilization of Particulate Nitrate from Teflon Filters, *J. Air Waste Manag. Assoc.*, 49(6),

947 725–733, 1999.

948 Hocking, M. B.: Indoor air quality: recommendations relevant to aircraft passenger cabins, *Am.*
949 *Ind. Hyg. Assoc. J.*, 59(7), 446–454, 1998.

950 Hodzic, A. and Duvel, J. P.: Impact of Biomass Burning Aerosols on the Diurnal Cycle of
951 Convective Clouds and Precipitation Over a Tropical Island: Fire aerosols effect on deep
952 convection, *J. Geophys. Res. D: Atmos.*, 123(2), 1017–1036, 2018.

953 Hodzic, A., Campuzano-Jost, P., Bian, H., Chin, M., Colarco, P. R., Day, D. A., Froyd, K. D.,
954 Heinold, B., Jo, D. S., Katich, J. M., Kodros, J. K., Nault, B. A., Pierce, J. R., Ray, E., Schacht,
955 J., Schill, G. P., Schroder, J. C., Schwarz, J. P., Sueper, D. T., Tegen, I., Tilmes, S., Tsigaridis, K.,
956 Yu, P. and Jimenez, J. L.: Characterization of Organic Aerosol across the Global Remote
957 Troposphere: A comparison of ATom measurements and global chemistry models, *Atmos.*
958 *Chem. Phys.*, 20(8), 4607–4635, 2020.

959 Hunt, E. W. and Space, D. R.: The Airplane Cabin Environment: Issues Pertaining to Flight
960 Attendant, in Comfort,” International in-flight Service Management Organization Conference.
961 [online] Available from:
962 <http://citeseerx.ist.psu.edu/viewdoc/similar?doi=10.1.1.304.7321&type=cc> (Accessed 25 March
963 2020), 1994.

964 Huntzicker, J. J., Cary, R. A. and Ling, C.-S.: Neutralization of sulfuric acid aerosol by ammonia,
965 *Environ. Sci. Technol.*, 14(7), 819–824, 1980.

966 Hu, W., Hu, M., Hu, W., Jimenez, J. L., Yuan, B., Chen, W., Wang, M., Wu, Y., Chen, C., Wang,
967 Z., Peng, J., Zeng, L. and Shao, M.: Chemical composition, sources, and aging process of
968 submicron aerosols in Beijing: Contrast between summer and winter, *J. Geophys. Res. D:*
969 *Atmos.*, 121(4), 1955–1977, 2016.

970 Hu, W., Campuzano-Jost, P., Day, D. A., Croteau, P., Canagaratna, M. R., Jayne, J. T., Worsnop,
971 D. R. and Jimenez, J. L.: Evaluation of the new capture vaporizer for aerosol mass spectrometers
972 (AMS) through field studies of inorganic species, *Aerosol Sci. Technol.*, 51(6), 735–754, 2017a.

973 Hu, W., Campuzano-Jost, P., Day, D. A., Croteau, P., Canagaratna, M. R., Jayne, J. T., Worsnop,
974 D. R. and Jimenez, J. L.: Evaluation of the new capture vapourizer for aerosol mass
975 spectrometers (AMS) through laboratory studies of inorganic species, *Atmospheric Measurement*
976 *Techniques*, 10(6), 2897–2921, 2017b.

977 Hu, W., Campuzano-Jost, P., Day, D. A., Nault, B. A., Park, T., Lee, T., Pajunoja, A., Virtanen,
978 A., Croteau, P., Canagaratna, M. R., Jayne, J. T., Worsnop, D. R. and Jimenez, J. L.: Ambient
979 Quantification and Size Distributions for Organic Aerosol in Aerosol Mass Spectrometers with
980 the New Capture Vaporizer, *ACS Earth Space Chem.*, doi:10.1021/acsearthspacechem.9b00310,
981 2020.

982 Jacob, D. J., Crawford, J. H., Maring, H., Clarke, A. D., Dibb, J. E., Emmons, L. K., Ferrare, R.
983 A., Hostetler, C. A., Russell, P. B., Singh, H. B., Thompson, A. M., Shaw, G. E., McCauley, E.,

984 Pederson, J. R. and Fisher, J. A.: The Arctic Research of the Composition of the Troposphere
985 from Aircraft and Satellites (ARCTAS) mission: design, execution, and first results, *Atmos.*
986 *Chem. Phys.*, 10(11), 5191–5212, 2010.

987 Jimenez, J. L., Canagaratna, M. R., Donahue, N. M., Prevot, A. S. H., Zhang, Q., Kroll, J. H.,
988 DeCarlo, P. F., Allan, J. D., Coe, H., Ng, N. L., Aiken, A. C., Docherty, K. S., Ulbrich, I. M.,
989 Grieshop, A. P., Robinson, A. L., Duplissy, J., Smith, J. D., Wilson, K. R., Lanz, V. A., Hueglin,
990 C., Sun, Y. L., Tian, J., Laaksonen, A., Raatikainen, T., Rautiainen, J., Vaattovaara, P., Ehn, M.,
991 Kulmala, M., Tomlinson, J. M., Collins, D. R., Cubison, M. J., Dunlea, E. J., Huffman, J. A.,
992 Onasch, T. B., Alfarra, M. R., Williams, P. I., Bower, K., Kondo, Y., Schneider, J., Drewnick, F.,
993 Borrmann, S., Weimer, S., Demerjian, K., Salcedo, D., Cottrell, L., Griffin, R., Takami, A.,
994 Miyoshi, T., Hatakeyama, S., Shimono, A., Sun, J. Y., Zhang, Y. M., Dzepina, K., Kimmel, J. R.,
995 Sueper, D., Jayne, J. T., Herndon, S. C., Trimborn, A. M., Williams, L. R., Wood, E. C.,
996 Middlebrook, A. M., Kolb, C. E., Baltensperger, U. and Worsnop, D. R.: Evolution of organic
997 aerosols in the atmosphere, *Science*, 326(5959), 1525–1529, 2009.

998 Kamp, J. N., Chowdhury, A., Adamsen, A. P. S. and Feilberg, A.: Negligible influence of
999 livestock contaminants and sampling system on ammonia measurements with cavity ring-down
1000 spectroscopy, *Atmos. Meas. Tech.*, 12(5), 2837–2850, 2019.

1001 Kim, H., Zhang, Q. and Heo, J.: Influence of intense secondary aerosol formation and long-range
1002 transport on aerosol chemistry and properties in the Seoul Metropolitan Area during spring time:
1003 results from KORUS-AQ, *Atmos. Chem. Phys.*, 18(10), 7149–7168, 2018.

1004 Kim, P. S., Jacob, D. J., Fisher, J. A., Travis, K., Yu, K., Zhu, L., Yantosca, R. M., Sulprizio, M.
1005 P., Jimenez, J. L., Campuzano-Jost, P., Froyd, K. D., Liao, J., Hair, J. W., Fenn, M. A., Butler, C.
1006 F., Wagner, N. L., Gordon, T. D., Welti, A., Wennberg, P. O., Crounse, J. D., St Clair, J. M.,
1007 Teng, A. P., Millet, D. B., Schwarz, J. P., Markovic, M. Z. and Perring, A. E.: Sources,
1008 seasonality, and trends of southeast US aerosol: an integrated analysis of surface, aircraft, and
1009 satellite observations with the GEOS-Chem chemical transport model, *Atmos. Chem. Phys.*, 15,
1010 10411–10433, 2015.

1011 Kline, J., Huebert, B., Howell, S., Blomquist, B., Zhuang, J., Bertram, T. and Carrillo, J.: Aerosol
1012 composition and size versus altitude measured from the C-130 during ACE-Asia, *J. Geophys.*
1013 *Res.*, 109(D19), 340, 2004.

1014 Klockow, D., Jablonski, B. and Nießner, R.: Possible artifacts in filter sampling of atmospheric
1015 sulphuric acid and acidic sulphates, *Atmos. Environ.*, 13(12), 1665–1676, 1979.

1016 Koutrakis, P., Wolfson, J. M. and Spengler, J. D.: An improved method for measuring aerosol
1017 strong acidity: Results from a nine-month study in St Louis, Missouri and Kingston, Tennessee,
1018 *Atmos. Environ.*, 22(1), 157–162, 1988.

1019 Kupc, A., Williamson, C., Wagner, N. L., Richardson, M. and Brock, C. A.: Modification,
1020 calibration, and performance of the Ultra-High Sensitivity Aerosol Spectrometer for particle size
1021 distribution and volatility measurements during the Atmospheric Tomography Mission (ATom)

- 1022 airborne campaign, *Atmos. Meas. Tech.*, 11(1), 369–383, 2018.
- 1023 Larson, T. V., Covert, D. S., Frank, R. and Charlson, R. J.: Ammonia in the human airways:
1024 neutralization of inspired acid sulfate aerosols, *Science*, 197(4299), 161–163, 1977.
- 1025 Lavery, T. F., Rogers, C. M., Baumgardner, R. and Mishoe, K. P.: Intercomparison of Clean Air
1026 Status and Trends Network Nitrate and Nitric Acid Measurements with Data from Other
1027 Monitoring Programs, *J. Air Waste Manag. Assoc.*, 59(2), 214–226, 2009.
- 1028 Liao, J., Froyd, K. D., Murphy, D. M., Keutsch, F. N., Yu, G., Wennberg, P. O., St Clair, J. M.,
1029 Crouse, J. D., Wisthaler, A., Mikoviny, T., Jimenez, J. L., Campuzano-Jost, P., Day, D. A., Hu,
1030 W., Ryerson, T. B., Pollack, I. B., Peischl, J., Anderson, B. E., Ziemba, L. D., Blake, D. R.,
1031 Meinardi, S. and Diskin, G.: Airborne measurements of organosulfates over the continental U.S.,
1032 *J. Geophys. Res. D: Atmos.*, 120(7), 2990–3005, 2015.
- 1033 Liggio, J., Li, S.-M., Vlasenko, A., Stroud, C. and Makar, P.: Depression of ammonia uptake to
1034 sulfuric acid aerosols by competing uptake of ambient organic gases, *Environ. Sci. Technol.*,
1035 45(7), 2790–2796, 2011.
- 1036 Li, M., Weschler, C. J., Bekö, G., Wargocki, P., Lucic, G. and Williams, J.: Human Ammonia
1037 Emission Rates under Various Indoor Environmental Conditions, *Environ. Sci. Technol.*,
1038 doi:10.1021/acs.est.0c00094, 2020.
- 1039 Liu, C.-N., Lin, S.-F., Awasthi, A., Tsai, C.-J., Wu, Y.-C. and Chen, C.-F.: Sampling and
1040 conditioning artifacts of PM_{2.5} in filter-based samplers, *Atmos. Environ.*, 85, 48–53, 2014.
- 1041 Liu, C.-N., Lin, S.-F., Tsai, C.-J., Wu, Y.-C. and Chen, C.-F.: Theoretical model for the
1042 evaporation loss of PM_{2.5} during filter sampling, *Atmos. Environ.*, 109, 79–86, 2015.
- 1043 Liu, M., Huang, X., Song, Y., Tang, J., Cao, J., Zhang, X., Zhang, Q., Wang, S., Xu, T., Kang, L.,
1044 Cai, X., Zhang, H., Yang, F., Wang, H., Yu, J. Z., Lau, A. K. H., He, L., Huang, X., Duan, L.,
1045 Ding, A., Xue, L., Gao, J., Liu, B. and Zhu, T.: Ammonia emission control in China would
1046 mitigate haze pollution and nitrogen deposition, but worsen acid rain, *Proc. Natl. Acad. Sci. U.*
1047 *S. A.*, 116(16), 7760–7765, 2019.
- 1048 Liu, T., Clegg, S. L. and Abbatt, J. P. D.: Fast oxidation of sulfur dioxide by hydrogen peroxide
1049 in deliquesced aerosol particles, *Proc. Natl. Acad. Sci. U. S. A.*, 117(3), 1354–1359, 2020.
- 1050 Liu, X., Zhang, Y., Huey, L. G., Yokelson, R. J., Wang, Y., Jimenez, J. L., Campuzano-Jost, P.,
1051 Beyersdorf, A. J., Blake, D. R., Choi, Y., St. Clair, J. M., Crouse, J. D., Day, D. A., Diskin, G.
1052 S., Fried, A., Hall, S. R., Hanisco, T. F., King, L. E., Meinardi, S., Mikoviny, T., Palm, B. B.,
1053 Peischl, J., Perring, A. E., Pollack, I. B., Ryerson, T. B., Sachse, G., Schwarz, J. P., Simpson, I.
1054 J., Tanner, D. J., Thornhill, K. L., Ullmann, K., Weber, R. J., Wennberg, P. O., Wisthaler, A.,
1055 Wolfe, G. M. and Ziemba, L. D.: Agricultural fires in the southeastern U.S. during SEAC⁴RS:
1056 Emissions of trace gases and particles and evolution of ozone, reactive nitrogen, and organic
1057 aerosol, *J. Geophys. Res. D: Atmos.*, 121(12), 7383–7414, 2016.

1058 Liu, X., Huey, L. G., Yokelson, R. J., Selimovic, V., Simpson, I. J., Müller, M., Jimenez, J. L.,
1059 Campuzano-Jost, P., Beyersdorf, A. J., Blake, D. R., Butterfield, Z., Choi, Y., Crouse, J. D.,
1060 Day, D. A., Diskin, G. S., Dubey, M. K., Fortner, E., Hanisco, T. F., Hu, W., King, L. E.,
1061 Kleinman, L., Meinardi, S., Mikoviny, T., Onasch, T. B., Palm, B. B., Peischl, J., Pollack, I. B.,
1062 Ryerson, T. B., Sachse, G. W., Sedlacek, A. J., Shilling, J. E., Springston, S., St. Clair, J. M.,
1063 Tanner, D. J., Teng, A. P., Wennberg, P. O., Wisthaler, A. and Wolfe, G. M.: Airborne
1064 measurements of western U.S. wildfire emissions: Comparison with prescribed burning and air
1065 quality implications, *J. Geophys. Res. D: Atmos.*, 122(11), 6108–6129, 2017.

1066 Malm, W. C., Sisler, J. F., Huffman, D., Eldred, R. A. and Cahill, T. A.: Spatial and seasonal
1067 trends in particle concentration and optical extinction in the United States, *J. Geophys. Res.*,
1068 99(D1), 1347, 1994.

1069 Malm, W. C., Schichtel, B. A., Hand, J. L. and Collett, J. L., Jr.: Concurrent Temporal and
1070 Spatial Trends in Sulfate and Organic Mass Concentrations Measured in the IMPROVE
1071 Monitoring Program, *J. Geophys. Res. D: Atmos.*, 122(19), 10,462–10,476, 2017.

1072 Martin, N. A., Ferracci, V., Cassidy, N. and Hoffnagle, J. A.: The application of a cavity
1073 ring-down spectrometer to measurements of ambient ammonia using traceable primary standard
1074 gas mixtures, *Appl. Phys. B*, 122(8), 219, 2016.

1075 Ma, S.-S., Yang, W., Zheng, C.-M., Pang, S.-F. and Zhang, Y.-H.: Subsecond measurements on
1076 aerosols: From hygroscopic growth factors to efflorescence kinetics, *Atmos. Environ.*, 210,
1077 177–185, 2019.

1078 McNaughton, C. S., Clarke, A. D., Howell, S. G., Pinkerton, M., Anderson, B., Thornhill, L.,
1079 Hudgins, C., Winstead, E., Dibb, J. E., Scheuer, E. and Maring, H.: Results from the DC-8 Inlet
1080 Characterization Experiment (DICE): Airborne versus surface sampling of mineral dust and sea
1081 salt aerosols, *Aerosol Sci. Technol.*, 41(2), 136–159, 2007.

1082 Meskhidze, N., Chameides, W. L., Nenes, A. and Chen, G.: Iron mobilization in mineral dust:
1083 Can anthropogenic SO₂ emissions affect ocean productivity?, *Geophys. Res. Lett.*, 30(21), 2085,
1084 2003.

1085 Mezuman, K., Bauer, S. E. and Tsigaridis, K.: Evaluating secondary inorganic aerosols in three
1086 dimensions, *Atmos. Chem. Phys.*, 16(16), 10651–10669, 2016.

1087 Middlebrook, A. M., Bahreini, R., Jimenez, J. L. and Canagaratna, M. R.: Evaluation of
1088 Composition-Dependent Collection Efficiencies for the Aerodyne Aerosol Mass Spectrometer
1089 using Field Data, *Aerosol Sci. Technol.*, 46(3), 258–271, 2012.

1090 Müller, M., Mikoviny, T., Feil, S., Haidacher, S., Hanel, G., Hartungen, E., Jordan, A., Märk, L.,
1091 Mutschlechner, P., Schottkowsky, R., Sulzer, P., Crawford, J. H. and Wisthaler, A.: A compact
1092 PTR-ToF-MS instrument for airborne measurements of volatile organic compounds at high
1093 spatiotemporal resolution, , doi:10.5194/amt-7-3763-2014, 2014.

1094 Murphy, D. M. and Thomson, D. S.: Laser Ionization Mass Spectroscopy of Single Aerosol

- 1095 *Particles, Aerosol Sci. Technol.*, 22(3), 237–249, 1995.
- 1096 Murphy, D. M., Froyd, K. D., Schwarz, J. P. and Wilson, J. C.: Observations of the chemical
1097 composition of stratospheric aerosol particles: The Composition of Stratospheric Particles, *Q.J.R.*
1098 *Meteorol. Soc.*, 140(681), 1269–1278, 2014.
- 1099 Murray, B. J. and Bertram, A. K.: Inhibition of solute crystallisation in aqueous
1100 $\text{H}^+\text{-NH}_4^+\text{-SO}_4^{2-}\text{-H}_2\text{O}$ droplets, *Phys. Chem. Chem. Phys.*, 10(22), 3287, 2008.
- 1101 Myhre, G., Shindell, D., Bréon, F.-M., Collins, W., Fuglestedt, J., Huang, J., Koch, D.,
1102 Lamarque, J.-F., Lee, D., Mendoza, B., Nakajima, T., Robock, A., Stephens, G., Takemura, T.
1103 and Zhang, H.: Anthropogenic and Natural Radiative Forcing, in *Climate Change 2013: The*
1104 *Physical Science Basis. Contribution of Working Group I to the Fifth Assessment Report of the*
1105 *Intergovernmental Panel on Climate Change*, edited by T. F. Stocker, D. Qin, G.-K. Plattner, M.
1106 Tignor, S. K. Allen, J. Boschung, A. Nauels, Y. Xia, V. Bex, and P. M. Midgley, p. 659,
1107 Cambridge University Press, Cambridge, United Kingdom and New York, NY, USA., 2013.
- 1108 National Research Council: *The Airliner Cabin Environment and the Health of Passengers and*
1109 *Crew*, The National Academies Press, Washington, DC., 2002.
- 1110 Nault, B. A., Campuzano-Jost, P., Day, D. A., Schroder, J. C., Anderson, B., Beyersdorf, A. J.,
1111 Blake, D. R., Brune, W. H., Choi, Y., Corr, C. A., de Gouw, J. A., Dibb, J., DiGangi, J. P., Diskin,
1112 G. S., Fried, A., Huey, L. G., Kim, M. J., Knute, C. J., Lamb, K. D., Lee, T., Park, T., Pusede, S.
1113 E., Scheuer, E., Thornhill, K. L., Woo, J.-H. and Jimenez, J. L.: Secondary Organic Aerosol
1114 Production from Local Emissions Dominates the Organic Aerosol Budget over Seoul, South
1115 Korea, during KORUS-AQ, *Atmos. Chem. Phys.*, 18, 17769–17800, 2018.
- 1116 Nenes, A., Pandis, S. N., Kanakidou, M., Russell, A., Song, S., Vasilakos, P. and Weber, R. J.:
1117 Aerosol acidity and liquid water content regulate the dry deposition of inorganic reactive
1118 nitrogen, *Atmos. Phys. Chem. Discuss.*, doi:10.5194/acp-2020-266, 2020a.
- 1119 Nenes, A., Pandis, S. N., Weber, R. J. and Russell, A.: Aerosol pH and liquid water content
1120 determine when particulate matter is sensitive to ammonia and nitrate availability, *Atmos. Chem.*
1121 *Phys.*, 20(5), 3249–3258, 2020b.
- 1122 Nguyen, T. K. V., Zhang, Q., Jimenez, J. L., Pike, M. and Carlton, A. G.: Liquid water:
1123 Ubiquitous contributor to aerosol mass, *Environ. Sci. Technol. Lett.*, 3, 257–263, 2016.
- 1124 Nie, W., Wang, T., Gao, X., Pathak, R. K., Wang, X., Gao, R., Zhang, Q., Yang, L. and Wang,
1125 W.: Comparison among filter-based, impactor-based and continuous techniques for measuring
1126 atmospheric fine sulfate and nitrate, *Atmos. Environ.*, 44(35), 4396–4403, 2010.
- 1127 Pagonis, D., Price, D. J., Algrim, L. B., Day, D. A., Handschy, A. V., Stark, H., Miller, S. L., de
1128 Gouw, J., Jimenez, J. L. and Ziemann, P. J.: Time-Resolved Measurements of Indoor Chemical
1129 Emissions, Deposition, and Reactions in a University Art Museum, *Environ. Sci. Technol.*,
1130 53(9), 4794–4802, 2019.

- 1131 Paulot, F., Jacob, D. J., Johnson, M. T., Bell, T. G., Baker, A. R., Keene, W. C., Lima, I. D.,
1132 Doney, S. C. and Stock, C. A.: Global oceanic emission of ammonia: Constraints from seawater
1133 and atmospheric observations, *Global Biogeochem. Cycles*, 29(8), 1165–1178, 2015.
- 1134 Pratt, K. A. and Prather, K. A.: Aircraft measurements of vertical profiles of aerosol mixing
1135 states, *J. Geophys. Res.*, 115(D11), D11305, 2010.
- 1136 Price, H. C., Mattsson, J., Zhang, Y., Bertram, A. K., Davies, J. F., Grayson, J. W., Martin, S. T.,
1137 O’Sullivan, D., Reid, J. P., Rickards, A. M. J. and Murray, B. J.: Water diffusion in
1138 atmospherically relevant α -pinene secondary organic material, *Chem. Sci.*, 6(8), 4876–4883,
1139 2015.
- 1140 Pye, H. O. T., Nenes, A., Alexander, B., Ault, A. P., Barth, M. C., Clegg, S. L., Collett, J. L., Jr.,
1141 Fahey, K. M., Hennigan, C. J., Herrmann, H., Kanakidou, M., Kelly, J. T., Ku, I.-T., McNeill, V.
1142 F., Riemer, N., Schaefer, T., Shi, G., Tilgner, A., Walker, J. T., Wang, T., Weber, R., Xing, J.,
1143 Zaveri, R. A. and Zuend, A.: The Acidity of Atmospheric Particles and Clouds, *Atmos. Chem.*
1144 *Phys.*, 20(8), 4809–4888, 2020.
- 1145 Robbins, R. C. and Cadle, R. D.: Kinetics of the Reaction between Gaseous Ammonia and
1146 Sulfuric Acid Droplets in an Aerosol, *J. Phys. Chem.*, 62(4), 469–471, 1958.
- 1147 Rumble, J. R., Ed.: *CRC Handbook of Chemistry and Physics*, 100th Edition, 2019 - 2020,
1148 Taylor & Francis Group., 2019.
- 1149 Schauer, C., Niessner, R. and Pöschl, U.: Polycyclic aromatic hydrocarbons in urban air
1150 particulate matter: decadal and seasonal trends, chemical degradation, and sampling artifacts,
1151 *Environ. Sci. Technol.*, 37(13), 2861–2868, 2003.
- 1152 Schroder, J. C., Campuzano-Jost, P., Day, D. A., Shah, V., Larson, K., Sommers, J. M., Sullivan,
1153 A. P., Campos, T., Reeves, J. M., Hills, A., Hornbrook, R. S., Blake, N. J., Scheuer, E., Guo, H.,
1154 Fibiger, D. L., McDuffie, E. E., Hayes, P. L., Weber, R. J., Dibb, J. E., Apel, E. C., Jaeglé, L.,
1155 Brown, S. S., Thornton, J. A. and Jimenez, J. L.: Sources and Secondary Production of Organic
1156 Aerosols in the Northeastern US during WINTER, *J. Geophys. Res. D: Atmos.*,
1157 doi:10.1029/2018JD028475, 2018.
- 1158 Seinfeld, J. H. and Pandis, S. N.: *Atmospheric Chemistry and Physics: From Air Pollution to*
1159 *Climate Change*, Second., John Wiley & Sons, Inc., Hoboken, NJ USA., 2006.
- 1160 Shingler, T., Crosbie, E., Ortega, A., Shiraiwa, M., Zuend, A., Beyersdorf, A., Ziemba, L.,
1161 Anderson, B., Thornhill, L., Perring, A. E., Schwarz, J. P., Campuzano-Jost, P., Day, D. A.,
1162 Jimenez, J. L., Hair, J. W., Mikoviny, T., Wisthaler, A. and Sorooshian, A.: Airborne
1163 characterization of subsaturated aerosol hygroscopicity and dry refractive index from the surface
1164 to 6.5 km during the SEAC⁴ RS campaign, *J. Geophys. Res. D: Atmos.*, 121(8), 4188–4210,
1165 2016.
- 1166 Shiraiwa, M., Ammann, M., Koop, T. and Pöschl, U.: Gas uptake and chemical aging of

- 1167 semisolid organic aerosol particles, *Proc. Natl. Acad. Sci. U. S. A.*, 108(27), 11003–11008, 2011.
- 1168 Slade, J. H., Ault, A. P., Bui, A. T., Ditto, J. C., Lei, Z., Bondy, A. L., Olson, N. E., Cook, R. D.,
1169 Desrochers, S. J., Harvey, R. M., Erickson, M. H., Wallace, H. W., Alvarez, S. L., Flynn, J. H.,
1170 Boor, B. E., Petrucci, G. A., Gentner, D. R., Griffin, R. J. and Shepson, P. B.: Bouncier Particles
1171 at Night: Biogenic Secondary Organic Aerosol Chemistry and Sulfate Drive Diel Variations in
1172 the Aerosol Phase in a Mixed Forest, *Environ. Sci. Technol.*, 53(9), 4977–4987, 2019.
- 1173 Solomon, P. A., Mitchell, W., Tolocka, M., Norris, G., Gemmill, D., Wiener, R., Vanderpool, R.,
1174 Murdoch, R., Natarajan, S. and Hardison, E.: Evaluation of PM_{2.5} Chemical Speciation
1175 Samplers for Use in the EPA National PM_{2.5} Chemical Speciation Network, EPA., 2000.
- 1176 Solomon, P. A., Crumpler, D., Flanagan, J. B., Jayanty, R. K. M., Rickman, E. E. and McDade,
1177 C. E.: U.S. national PM_{2.5} Chemical Speciation Monitoring Networks-CSN and IMPROVE:
1178 description of networks, *J. Air Waste Manag. Assoc.*, 64(12), 1410–1438, 2014.
- 1179 Song, S., Gao, M., Xu, W., Shao, J., Shi, G., Wang, S., Wang, Y., Sun, Y. and McElroy, M. B.:
1180 Fine-particle pH for Beijing winter haze as inferred from different thermodynamic equilibrium
1181 models, *Atmos. Chem. Phys.*, 18(10), 7423–7438, 2018.
- 1182 Spiller, L. L.: Determination of Ammonia/Air Diffusion Coefficient Using Nafion Lined Tube,
1183 *Anal. Lett.*, 22(11-12), 2561–2573, 1989.
- 1184 Stith, J. L., Ramanathan, V., Cooper, W. A., Roberts, G. C., DeMott, P. J., Carmichael, G., Hatch,
1185 C. D., Adhikary, B., Twohy, C. H., Rogers, D. C., Baumgardner, D., Prenni, A. J., Campos, T.,
1186 Gao, R., Anderson, J. and Feng, Y.: An overview of aircraft observations from the Pacific Dust
1187 Experiment campaign, *J. Geophys. Res.*, 114(D5), 833, 2009.
- 1188 Sueper, D.: ToF-AMS Data Analysis Software Webpage, [online] Available from:
1189 http://cires1.colorado.edu/jimenez-group/wiki/index.php/ToF-AMS_Analysis_Software, 2018.
- 1190 Sun, K., Cady-Pereira, K., Miller, D. J., Tao, L., Zondlo, M. A., Nowak, J. B., Neuman, J. A.,
1191 Mikoviny, T., Müller, M., Wisthaler, A., Scarino, A. J. and Hostetler, C. A.: Validation of TES
1192 ammonia observations at the single pixel scale in the San Joaquin Valley during
1193 DISCOVER-AQ, *J. Geophys. Res. D: Atmos.*, 120(10), 5140–5154, 2015.
- 1194 Sun, Y., Zhang, Q., Macdonald, A. M., Hayden, K., Li, S. M., Liggió, J., Liu, P. S. K., Anlauf, K.
1195 G., Leaitch, W. R., Steffen, A., Cubison, M., Worsnop, D. R., van Donkelaar, A. and Martin, R.
1196 V.: Size-resolved aerosol chemistry on Whistler Mountain, Canada with a high-resolution aerosol
1197 mass spectrometer during INTEX-B, *Atmos. Chem. Phys.*, 9(9), 3095–3111, 2009.
- 1198 Sutton, M. A., Dragosits, U., Tang, Y. S. and Fowler, D.: Ammonia emissions from
1199 non-agricultural sources in the UK, *Atmos. Environ.*, 34(6), 855–869, 2000.
- 1200 Sutton, M. A., Reis, S., Riddick, S. N., Dragosits, U., Nemitz, E., Theobald, M. R., Tang, Y. S.,
1201 Braban, C. F., Vieno, M., Dore, A. J., Mitchell, R. F., Wanless, S., Daunt, F., Fowler, D.,
1202 Blackall, T. D., Milford, C., Flechard, C. R., Loubet, B., Massad, R., Cellier, P., Personne, E.,

1203 Coheur, P. F., Clarisse, L., Van Damme, M., Ngadi, Y., Clerbaux, C., Skjøth, C. A., Geels, C.,
1204 Hertel, O., Wichink Kruit, R. J., Pinder, R. W., Bash, J. O., Walker, J. T., Simpson, D., Horváth,
1205 L., Misselbrook, T. H., Bleeker, A., Dentener, F. and de Vries, W.: Towards a climate-dependent
1206 paradigm of ammonia emission and deposition, *Philos. Trans. R. Soc. Lond. B Biol. Sci.*,
1207 368(1621), 20130166, 2013.

1208 Swartz, E., Shi, Q., Davidovits, P., Jayne, J. T., Worsnop, D. R. and Kolb, C. E.: Uptake of
1209 Gas-Phase Ammonia. 2. Uptake by Sulfuric Acid Surfaces, *J. Phys. Chem. A*, 103(44),
1210 8824–8833, 1999.

1211 Talbot, R. W., Dibb, J. E., Lefer, B. L., Scheuer, E. M., Bradshaw, J. D., Sandholm, S. T., Smyth,
1212 S., Blake, D. R., Blake, N. J., Sachse, G. W., Collins, J. E. and Gregory, G. L.: Large-scale
1213 distributions of tropospheric nitric, formic, and acetic acids over the western Pacific basin during
1214 wintertime, *J. Geophys. Res.: Atmos.*, 102(D23), 28303–28313, 1997.

1215 Tao, Y. and Murphy, J. G.: The sensitivity of PM_{2.5} acidity to meteorological parameters and
1216 chemical composition changes: 10-year records from six Canadian monitoring sites, *Atmos.*
1217 *Chem. Phys.*, 19(14), 9309–9320, 2019.

1218 Thomson, D. S., Schein, M. E. and Murphy, D. M.: Particle Analysis by Laser Mass
1219 Spectrometry WB-57F Instrument Overview, *Aerosol Sci. Technol.*, 33(1-2), 153–169, 2000.

1220 Toon, O. B., Maring, H., Dibb, J., Ferrare, R., Jacob, D. J., Jensen, E. J., Luo, Z. J., Mace, G. G.,
1221 Pan, L. L., Pfister, L., Rosenlof, K. H., Redemann, J., Reid, J. S., Singh, H. B., Thompson, A.
1222 M., Yokelson, R., Minnis, P., Chen, G., Jucks, K. W. and Pszenny, A.: Planning, implementation,
1223 and scientific goals of the Studies of Emissions and Atmospheric Composition, Clouds and
1224 Climate Coupling by Regional Surveys (SEAC⁴RS) field mission, *J. Geophys. Res. D: Atmos.*,
1225 121(9), 4967–5009, 2016.

1226 Vay, S. A., Woo, J.-H., Anderson, B. E., Thornhill, K. L., Blake, D. R., Westberg, D. J., Kiley, C.
1227 M., Avery, M. A., Sachse, G. W., Streets, D. G., Tsutsumi, Y. and Nolf, S. R.: Influence of
1228 regional-scale anthropogenic emissions on CO₂ distributions over the western North Pacific, *J.*
1229 *Geophys. Res.*, 108(D20), 213, 2003.

1230 Vay, S. A., Choi, Y., Vadrevu, K. P., Blake, D. R., Tyler, S. C., Wisthaler, A., Hecobian, A.,
1231 Kondo, Y., Diskin, G. S., Sachse, G. W., Woo, J.-H., Weinheimer, A. J., Burkhardt, J. F., Stohl, A.
1232 and Wennberg, P. O.: Patterns of CO₂ and radiocarbon across high northern latitudes during
1233 International Polar Year 2008, *J. Geophys. Res.*, 116(D14), 4039, 2011.

1234 Walker, J. M., Philip, S., Martin, R. V. and Seinfeld, J. H.: Simulation of nitrate, sulfate, and
1235 ammonium aerosols over the United States, *Atmos. Chem. Phys.*, 12(22), 11213–11227, 2012.

1236 Wang, J., Hoffmann, A. A., Park, R. J., Jacob, D. J. and Martin, S. T.: Global distribution of solid
1237 and aqueous sulfate aerosols: Effect of the hysteresis of particle phase transitions, *J. Geophys.*
1238 *Res.*, 113(D11), 1770, 2008a.

1239 Wang, J., Jacob, D. J. and Martin, S. T.: Sensitivity of sulfate direct climate forcing to the

hysteresis of particle phase transitions, *J. Geophys. Res.*, 113(D11), 13791, 2008b.

Warneke, C., Schwarz, J. P., Ryerson, T., Crawford, J., Dibb, J., Lefer, B., Roberts, J., Trainer, M., Murphy, D., Brown, S., Brewer, A., Gao, R.-S. and Fahey, D.: Fire Influence on Regional to Global Environments and Air Quality (FIREX-AQ): A NOAA/NASA Interagency Intensive Study of North American Fires, NOAA/NASA. [online] Available from: <https://esrl.noaa.gov/csd/projects/firex-aq/whitepaper.pdf>, 2018.

Warner, J. X., Wei, Z., Larrabee Strow, L., Dickerson, R. R. and Nowak, J. B.: The global tropospheric ammonia distribution as seen in the 13-year AIRS measurement record, *Atmos. Chem. Phys.*, 16(8), 5467–5479, 2016.

Warner, J. X., Dickerson, R. R., Wei, Z., Strow, L. L., Wang, Y. and Liang, Q.: Increased atmospheric ammonia over the world's major agricultural areas detected from space, *Geophys. Res. Lett.*, 44(6), 2875–2884, 2017.

Watson, J. G., Chow, J. C., Chen, L. W. A. and Frank, N. H.: Methods to assess carbonaceous aerosol sampling artifacts for IMPROVE and other long-term networks, *J. Air Waste Manag. Assoc.*, 59(8), 898–911, 2009.

Weber, R. J., Orsini, D., Daun, Y., Lee, Y.-N., Klotz, P. J. and Brechtel, F.: A Particle-into-Liquid Collector for Rapid Measurement of Aerosol Bulk Chemical Composition, *Aerosol Sci. Technol.*, 35(3), 718–727, 2001.

Weber, R. J., Guo, H., Russell, A. G. and Nenes, A.: High aerosol acidity despite declining atmospheric sulfate concentrations over the past 15 years, *Nat. Geosci.*, 9(4), 282–285, 2016.

Williamson, C., Kupc, A., Wilson, J., Gesler, D. W., Reeves, J. M., Erdesz, F., McLaughlin, R. and Brock, C. A.: Fast time response measurements of particle size distributions in the 3–60 nm size range with the nucleation mode aerosol size spectrometer, *Atmos. Meas. Tech.*, 11(6), 3491–3509, 2018.

Wilson, R. E.: Humidity Control by Means of Sulfuric Acid Solutions, with Critical Compilation of Vapor Pressure Data, *J. Ind. Eng. Chem.*, 13(4), 326–331, 1921.

Worsnop, D. R., Williams, L. R., Kolb, C. E., Mozurkewich, M., Gershenson, M. and Davidovits, P.: Comment on “The NH₃ Mass Accommodation Coefficient for Uptake onto Sulfuric Acid Solution,” *J. Phys. Chem. A*, 108(40), 8546–8548, 2004.

Yao, X. H. and Zhang, L.: Supermicron modes of ammonium ions related to fog in rural atmosphere, *Atmos. Chem. Phys.*, 12(22), 11165–11178, 2012.

Zakoura, M., Kakavas, S., Nenes, A. and Pandis, S. N.: Size-resolved aerosol pH over Europe during summer, *Atmos. Chem. Phys. Discuss.*, doi:10.5194/acp-2019-1146, 2020.

Zhang, X., Smith, K. A., Worsnop, D. R., Jimenez, J., Jayne, J. T. and Kolb, C. E.: A Numerical Characterization of Particle Beam Collimation by an Aerodynamic Lens-Nozzle System: Part I.

An Individual Lens or Nozzle, *Aerosol Sci. Technol.*, 36(5), 617–631, 2002.

Zhang, X., Smith, K. A., Worsnop, D. R., Jimenez, J. L., Jayne, J. T., Kolb, C. E., Morris, J. and Davidovits, P.: Numerical Characterization of Particle Beam Collimation: Part II Integrated Aerodynamic-Lens–Nozzle System, *Aerosol Sci. Technol.*, 38(6), 619–638, 2004.

Zhou, S., Collier, S., Jaffe, D. A. and Zhang, Q.: Free tropospheric aerosols at the Mt. Bachelor Observatory: more oxidized and higher sulfate content compared to boundary layer aerosols, *Atmos. Chem. Phys.*, 19(3), 1571–1585, 2019.

1 **Supplemental Information of**

2 **Interferences on Aerosol Acidity Quantification due to Gas-phase Ammonia Uptake onto**

3 **Acidic Sulfate Filter Samples**

4

5 **Benjamin A. Nault et al.**

6

7 *Correspondence to:* Jose L. Jimenez (jose.jimenez@colorado.edu)

8 **S1. GEOS-Chem Model**

9 We used a global chemical transport model (GEOS-Chem 11-02-rc, (Bey et al., 2001)) to
10 estimate sulfate mass concentration distributions in the troposphere. The GEOS-Chem model
11 was driven by assimilated meteorological fields from the Goddard Earth Observing System
12 Forward Processing (GEOS-FP) for a year (May 2013 to June 2014, with the first two months
13 discarded for spin-up). The simulation was conducted at 2° (latitude)×2.5° (longitude) with 47
14 vertical layers up to 0.01 hPa and ~30 layers under 250 hPa. We used the EDGAR v4.3 global
15 anthropogenic emissions (Crippa et al., 2018). The global fire emissions database version 4
16 (GFED4) was used for biomass burning emissions (Giglio et al., 2013). Gas-particle partitioning
17 of inorganic aerosols was calculated with the ISORROPIA II thermodynamic model (Fountoukis
18 and Nenes, 2007; Pye et al., 2009), but we excluded sea salt in the ISORROPIA calculation
19 based on Nault et al. (2020).

20

21 **S2. SAGA Filter Extraction**

22 The 20 mL is thought to be a balance between a couple of competing factors. (1) The
23 SAGA team wants to be confident that they are completely extracting the soluble material from
24 the filters (recall, the filters are 90 mm in diameter). They had conducted testing when they first
25 started operating on the NASA DC-8 (late 1980's-early 1990's) and established that this amount
26 of water was necessary to fully extract the material. (2) To counter the dilution, the SAGA team
27 uses a pre-concentrator column and large volume injections into the IC (~5 mL). These two
28 aspects compensate for the greater dilution. (3) Finally, 5 mL is injected for both anions and

29 cations (total 10 mL), and enough sample is left to conduct a follow-up injection if there was any
30 concern about the data.

31

32 **S32. Equations for the Ammonia Flux Model**

33

$$34 \quad v_{NH_3} = \sqrt{\frac{8 \times k_B \times T_{cabin} \times 1000 \times Av}{\pi \times MW_{NH_3}}} \quad \text{Eq. S1}$$

35

$$36 \quad AeroConc = \frac{\frac{4}{3} \times \pi \times (0.5 \times D_{particle} \times 10^{-7})^3 \times \rho_{particle} \times Av}{MW_{particle}} \quad \text{Eq. S2}$$

37

$$38 \quad NH_{3,Flux} = \pi \times (0.5 \times D_{particle} \times 10^{-9})^2 \times v_{NH_3} \times \alpha \times [NH_3] \times (J/J_c) \quad \text{Eq. S3}$$

39

$$40 \quad Time = \frac{AeroConc}{NH_{3,Flux}} \quad \text{Eq. S4}$$

41

42 Above, are the equations used in the theoretical ammonia uptake model (Sect. 2.4) (Seinfeld. and
43 Pandis, 2006). v_{NH_3} (Eq. S1) is the velocity of ammonia gas (m/s). AeroConc (Eq. S2) is the
44 aerosol concentration, in molecules, for a given aerosol diameter. $NH_{3,Flux}$ (Eq. S3) is the flux of
45 ammonia (molecule s^{-1}). Finally, *Time* is the time needed for one ammonia molecule to interact
46 with one sulfuric acid (s).

47 The remaining variables are defined here. In Eq. S1, k_B is the Boltzmann constant
48 (1.38×10^{-23} J K^{-1}), T_{cabin} is the temperature in the cabin of the DC-8 (298 K), Av is Avogadro's
49 number (6.02×10^{23} molecules mol^{-1}), MW_{NH_3} is the molecular weight of gas-phase ammonia (17 g

50 mol⁻¹), and the 1000 is a conversion factor from g to kg. For Eq. S2, $D_{particle}$ is the diameter of the
 51 particle in nm (100 – 1000 nm), 10^{-7} is a conversion factor from nm to cm, $\rho_{particle}$ is the density
 52 of sulfuric acid (1.8 g cm⁻³), and $MW_{particle}$ is the molecular weight of sulfuric acid (98 g mol⁻¹). In
 53 Eq. S3, $D_{particle}$ is the diameter of the particle (100 – 1000 nm), 10^{-9} is a conversion factor from
 54 nm to m, v_{NH_3} is from Eq. S1 (m/s), α is the accommodation coefficient for ammonia with
 55 sulfuric acid (1), $[NH_3]$ is the concentration of ammonia in ppbv, and J/J_c is the Fuchs-Sutugin
 56 correction for a transition regime.

57 The above equations assume a spherical aerosol on the filter. It is possible that the liquid
 58 particle adopts a more elongated shape upon contact with the filter fiber. To estimate the impact
 59 of change of liquid aerosol into more cylindrical shape, we use the following equations:

$$60 \quad volume_{cylinder} = volume_{sphere} \quad \text{Eq. S5}$$

$$61 \quad r_{cylinder} = \sqrt{volume_{sphere}/(\pi h_{cylinder})} \quad \text{Eq. S6}$$

62 where r is the radius of the sphere, $r_{cylinder}$ is the radius and $h_{cylinder}$ is the height for the cylinder.
 63 We assume volume of the sphere is conserved, and take a few values for $h_{cylinder}$: $h_{cylinder}$ is 1 nm,
 64 $h_{cylinder}$ is 25 nm, or $h_{cylinder}$ is radius of the sphere. $r_{cylinder}$ from Eq. S6 is then used in Eq. S3 to
 65 calculate flux.

66

67 **S4. Estimated Influence of Ammonia Offgasing from Polyethylene Bags**

68 Research from co-authors on a prior paper showed that films of water are the most likely
 69 reason for the retention and slow release of sticky volatile gases from surfaces coated by Teflon
 70 and other surfaces. An upper limit water thickness is ~10 μm (Liu et al., 2019). The Henry's Law
 71 Coefficient for ammonia is 62 M atm⁻¹ (Seinfeld. and Pandis, 2006). With the bags being

72 $\sim 1.6 \times 10^4 \text{ mm}^2$ ($\sim 1.6 \times 10^{-2} \text{ m}^2$), that would put an upper limit of water volume of $\sim 1.6 \times 10^{-7} \text{ m}^3$
73 ($\sim 1.6 \times 10^{-4} \text{ L}$). The average ammonia in the cabin of the DC-8 was $\sim 45 \text{ ppbv}$ ($\sim 4.5 \times 10^{-9} \text{ atm}$),
74 leading to $\sim 2.8 \times 10^{-7} \text{ M}$ ammonia partitioned to the water in the bag. Thus, that would lead to
75 $\sim 4.5 \times 10^{-11} \text{ mol}$ ammonia on the walls, or $\sim 2.7 \times 10^{13}$ molecules ammonia. The average number of
76 sulfate molecules on the filters was $\sim 3.8 \times 10^{15}$. Thus, at the upper limit for the water thickness of
77 the bags, there is $\sim 0.7\%$ ammonia:sulfate molecules. As the bags are blown with dry air prior to
78 placing the filters into the bags, the water thickness is expected to be lower ($\sim 0.1 \mu\text{m}$), leading to
79 a three order magnitude decrease for ammonia molecules in the bag. Thus, the bags are not
80 expected to be a large source of ammonia contamination. However, this effect has not been
81 directly investigated.

82

83 **S53. DC-8 Cabin Air Exchange Rates**

84 Air inside the cabin of the DC-8 is constantly being exchanged with ambient air to
85 minimize build-up of carbon dioxide mixing ratios from human emissions, to increase comfort,
86 and to improve human health (Hunt and Space, 1994; Hocking, 1998; Brundrett, 2001; National
87 Research Council, 2002). This exchange rate is factors to an order of magnitude higher than the
88 exchange rates in typical indoor environments (Hunt and Space, 1994). The exchange rate will
89 impact the ammonia mixing ratio in the cabin, as ambient ammonia can be drawn into the
90 airplane and the ventilation will generally reduce the ammonia mixing ratio due to human
91 emissions, similar to carbon dioxide.

92 To calculate the exchange rate, a mass balance method . (Pagonis et al., 2019) was used
93 where the cabin of the DC-8 is assumed to be well-mixed (Eq. S7 and Eq. S8 below). For this

94 method, ambient carbon dioxide, measured by AVOCET (Vay et al., 2003, 2011), and cabin
 95 carbon dioxide, measured by the HOBO MX1102 Carbon Dioxide Data Logger, were used. The
 96 maximum number of passengers on the NASA DC-8 during FIREX-AQ was 40 people, which is
 97 used in this calculation. Finally, the volume of the portion of the DC-8 accessed by passengers is
 98 ~258 m³ (Anon, 2011). These values are used in Eq. S7 and Eq. S8 to estimate the exchange rate.
 99 Here, we assumed that carbon dioxide was in steady-state to estimate the air exchange rate.

100

$$101 \quad \frac{dCO_{2,DC-8}}{dt} = \frac{AER_{DC-8}([CO_{2,ambient}] - [CO_{2,DC-8}]) + (E_{CO_2,Person} \times N)}{V_{DC-8}} \quad \text{Eq. S7}$$

102

$$103 \quad AER_{DC-8} = \frac{-(E_{CO_2,Person} \times N) / V_{DC-8}}{([CO_{2,ambient}] - [CO_{2,DC-8}])} \quad \text{Eq. S8}$$

104

105 Above, for Eq. S7 and Eq. S8, AER_{DC-8} is the air exchange rate, in hr⁻¹, $[CO_{2,ambient}]$ is the ambient
 106 mixing ratio of carbon dioxide, $[CO_{2,DC-8}]$ is the carbon dioxide mixing ratio in the cabin of the
 107 DC-8, $E_{CO_2,Person}$ is the emission rate of carbon dioxide per person (21 g hr⁻¹ person⁻¹ (Tang et al.,
 108 2016)), N is the number of people in the cabin (40), and V_{DC-8} is the volume of the cabin (258
 109 m³).

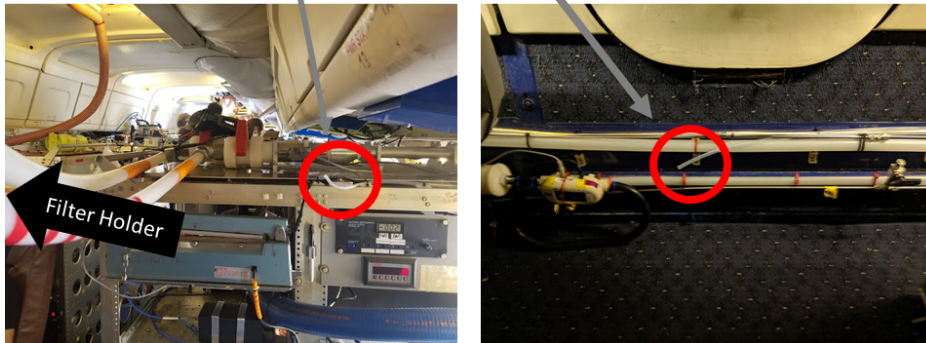
110 After solving for the exchange rate (AER_{DC-8}), Eq. S8 can be rearranged to estimate the
 111 mixing ratio of ammonia in the cabin of the DC-8. Using 1940 µg hr⁻¹ person⁻¹ as the ammonia
 112 emission rate per person, the cabin ammonia mixing ratio is 43.4 ppbv. There have been minimal
 113 studies (two to the best of our knowledge) that have measured total ammonia emissions from
 114 human activity. For one study, which investigated the emissions from hard activity (workout), the
 115 value of 1940 µg hr⁻¹ person⁻¹ is at the lower end (Finewax et al., 2020); however, the total

116 human emissions during this study were potentially higher to higher sweating from exercise,
117 which leads to the hydrolysis of urea to form gas-phase ammonia (Healy et al., 1970; Sutton et
118 al., 2000). For the other study that measured total ammonia emission (Li et al., 2020), the value
119 of $1940 \mu\text{g hr}^{-1} \text{ person}^{-1}$ is similar to the values observed for humans doing low to medium
120 activity.

121 **Figures**

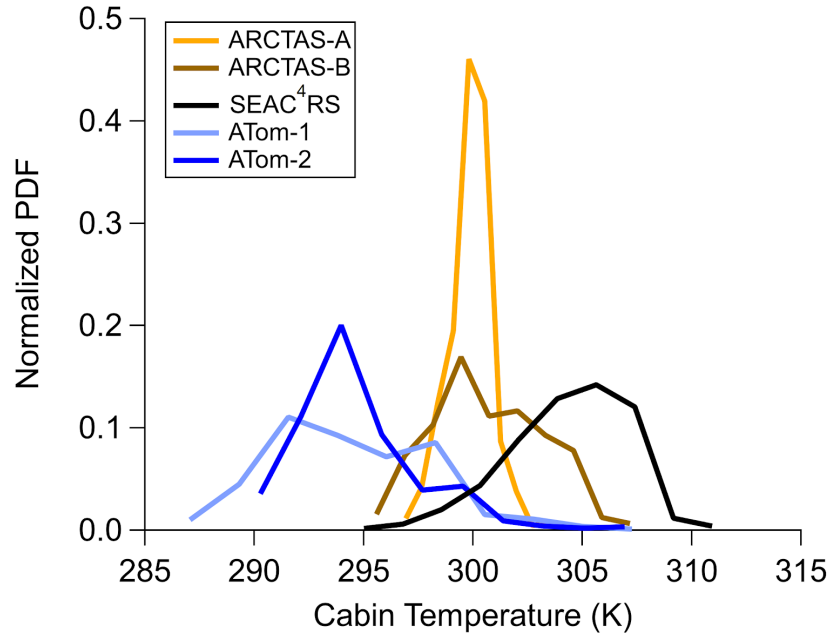


122



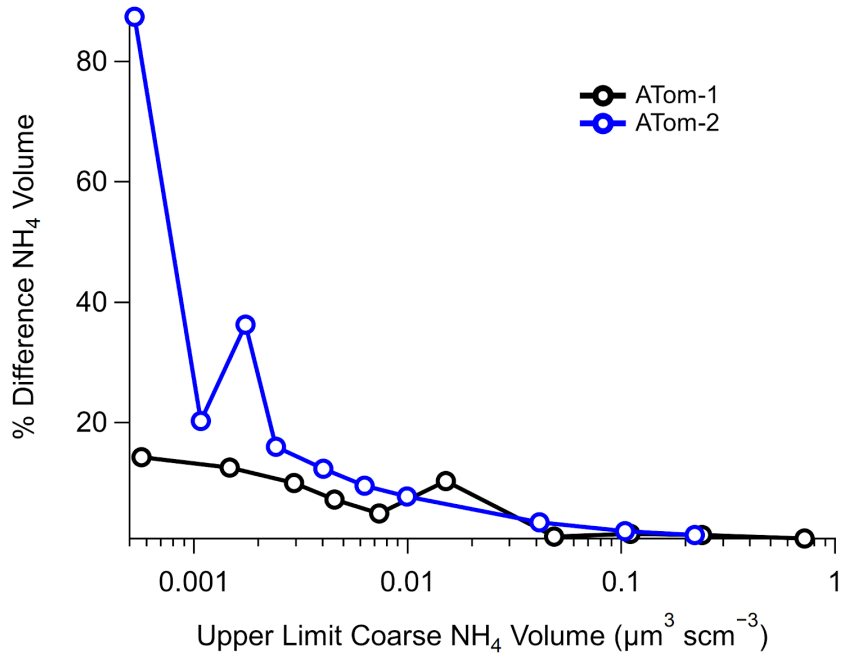
123 *Figure S1. (Top) Floor plan of the DC-8 for the FIREX-AQ campaign (Webster, 2019). Location*
124 *of where the Picarro instrument, aerosol filter sampling, and sampling of cabin ammonia*
125 *locations (red circles) during the campaign are shown. Photos of the sampling by the filter*
126 *collection (bottom left) and mid-cabin sampling (bottom right) are shown. The actual filter*
127 *holder in the bottom left is in the direction of the arrow and not pictured.*

128

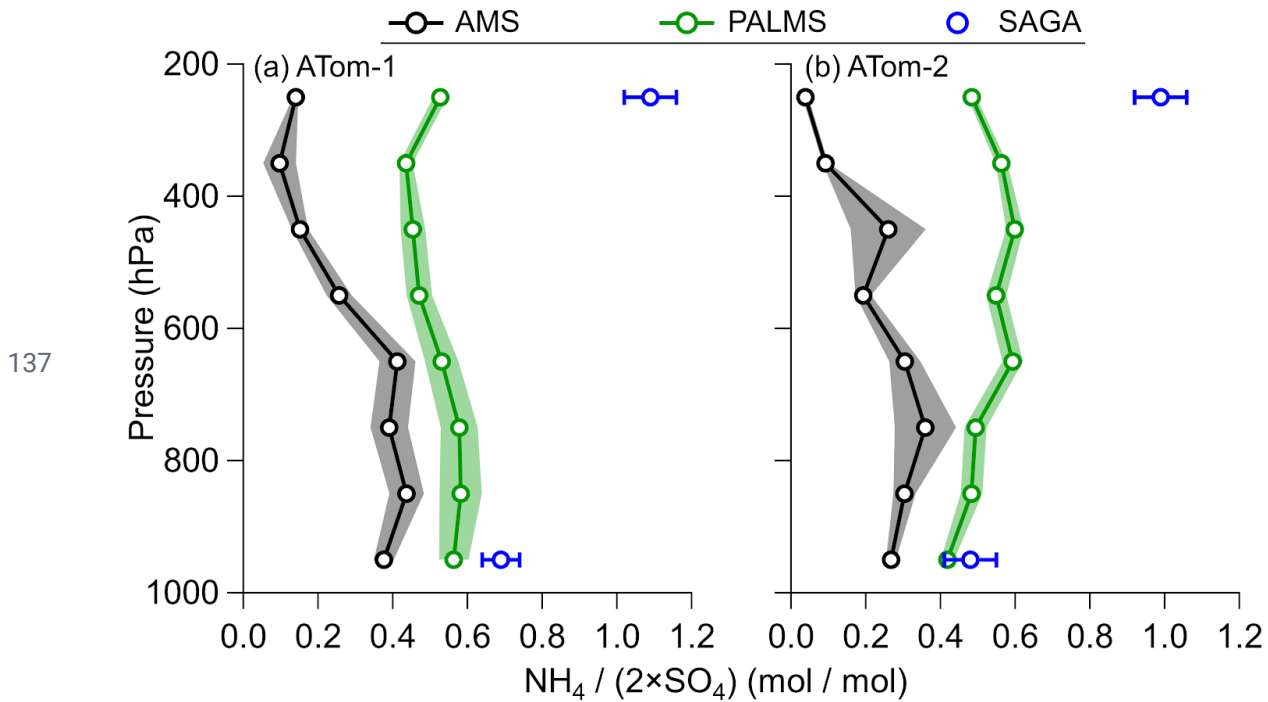


129 *Figure S2. Normalized probability distribution function (PDF) of cabin temperature (K) during*
130 *five aircraft campaigns.*

131

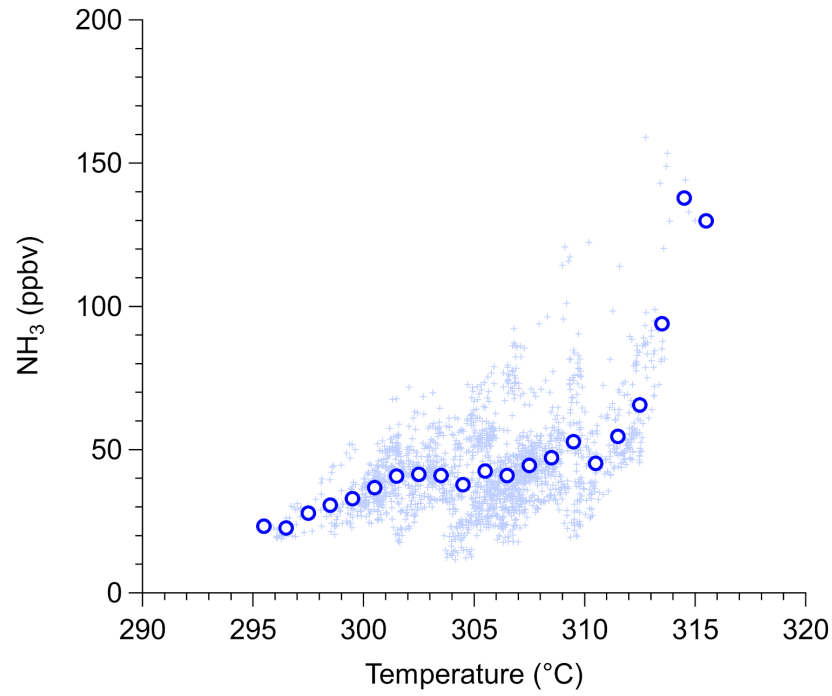


132 *Figure S3. Percent difference in measured ammonium volume ($((\text{filter NH}_4 - \text{AMS}$*
133 *$\text{NH}_4)/1.78)/(\text{AMS NH}_4/1.78) \times 100$) versus upper limit coarse NH₄ volume. The 1.78 is the density*
134 *of ammonium in g cm⁻³ (Rumble, 2019), and the upper limit coarse NH₄ volume was estimated by*
135 *multiplying the coarse volume (from LAS) by 0.1, the highest fraction of ammonium observed in*
136 *coarse aerosol from prior studies (Kline et al., 2004; Cozic et al., 2008).*

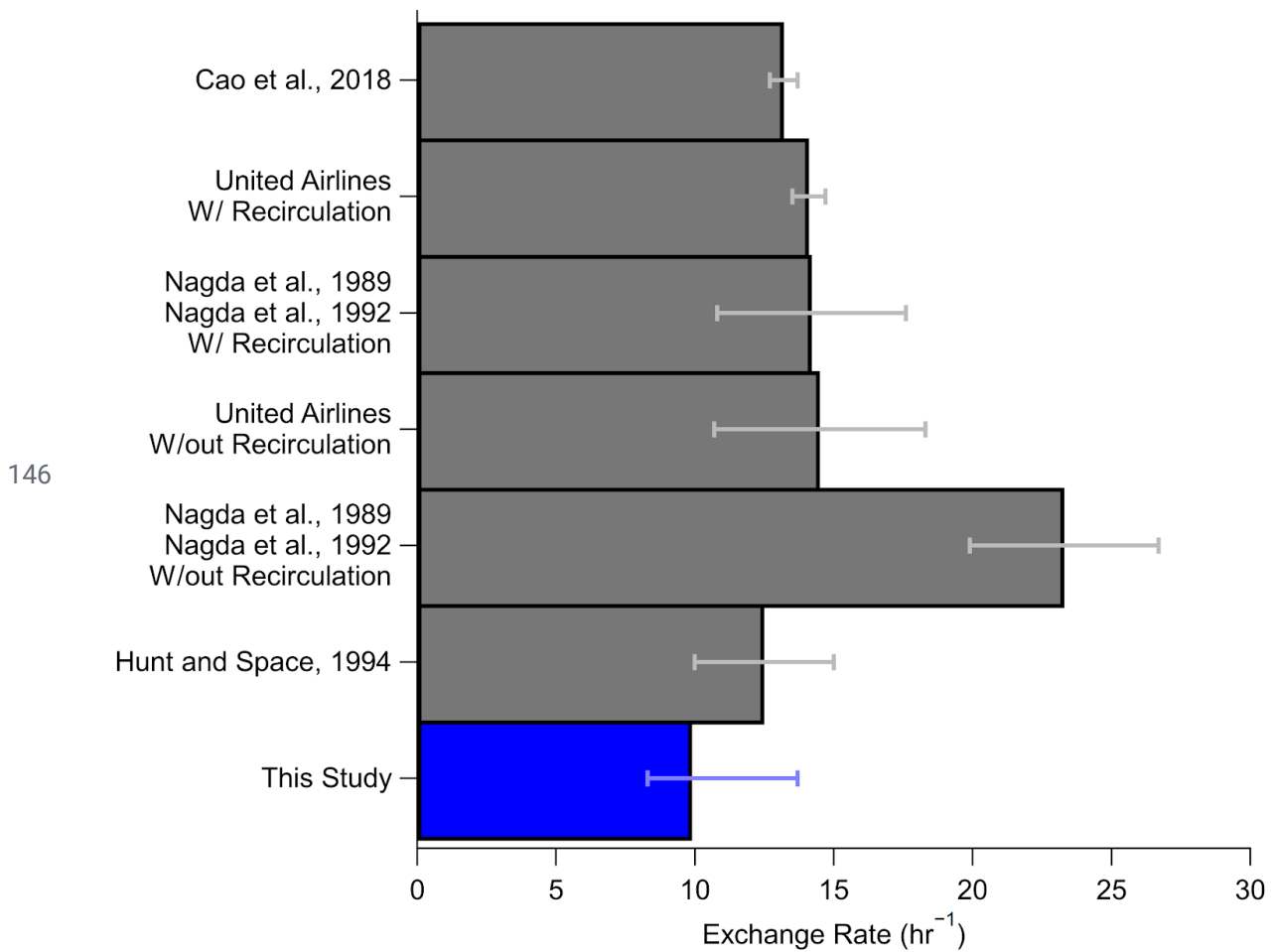


138 *Figure S4. Similar to Fig. 3, but for AMS, PALMS, and SAGA during ATom-1 (a) and ATom-2 (b).*
 139 *However, unlike Fig. 3, the x-axis is defined as $\text{NH}_4 / (2 \times \text{SO}_4)$ instead of $\text{NH}_4 / (2 \times \text{SO}_4 + \text{NO}_3)$, to*
 140 *be consistent with the data product from PALMS (Froyd et al., 2009). The shaded area and error*
 141 *bar is the standard error about the mean.*

142

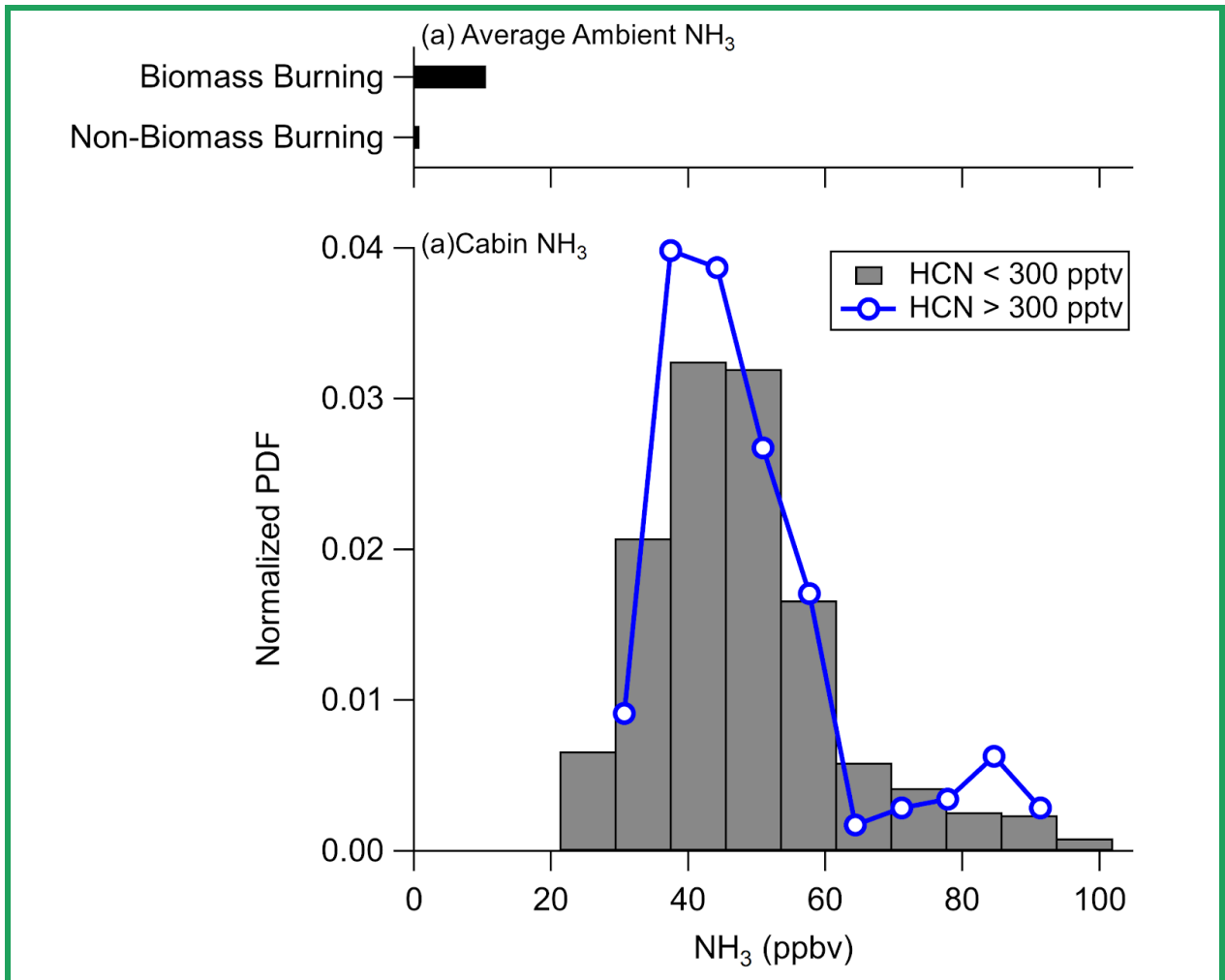


143 *Figure S5. Gas-phase ammonia (NH₃) versus temperature, measured inside the cabin of the*
144 *NASA DC-8, during FIREX-AQ. Light blue crosses are all data, and the blue circles are the*
145 *binned data.*

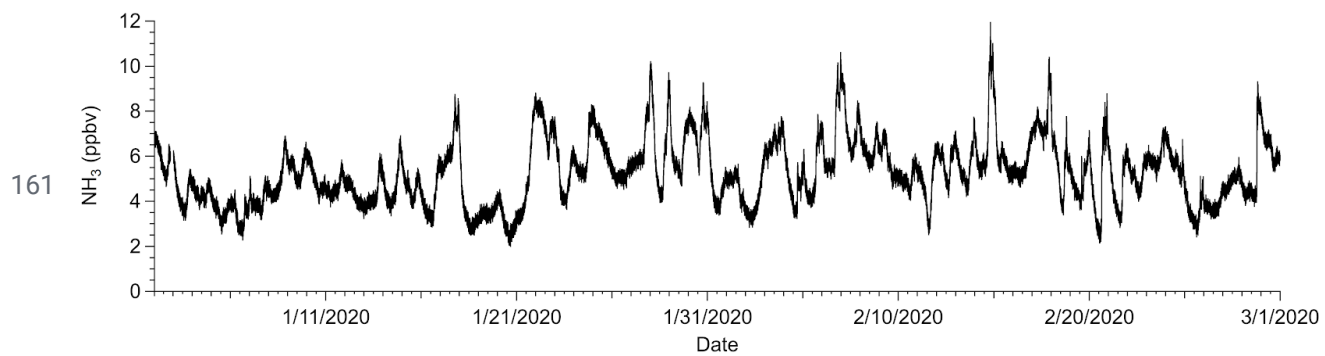


147 *Figure S6. Exchange rates for air in the cabin of the DC-8 (blue), determined by the methods*
 148 *described in SI Sect. 52, compared with exchange rates cited in other studies from various*
 149 *aircraft cabins (Nagda et al., 1989, 1992; Hunt and Space, 1994; United Airlines, 1994; Cao et*
 150 *al., 2019).*

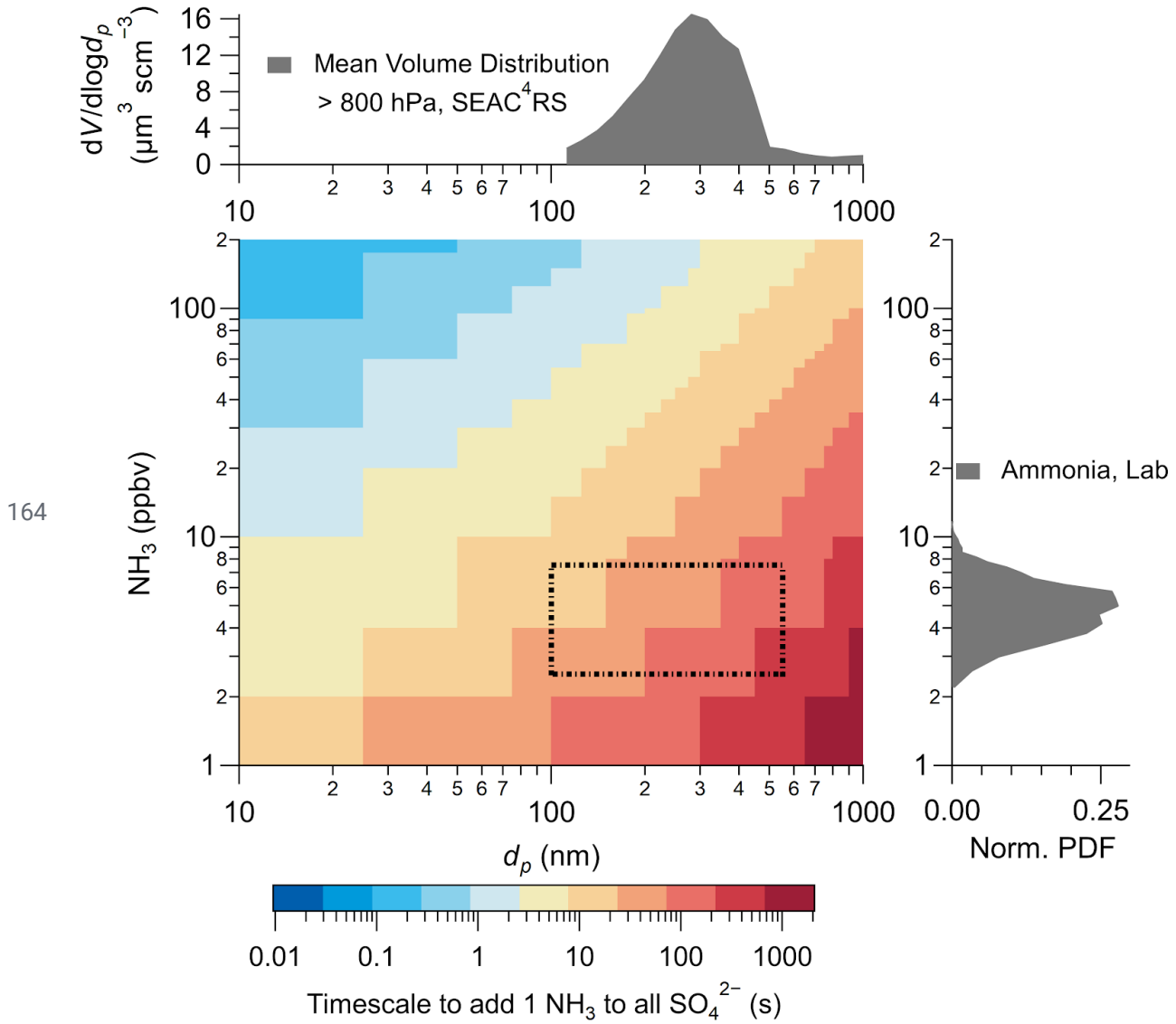
151



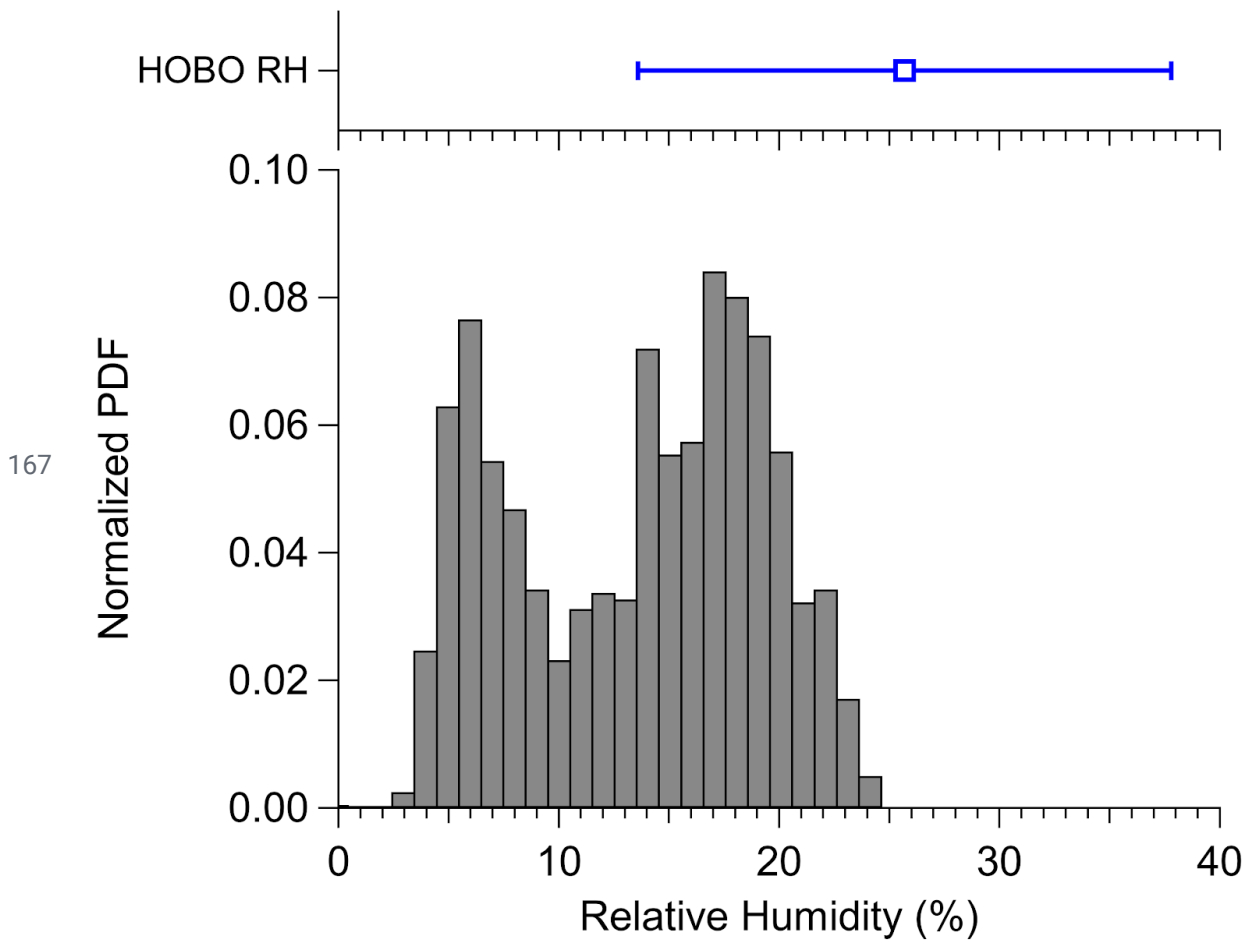
152 *Figure S7.* (top) Average ambient ammonia, measured by PTR-MS (Müller et al., 2014), sampled
 153 in air influenced (HCN > 300 pptv) and not influenced (HCN < 300 pptv) by biomass burning
 154 during the time period cabin was being sampled by Picarro. Note, this sampling was weighted
 155 towards the time period that the DC-8 was sampling agricultural fires, where the plumes were
 156 significantly smaller (seconds) versus the western fires at the beginning of the campaign
 157 (minutes - hours). (b) Normalized probability density function (PDF) of gas-phase ammonia
 158 (NH₃) measured in the cabin of the DC-8 during FIREX-AQ for when the DC-8 was sampling
 159 air influenced by biomass burning (HCN > 300 pptv) and not influenced by biomass burning
 160 (HCN < 300 pptv).



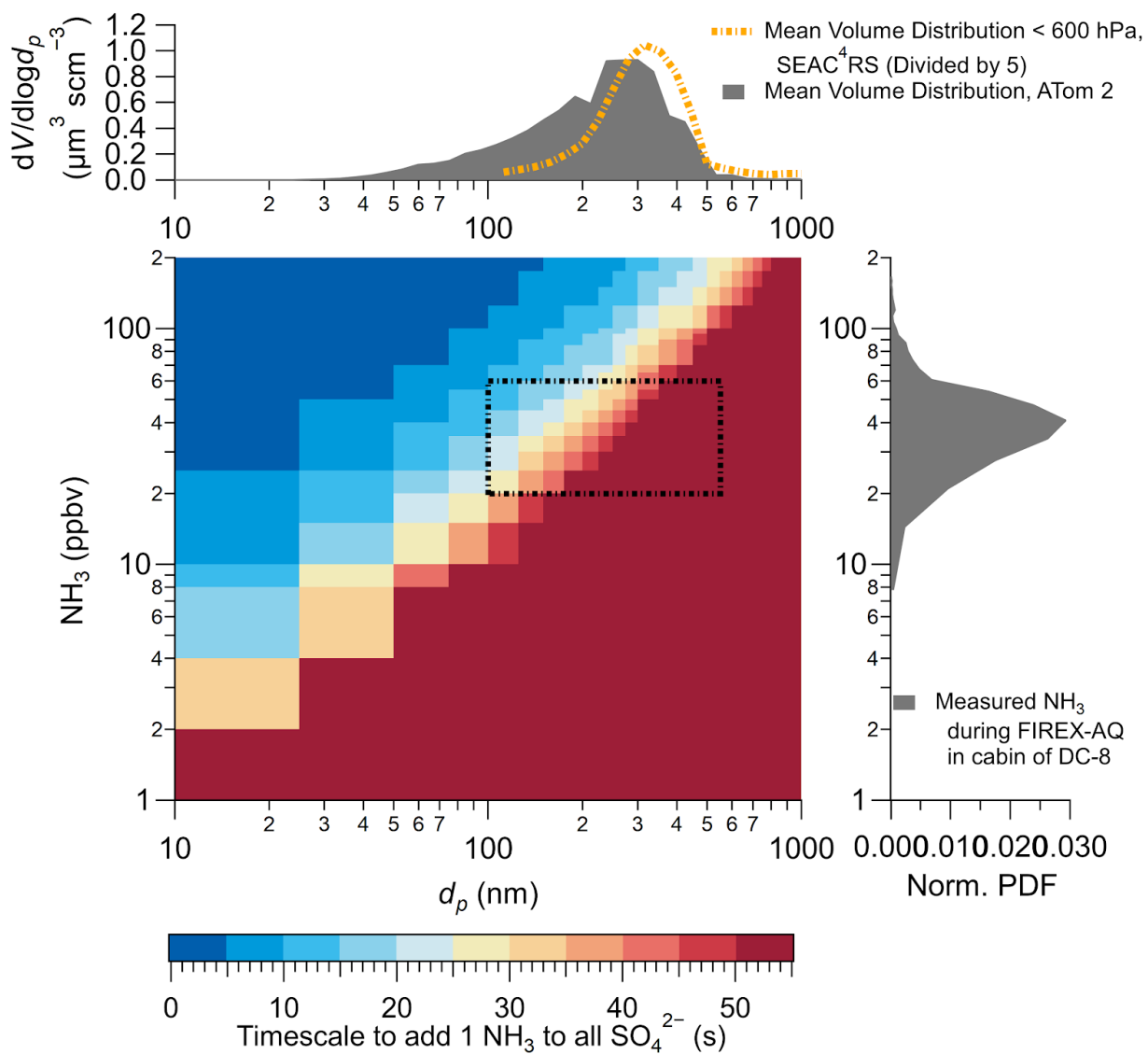
162 *Figure S7. Gas-phase ammonia measured in the Jimenez Group laboratory at the University of*
163 *Colorado at Boulder (room Cristol 343) for ~2 months.*



165 Figure S8. Same as Fig. 7, but with histogram of laboratory ammonia (Fig. S7) and average
 166 boundary layer volume distribution, measured during SEAC⁴RS.



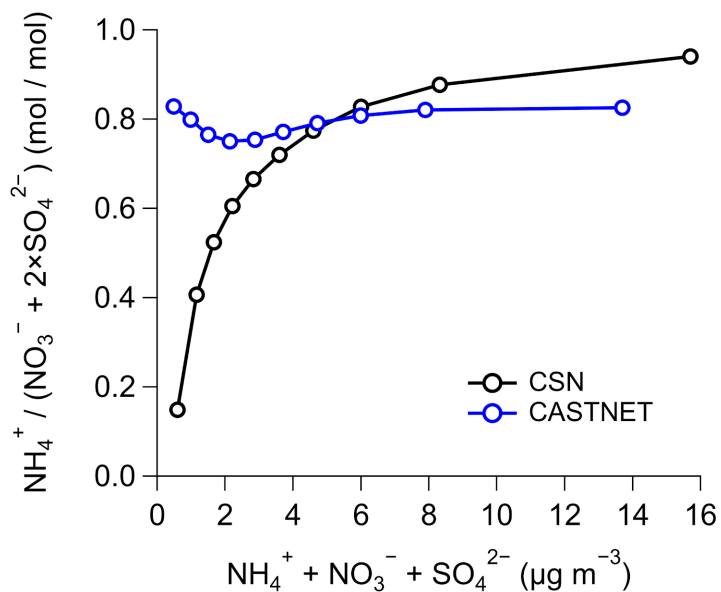
168 *Figure S9. (top) Mean and standard deviation of relative humidity measured inside the NASA*
 169 *DC-8 cabin by the HOBO sensor. (bottom) Normalized probability distribution function (PDF) of*
 170 *relative humidity for inside the cabin of the NASA DC-8, calculated from the water vapor*
 171 *measured by the Picarro. Note that the periods of measurement of the two sensors do not*
 172 *completely overlap, therefore some difference is expected.*



173

174 Figure S10. Same as Fig. 7, but with accommodation coefficient of 0.1 instead of 1.

175



176 Figure S11. Comparison of binned data from Chemical Speciation Monitoring Network (CSN)
177 (Solomon et al., 2000, 2014) and Clean Air Status and Trends Network (CASTNET) (Lavery et
178 al., 2009; Solomon et al., 2014) ammonium balance versus total inorganic mass concentration
179 for the continental United States.

180 **Tables**

181

182 Table S1. *References for studies used in Fig. 6.*

Name of Study in Fig. 6	Reference for Measurement/Predicted NH₃
ATom-1 & -2	(Nault et al., 2020)
DISCOVER-AQ CO	(Battye et al., 2016)
CalNex	(Guo et al., 2017)
SOAS	(Guo et al., 2015)
WINTER	(Guo et al., 2016)
Cabauw Netherlands	(Guo et al., 2018)
Beijing	(Wang et al., 2016)
HomeChem	(Ampollini et al., 2019)
Average Homes	(Brauer et al., 1991; Atkins and Lee, 1993; Tidy and Neil Cape, 1993; Suh et al., 1994; Leaderer B P et al., 1999; Tuomainen et al., 2001; Fischer et al., 2003; Lunden et al., 2003; Järnström et al., 2006)
Average Offices	(Šišović et al., 1987; Salonen et al., 2009)
Average Schools	(Li and Harrison, 1990; Gomzi, 1999; Meininghaus et al., 2003)
ATHLETIC, All	(Finewax et al., 2020)

183

184 References

- 185 Ampollini, L., Katz, E. F., Bourne, S., Tian, Y., Novoselac, A., Goldstein, A. H., Lucic, G.,
186 Waring, M. S. and DeCarlo, P. F.: Observations and Contributions of Real-Time Indoor
187 Ammonia Concentrations during HOMEChem, *Environ. Sci. Technol.*, 53(15), 8591–8598,
188 2019.
- 189 Anon: DC-8 Airborne Science Experimenter Handbook, NASA. [online] Available from:
190 https://espo.nasa.gov/sites/default/files/DC8_Experimenter_Handbook_Jan2011v2.pdf, 2011.
- 191 Atkins, D. H. F. and Lee, D. S.: Indoor concentrations of ammonia and the potential contribution
192 of humans to atmospheric budgets, *Atmos. Environ.*, 27(1), 1–7, 1993.
- 193 Battye, W. H., Bray, C. D., Aneja, V. P., Tong, D., Lee, P. and Tang, Y.: Evaluating ammonia
194 (NH₃) predictions in the NOAA National Air Quality Forecast Capability (NAQFC) using in situ
195 aircraft, ground-level, and satellite measurements from the DISCOVER-AQ Colorado campaign,
196 *Atmos. Environ.*, 140, 342–351, 2016.
- 197 Bey, I., Jacob, D. J., Yantosca, R. M., Logan, J. A., Field, B. D., Fiore, A. M., Li, Q., Liu, H. Y.,
198 Mickley, L. J. and Schultz, M. G.: Global modeling of tropospheric chemistry with assimilated
199 meteorology: Model description and evaluation, *J. Geophys. Res.*, 106(D19), 23073–23095,
200 2001.
- 201 Brauer, M., Koutrakis, P., Keeler, G. J. and Spengler, J. D.: Indoor and outdoor concentrations of
202 inorganic acidic aerosols and gases, *J. Air Waste Manage. Assoc.*, 41(2), 171–181, 1991.
- 203 Brundrett, G.: Comfort and health in commercial aircraft: a literature review, *J. R. Soc. Promot.*
204 *Health*, 121(1), 29–37, 2001.
- 205 Cao, X., Zevitas, C. D., Spengler, J. D., Coull, B., McNeely, E., Jones, B., Loo, S. M.,
206 MacNaughton, P. and Allen, J. G.: The on-board carbon dioxide concentrations and ventilation
207 performance in passenger cabins of US domestic flights, *Indoor Built Environ.*, 28(6), 761–771,
208 2019.
- 209 Cozic, J., Verheggen, B., Weingartner, E., Crosier, J., Bower, K. N., Flynn, M., Coe, H.,
210 Henning, S., Steinbacher, M., Henne, S., Collaud Coen, M., Petzold, A. and Baltensperger, U.:
211 Chemical composition of free tropospheric aerosol for PM₁ and coarse mode at the high alpine
212 site Jungfraujoch, *Atmos. Chem. Phys.*, 8(2), 407–423, 2008.
- 213 Crippa, M., Guizzardi, D., Muntean, M., Schaaf, E., Dentener, F., van Aardenne, J. A., Monni,
214 S., Doering, U., Olivier, J. G. J., Pagliari, V. and Janssens-Maenhout, G.: Gridded emissions of
215 air pollutants for the period 1970–2012 within EDGAR v4.3.2, *Earth Syst. Sci. Data*, 10(4),
216 1987–2013, 2018.
- 217 Finewax, Z., Pagonis, D., Claflin, M. S., Handschy, A. V., Brown, W. L., Ba, J. O. N., Lerner, B.
218 M., Jimenez, J. L., Ziemann, P. J. and de Gouw, J. A.: Quantification and source characterization
219 of volatile organic compounds from exercising and application of chlorine-based cleaning

220 products in a university athletic center, *Indoor Air*, Submitted, 2020.

221 Fischer, M. L., Littlejohn, D., Lunden, M. M. and Brown, N. J.: Automated measurements of
222 ammonia and nitric acid in indoor and outdoor air, *Environ. Sci. Technol.*, 37(10), 2114–2119,
223 2003.

224 Fountoukis, C. and Nenes, A.: ISORROPIA II: a computationally efficient thermodynamic
225 equilibrium model for K^+ - Ca^{2+} - Mg^{2+} - NH_4^+ - Na^+ - SO_4^{2-} - NO_3^- - Cl^- - H_2O aerosols, *Atmos. Chem.*
226 *Phys.*, 7(17), 4639–4659, 2007.

227 Froyd, K. D., Murphy, D. M., Sanford, T. J., Thomson, D. S., Wilson, J. C., Pfister, L. and Lait,
228 L.: Aerosol composition of the tropical upper troposphere, *Atmos. Chem. Phys.*, 9(13),
229 4363–4385, 2009.

230 Giglio, L., Randerson, J. T. and van der Werf, G. R.: Analysis of daily, monthly, and annual
231 burned area using the fourth-generation global fire emissions database (GFED4), *J. Geophys.*
232 *Res.: Biogeosci.*, 118(1), 317–328, 2013.

233 Gomzi, M.: Indoor air and respiratory health in preadolescent children, *Atmos. Environ.*, 33(24),
234 4081–4086, 1999.

235 Guo, H., Xu, L., Bougiatioti, A., Cerully, K. M., Capps, S. L., Hite, J. R., Carlton, A. G., Lee,
236 S.-H., Bergin, M. H., Ng, N. L., Nenes, A. and Weber, R. J.: Fine-particle water and pH in the
237 southeastern United States, *Atmos. Chem. Phys.*, 15(9), 5211–5228, 2015.

238 Guo, H., Sullivan, A. P., Campuzano-Jost, P., Schroder, J. C., Lopez-Hilfiker, F. D., Dibb, J. E.,
239 Jimenez, J. L., Thornton, J. A., Brown, S. S., Nenes, A. and Weber, R. J.: Fine particle pH and
240 the partitioning of nitric acid during winter in the northeastern United States, *J. Geophys. Res. D:*
241 *Atmos.*, 121(17), 10,355–10,376, 2016.

242 Guo, H., Liu, J., Froyd, K. D., Roberts, J. M., Veres, P. R., Hayes, P. L., Jimenez, J. L., Nenes, A.
243 and Weber, R. J.: Fine particle pH and gas–particle phase partitioning of inorganic species in
244 Pasadena, California, during the 2010 CalNex campaign, *Atmos. Chem. Phys.*, 17(9),
245 5703–5719, 2017.

246 Guo, H., Nenes, A. and Weber, R. J.: The underappreciated role of nonvolatile cations in aerosol
247 ammonium-sulfate molar ratios, *Atmos. Chem. Phys.*, 18(23), 17307–17323, 2018.

248 Healy, T. V., McKay, H. A. C., Pilbeam, A. and Scargill, D.: Ammonia and ammonium sulfate in
249 the troposphere over the United Kingdom, *J. Geophys. Res.*, 75(12), 2317–2321, 1970.

250 Hocking, M. B.: Indoor air quality: recommendations relevant to aircraft passenger cabins, *Am.*
251 *Ind. Hyg. Assoc. J.*, 59(7), 446–454, 1998.

252 Hunt, E. W. and Space, D. R.: The Airplane Cabin Environment: Issues Pertaining to Flight
253 Attendant, in *Comfort,” International in-flight Service Management Organization Conference.*
254 [online] Available from:

255 <http://citeseerx.ist.psu.edu/viewdoc/similar?doi=10.1.1.304.7321&type=cc> (Accessed 25 March
256 2020), 1994.

257 Järnström, H., Saarela, K., Kalliokoski, P. and Pasanen, A.-L.: Reference values for indoor air
258 pollutant concentrations in new, residential buildings in Finland, *Atmos. Environ.*, 40(37),
259 7178–7191, 2006.

260 Kline, J., Huebert, B., Howell, S., Blomquist, B., Zhuang, J., Bertram, T. and Carrillo, J.: Aerosol
261 composition and size versus altitude measured from the C-130 during ACE-Asia, *J. Geophys.*
262 *Res.*, 109(D19), 340, 2004.

263 Lavery, T. F., Rogers, C. M., Baumgardner, R. and Mishoe, K. P.: Intercomparison of Clean Air
264 Status and Trends Network Nitrate and Nitric Acid Measurements with Data from Other
265 Monitoring Programs, *J. Air Waste Manag. Assoc.*, 59(2), 214–226, 2009.

266 Leaderer B P, Naeher L, Jankun T, Balenger K, Holford T R, Toth C, Sullivan J, Wolfson J M
267 and Koutrakis P: Indoor, outdoor, and regional summer and winter concentrations of PM₁₀,
268 PM_{2.5}, SO₄²⁻, H⁺, NH₄⁺, NO₃⁻, NH₃, and nitrous acid in homes with and without kerosene space
269 heaters, *Environ. Health Perspect.*, 107(3), 223–231, 1999.

270 Li, M., Weschler, C. J., Bekö, G., Wargocki, P., Lucic, G. and Williams, J.: Human Ammonia
271 Emission Rates under Various Indoor Environmental Conditions, *Environ. Sci. Technol.*,
272 doi:10.1021/acs.est.0c00094, 2020.

273 Li, Y. and Harrison, R. M.: Comparison of indoor and outdoor concentrations of acid gases,
274 ammonia and their associated salts, *Environ. Technol.*, 11(4), 315–326, 1990.

275 Lunden, M. M., Revzan, K. L., Fischer, M. L., Thatcher, T. L., Littlejohn, D., Hering, S. V. and
276 Brown, N. J.: The transformation of outdoor ammonium nitrate aerosols in the indoor
277 environment, *Atmos. Environ.*, 37(39), 5633–5644, 2003.

278 Meininghaus, R., Kouniali, A., Mandin, C. and Cicolella, A.: Risk assessment of sensory irritants
279 in indoor air--a case study in a French school, *Environ. Int.*, 28(7), 553–557, 2003.

280 Müller, M., Mikoviny, T., Feil, S., Haidacher, S., Hanel, G., Hartungen, E., Jordan, A., Märk, L.,
281 Mutschlechner, P., Schottkowsky, R., Sulzer, P., Crawford, J. H. and Wisthaler, A.: A compact
282 PTR-ToF-MS instrument for airborne measurements of volatile organic compounds at high
283 spatiotemporal resolution, , doi:10.5194/amt-7-3763-2014, 2014.

284 Nagda, N. L., Fortmann, R. C., Koontz, M. D., Baker, S. R. and Ginevan, M. E.: *Airliner Cabin
285 Environment: Contaminant Measurements, Health Risks, and Mitigation Options*, US
286 Department of Transportation., 1989.

287 Nagda, N. L., Koontz, M. D., Konheim, A. G. and Katharine Hammond, S.: Measurement of
288 cabin air quality aboard commercial airliners, *Atmospheric Environment. Part A. General
289 Topics*, 26(12), 2203–2210, 1992.

290 National Research Council: The Airliner Cabin Environment and the Health of Passengers and
291 Crew, The National Academies Press, Washington, DC., 2002.

292 Nault, B. A., Campuzano-Jost, P., Jo, D., Day, D., Bahreini, R., Bian, H., Chin, M., Clegg, S.,
293 Colarco, P., Kodros, J., Lopez-Hilfiker, F., Marais, E., Middlebrook, A., Neuman, A., Nowak,
294 J., Pierce, J., Thornton, J., Tsigaridis, K., Jimenez, J. and ATom Science Team: Global Survey of
295 Aerosol Acidity from Polluted to Remote Locations: Measurements and Comparisons with
296 Global Models, , doi:10.5194/egusphere-egu2020-11366, 2020.

297 Pagonis, D., Price, D. J., Algrim, L. B., Day, D. A., Handschy, A. V., Stark, H., Miller, S. L., de
298 Gouw, J., Jimenez, J. L. and Ziemann, P. J.: Time-Resolved Measurements of Indoor Chemical
299 Emissions, Deposition, and Reactions in a University Art Museum, *Environ. Sci. Technol.*,
300 53(9), 4794–4802, 2019.

301 Pye, H. O. T., Liao, H., Wu, S., Mickley, L. J., Jacob, D. J., Henze, D. K. and Seinfeld, J. H.:
302 Effect of changes in climate and emissions on future sulfate-nitrate-ammonium aerosol levels in
303 the United States, *J. Geophys. Res.*, 114(D1), 1097, 2009.

304 Rumble, J. R., Ed.: *CRC Handbook of Chemistry and Physics*, 100th Edition, 2019 - 2020,
305 Taylor & Francis Group., 2019.

306 Salonen, H. J., Pasanen, A.-L., Lappalainen, S. K., Riuttala, H. M., Tuomi, T. M., Pasanen, P. O.,
307 Bäck, B. C. and Reijula, K. E.: Airborne concentrations of volatile organic compounds,
308 formaldehyde and ammonia in Finnish office buildings with suspected indoor air problems, *J.*
309 *Occup. Environ. Hyg.*, 6(3), 200–209, 2009.

310 Seinfeld, J. H. and Pandis, S. N.: *Atmospheric Chemistry and Physics: From Air Pollution to*
311 *Climate Change*, Second., John Wiley & Sons, Inc., Hoboken, NJ USA., 2006.

312 Šišović, A., Šega, K. and Kalinić, N.: Indoor/outdoor relationship of ammonia concentrations in
313 selected office buildings, *Sci. Total Environ.*, 61, 73–77, 1987.

314 Solomon, P. A., Mitchell, W., Tolocka, M., Norris, G., Gemmill, D., Wiener, R., Vanderpool, R.,
315 Murdoch, R., Natarajan, S. and Hardison, E.: Evaluation of PM_{2.5} Chemical Speciation
316 Samplers for Use in the EPA National PM_{2.5} Chemical Speciation Network, EPA., 2000.

317 Solomon, P. A., Crumpler, D., Flanagan, J. B., Jayanty, R. K. M., Rickman, E. E. and McDade,
318 C. E.: U.S. national PM_{2.5} Chemical Speciation Monitoring Networks-CSN and IMPROVE:
319 description of networks, *J. Air Waste Manag. Assoc.*, 64(12), 1410–1438, 2014.

320 Suh, H. H., Koutrakis, P. and Spengler, J. D.: The relationship between airborne acidity and
321 ammonia in indoor environments, *J. Expo. Anal. Environ. Epidemiol.*, 4(1), 1–22, 1994.

322 Sutton, M. A., Dragosits, U., Tang, Y. S. and Fowler, D.: Ammonia emissions from
323 non-agricultural sources in the UK, *Atmos. Environ.*, 34(6), 855–869, 2000.

324 Tang, X., Misztal, P. K., Nazaroff, W. W. and Goldstein, A. H.: Volatile Organic Compound

- 325 Emissions from Humans Indoors, *Environ. Sci. Technol.*, 50(23), 12686–12694, 2016.
- 326 Tidy, G. and Neil Cape, J.: Ammonia concentrations in houses and public buildings,
327 *Atmospheric Environment. Part A. General Topics*, 27(14), 2235–2237, 1993.
- 328 Tuomainen, M., Pasanen, A.-L., Tuomainen, A., Jyrki Liesivuori and Juvonen, P.: Usefulness of
329 the Finnish classification of indoor climate, construction and finishing materials: comparison of
330 indoor climate between two new blocks of flats in Finland, *Atmos. Environ.*, 35(2), 305–313,
331 2001.
- 332 United Airlines: Cabin Air Quality., 1994.
- 333 Vay, S. A., Woo, J.-H., Anderson, B. E., Thornhill, K. L., Blake, D. R., Westberg, D. J., Kiley, C.
334 M., Avery, M. A., Sachse, G. W., Streets, D. G., Tsutsumi, Y. and Nolf, S. R.: Influence of
335 regional-scale anthropogenic emissions on CO₂ distributions over the western North Pacific, J.
336 *Geophys. Res.*, 108(D20), 213, 2003.
- 337 Vay, S. A., Choi, Y., Vadrevu, K. P., Blake, D. R., Tyler, S. C., Wisthaler, A., Hecobian, A.,
338 Kondo, Y., Diskin, G. S., Sachse, G. W., Woo, J.-H., Weinheimer, A. J., Burkhart, J. F., Stohl, A.
339 and Wennberg, P. O.: Patterns of CO₂ and radiocarbon across high northern latitudes during
340 International Polar Year 2008, *J. Geophys. Res.*, 116(D14), 4039, 2011.
- 341 Wang, G., Zhang, R., Gomez, M. E., Yang, L., Levy Zamora, M., Hu, M., Lin, Y., Peng, J., Guo,
342 S., Meng, J., Li, J., Cheng, C., Hu, T., Ren, Y., Wang, Y., Gao, J., Cao, J., An, Z., Zhou, W., Li,
343 G., Wang, J., Tian, P., Marrero-Ortiz, W., Secrest, J., Du, Z., Zheng, J., Shang, D., Zeng, L.,
344 Shao, M., Wang, W., Huang, Y., Wang, Y., Zhu, Y., Li, Y., Hu, J., Pan, B., Cai, L., Cheng, Y., Ji,
345 Y., Zhang, F., Rosenfeld, D., Liss, P. S., Duce, R. A., Kolb, C. E. and Molina, M. J.: Persistent
346 sulfate formation from London Fog to Chinese haze, *Proc. Natl. Acad. Sci. U. S. A.*, 113(48),
347 13630–13635, 2016.
- 348 Webster, A.: DC-8 Floor Plan, FIREX-AQ ESPO [online] Available from:
349 <https://espo.nasa.gov/sites/default/files/documents/DC800XXX%2C%20Preliminary%20-%20FIREX-AQ%20Loading%20Floorplan%2C%204-4-19.pdf> (Accessed 27 April 2020), 2019.

351